The importance of the ribosomal elongation factor 4 (LepA)

Dissertation zur Erlangung des akademischen Grades des Doktors der Naturwissenschaften (Dr. rer. nat.)

Eingereicht im Fachbereich Biologie, Chemie, Pharmazie

der Freien Universität Berlin

Vorgelegt von Zhala Karim

aus Sulaymaniah, Kurdistan, Iraq

Dezember 2009

Gutachter

1. Prof. Dr. Kürsad Turgay

2. Prof. Dr. Knud H. Nierhaus

Disputation am 04.02.2010

Summary

EF4 (LepA) is a recently detected elongation factor in bacteria, which has the unique function of back-translocating ribosomes from the post-translocated state and thus catalyzes just the opposite reaction of the translocase EF-G. EF 4 is widely distributed – practically present in all bacteria, mitochondria and chloroplasts – and highly conserved; therefore it is astonishing that a knock-out of its gene *lepA* has no phenotype. Since EF4 increases the active fraction of the synthesized proteins *in vitro*, it was speculated that it might improve the accuracy, perhaps simply via retardation of protein synthesis.

Here we demonstrate that the underlying assumption mentioned above is incorrect. Furthermore, we present *in vivo* and *in vitro* data that for the first time can explain the importance of this factor:

1: In rich medium under non-stress conditions EF4 is present only in trace-amounts in the cytoplasm, but in larger quantities in the membrane fraction. Under stress conditions the ratio membrane-cytoplasm is changed dramatically: Most of the factor is now in the cytoplasm and minor amounts are in the membrane saying that the membrane is a storage organ for this factor.

2: Growth competition experiments show that under non-stress conditions the absence or presence of EF4 in the cell hardly makes a difference, but that stress conditions that increase the intracellular ionic strength, cells lacking this factor are overgrown by wild-type cells in a few generations.

3: Antibiotics that affect EF-G functions have been tested also with EF4 (both factors are structurally related). Thiostrepton blocks the uncoupled GTPase from both EF-G and EF4, whereas micrococcin shows a diverse effect: EF-G dependent GTPase is stimulated, whereas that of EF4 is blocked. Fusidic acid binds directly to EF-G and blocks its GTPase and interestingly also that of EF4.

4: EF4 does not affect the accuracy of protein synthesis at any Mg^{2+} concentration, but surprisingly accelerates the synthesis rate by up to five-fold exclusively under unfavorable ionic conditions.

These observations could be reconciled to the following picture of the EF4 importance: For osmoregulation bacteria can change their intracellular ionic strength in a wide range, e.g. the K^+ concentration from optimal about 100 mM to 1,000 mM, which affects the structure of ribonucleo-particles such as the ribosome.

Unfavourable ionic conditions increase the fraction of stalled ribosomes that block protein synthesis. EF4 is mobilizing these stalled ribosomes and thus overall accelerates protein synthesis. It is known that a ribosome that pauses during protein synthesis within a domain impairs co-translational folding. Therefore it is conceivable that unscheduled stalled ribosomes within a domain also impair the co-translational folding. Mobilization of these ribosomes will improve the active fraction of the co-translational folded protein. In this way EF4 is required under unfavorable ionic conditions and will be provided by the membrane fraction of the cell. It follows that both accelerating protein synthesis and increasing the active protein fraction are consequence of the unique function of EF4, namely back-translocating and mobilizing stalled ribosomes.

Zusammenfassung

EF4 (LepA) ist ein kürzlich entdeckter Elongationsfaktor in Bakterien, der eine einzigartige Funktion ausübt: Er rück-translozíert post-translokationale Ribosomen und katalysiert damit die umgekehrte Reaktion der Translokase EF-G. Seine weite Verbreitung – EF4 kommt praktisch in allen Bakterien, in Mitochondrien und Chloroplasten vor – und hohe Konservierung läßt eine wichtige Funktion vermuten, deshalb ist es eine erstaunlich Tatsache, das ein Knock-out des EF4 Gens keinen ausgeprägten Phänotyp hat. Da es die aktive Fraktion von Proteinen erhöht, vermutete man, daß er die Genauigkeit der Proteinsynthese verbessert, vermutlich einfach über eine Verlangsamung derselben.

Hier zeigen wir, daß die oben erwähnte, zugrunde liegende Annahme unrichtig ist. Unsere *in vivo* und *in vitro* Ergebnisse können zum ersten mal die Rolle und Bedeutung dieses Faktors erklären:

1: In reichem Medium und abwesenden Streßbedingungen (hohe/niedrige Temperaturen, hohe Salze u.a.) findet sich EF4 nur in geringen Mengen im Zytoplasma, ist aber in größeren Mengen in der Membranfraktion zu finden. Unter Streßbedingungen, die die intrazelluläre Ionenstärke anschwellen lassen, verändert sich die Verteilung dramatisch: Nun ist der größere Anteil des Faktors im Zytoplasma. Offenbar fungiert die Membran als Vorratsorgan für EF4.

2: Wachstumswettbewerb-Experimente zeigen, das bei Abwesenheit von Streß EF4, ob in der Zelle vorhanden oder nicht, nur eine unbedeutende Rolle, wenn überhaupt, spielt. Unter Streßbedingungen jedoch werden die Zellen, denen EF4 fehlt, nach wenigen Generationen von Wild-Typ Zellen überwachsen.

3: Antibiotika, die EF-G Funktionen beeinflussen, wurden auch mit EF4 getestet (EF-G und EF4 habe eine sehr ähnliche Struktur). Thiostrepton blockiert die entkoppelte EF-G abhängige GTPase wie auch die von EF4, während Micrococcin unterschiedlich die Funktion beider Faktoren affiziert: EFG abhängige GTPase wird stimuliert und die von EF4 blockiert. Fusidinsäure bindet an EF-G und blockiert die GTPases, und ebenfalls die von EF4, was mit der fast identischen Bindungstasche von Fusidinsäure erklärt werden kann.

4: EF4 verbessert nicht die Genauigkeit der Proteinsynthese bei allen möglichen Mg^{2+} Konzentrationen, aber überraschenderweise beschleunigt es die Proteinsynthese bei hohen Mg^{2+} Konzentrationen bis zu fünffach. Hohe Mg^{2+}

Konzentrationen verlangsamen die Proteinsythese, was auch einen Anstieg der auf einer mRNA blockierten Ribosomen einschließt.

Diese Ergebnisse können zu folgendem Bild der Rolle und Bedeutung von EF4 zusammen gesetzt werden: Merkmal der bakteriellen Osmoregulation ist, daß Bakterien die intrazelluläre K^+ Konzentration in weiten Grenzen variieren können, von z.B. 100 mM bis auf 1,000 mM, letztere Konzentration verändert stark die Struktur von Ribonukleopartikeln wie die des Ribosoms. Die Folge ist eine verstärktes Stehenbleiben eines Ribosomes auf der mRNA eines Polysoms, was einen totalen Ausfall der Proteinsythese auf dieser mRNA nach sich zieht. EF4 erkennt und mobilisiert diese angehaltenen Ribosomen und beschleunigt so insgesamt die Proteinsynthese einer Zelle. Es ist ferner bekannt, daß ein Pausieren von Ribosomen während der Proteinsynthese inmitten einer Domäne die co-translationale Faltung des Proteins verschlechtert. Deshalb darf man annehmen, daß wenn hohe Ionenstärke die Fraktion der angehaltenen Ribosomen vermehrt, die Verminderung derselben mittels EF4 auch die aktive Fraktion der Proteine vermehrt. Auf diese Wiese ist unter ungünstigen Wachstumsbedingungen EF4 im Cytoplasma erforderlich und wird dazu aus der Membran bereitgestellt. Wir sehen, daß beides – Beschleunigung der Proteinsynthese und Verbesserung der aktiven Fraktion – Folgen der einzigartigen EF4 Funktion sind: Rücktranslokation und Mobilisierung von zufällig angehaltenen Ribosomen unter ungünstigen Ionenbedingungen.

Table of contents

Abbreviations

A	Ampere
AA	Acryl Amide
aa-tRNA	Aminoacyl-tRNA
AcPhe-tRNAPhe	N-Acetyl-Phe-tRNA^{Phe}
Å	Ångström
Asp	Aspartic acid
ATP	Adenosine triphosphate
BAA	Bis-acrylamide
BPB	Bromophenol blue
BSA	Bovine Serum albumine
Ci	Curie
Da	Dalton
dpm	disintegration per minute
dsDNA	double strand DNA
E. coli	*Escherichia coli*
EF4	Elongation factor 4 (LepA)
EF-G	Elongation factor G
EF-Ts	Elongation factor thermo stable
EF-Tu	Elongation factor thermo unstable
EM	Electron Microscopy
F	Farad
f. c	final concentration
GDP	guanosine diphosphate
GFP	green fluorescent protein
GTP	guanosine triphosphate
IPTG	isopropyl-ß-D-1 thiogalactopyranoside
kb	kilo bases (1,000 bases)
kJ	kilo Joules
mRNA	messenger RNA

MQ	milli Q water
MW	molecular weight
NH_4Ac	ammonium acetate
nt(s)	nucleotide(s)
NTP	Nucleoside tri-phosphate
P1Kc	Phage 1 transduction
PAGE	Poly acrylamide gel electrophoresis
PCR	polymerase chain reaction
PEP	Phospho*enol*pyruvate
PK	Pyruvate kinase
Phe	phenylalanine
Poly(U)	Long poly-uridine mRNA
PPi	Inorganic pyrophosphate
PTC	Peptidyltransferase centre
RF	Release factor
rpm	revolutions per minute
rRNA	ribosomal RNA
RRF	Ribosome recycling factor
RTS	rapid translation system
SD	Shine Dalgarno sequence
SDS	Sodium Dodecyl Sulphate
30S	small ribosomal subunit
50S	large ribosomal subunit
70S	Prokaryotic ribosome
V	Volts
v/ v	volume/volume
w/ v	weight/volume

1 Introduction

1.1 Protein biosynthesis

In all organisms ribosomes are the core of the translation machinery. The central dogma of molecular biology is the simplest description of translation and describes the conversion of the genetic information encoded in mRNA into a continuous chains of amino acids (polypeptides or proteins) with structural tasks or catalytic activity. Transfer RNAs (tRNAs) are bridging the world of nucleic acids with that of proteins, this L shaped small RNA is holds at the 3`CCA end the amino acid and at the other end an anticodon complementary to a codon on the mRNA.

1.2 Ribosome structure

A ribosome consists of two unequal subunits. In bacteria, a ribosome has a sedimentation constant of 70S and a mass of 2.6-2.8 mega Daltons (Mda) with a diameter of ~20 nm. 70S ribosome can be separated into a large 50S subunit (33 proteins) and 30S (21 proteins) small subunit containing 5S (120 nucleotides), 23S rRNA (2900 nucleotides) and 16S rRNA (1500 nucleotides), respectively (**Figure 1.1**). Eukaryotic ribosomes are larger e.g. in *Saccharomyces cerevisiae* the ribosome has a sedimentation constant of 80S, which can separate into 60S and 40S subunits. Previously it was believed that the ribosomal proteins were main players in protein synthesis, but this idea has become outdated as a result of overwhelming evidence showing that the rRNA is the main player at two essential activities, viz. decoding and peptide bond formation (Green and Noller 1997; Nissen, Hansen et al. 2000). Nevertheless the interplay between ribosomal proteins (r-proteins) and ribosomal RNA provides the fine tuning for the ribosomal functions.

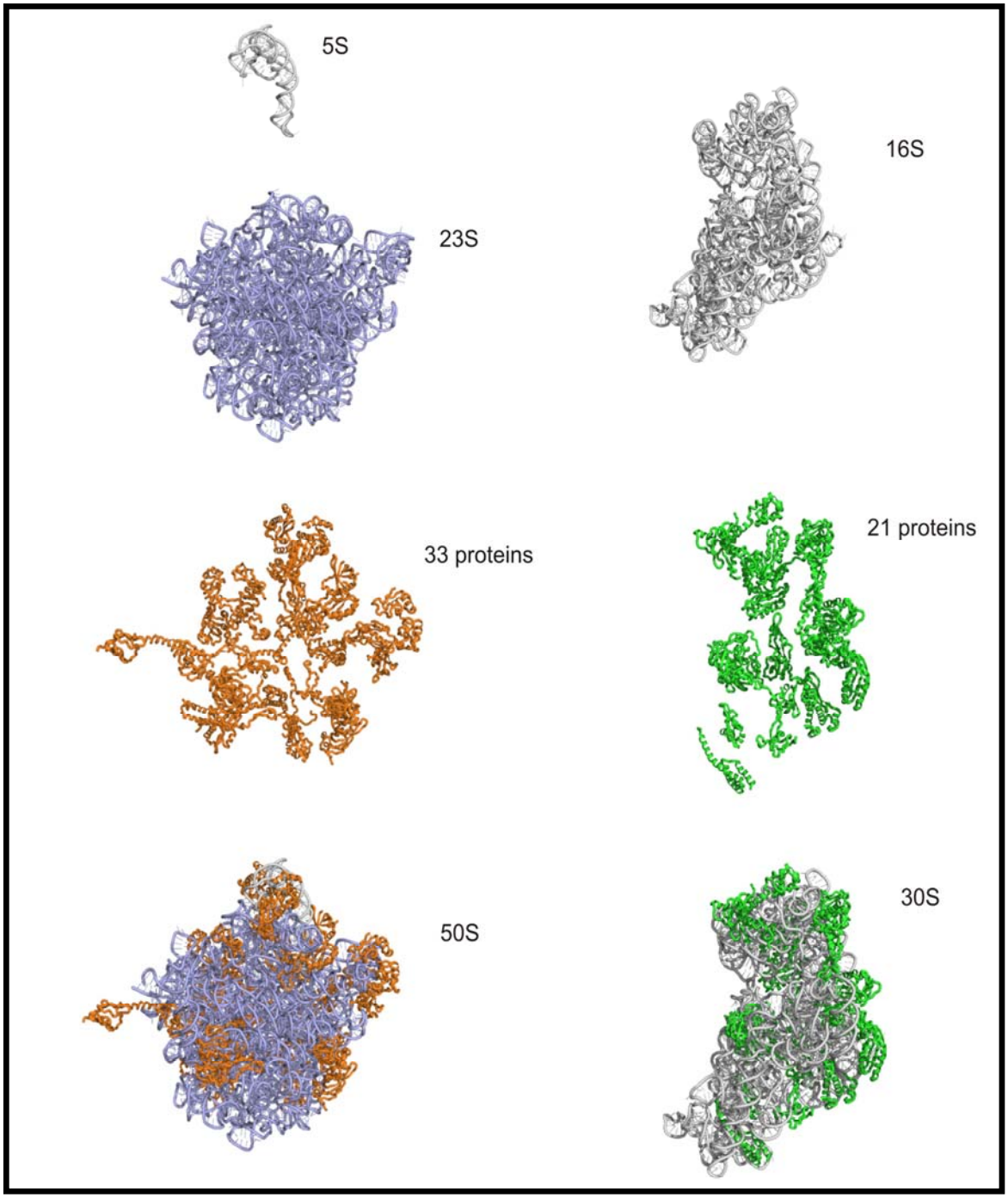

Figure 1.1 The rRNA and protein components of the ribosome. The 30S and 50S PDB files were 2AVY and 2AW4, respectively.

For the first time, the crystallization of the complicated complex ribosome particles was made possible by Yonath and Wittmann (Yonath, Müssig et al. 1980), two decades after this report, the structure of the 50S subunit from the archaean *Haloarcula marismortui* at 2.4 Å was solved (Ban, Nissen et al. 2000) comprising the peptidyl transferase center, whereas the flexible L7/L12 stalk was resolved. This breakthrough was followed by a bacterial 50S structure from *Deinococcus*

radiodurans at 3.1 Å (Harms, Schluenzen et al. 2001). During the same year some other groups solved the structures independently. An immense impact came from Ramakrishnan, by solving the principles of the decoding mechanism at the A site of the small subunit by crystallizing the small ribosomal subunit (Brodersen, Clemons et al. 2002).

Moreover the crystal structure of the *Thermus thermophilus* ribosome was solved by a few groups (Cate, Yusupov et al. 1999; Yusupov, Yusupova et al. 2001), the information obtained from the structures was immensely useful, however the main goal was to crystallize 70S ribosomes from *E. coli*, which was resolved finally by the group of Jamie Cate in 2005 at 3.5 Å resolution, which shed light to many corners on the ribosome above that the ribosome dynamic and movement were observed (Schuwirth, Borovinskaya et al. 2005). These breakthroughs were honoured with Nobel Prizes.

A complementing method is the cryo electron microscopy (cryoEM), which provided medium resolution structures of the ribosome (Gao, Sengupta et al. 2003; Valle, Zavialov et al. 2003; Halic, Becker et al. 2004), in different functional states and also in complex with different translational factors (Spahn, Gomez-Lorenzo et al. 2004; Schuette, Murphy et al. 2009).

1.3 Three tRNA binding sites on the ribosome

1964/5 James Watson (Watson 1964) and Fritz Lipmann (Lipmann 1963) presented for theoretical reasons a model for the functioning ribosome containing two tRNA binding sites A and P sites A for aminoacyl-tRNA and P for peptidyl-tRNA, respectively, the two site model was general wisdom until Nierhaus and Rheinberger discovered the third tRNA binding site (Rheinberger, Sternbach et al. 1981) named E site (exit site) for deacylated-tRNA leaving the ribosome. The *thermus thermophilus* ribosome crystal structure was found with three tRNAs, at A, P and E sites (Yusupov, Yusupova et al. 2001), **(Figure 1.2)**.

The importance of E site was controversially discussed for many years, however this conserved feature of ribosome was finally proven to be important for the accuracy of ribosomes (Di Giacco, Marquez et al. 2008) and for maintaining the reading frame (Marquez, Wilson et al. 2004). After peptide bond formation the deacylated tRNA moves from P site to E site from where it is released upon A site binding, this discovery has led to the allosteric three site model. The allosterically linkage

describes the fact that the occupation of the A site is reducing the binding affinity of the E site and vice versa (the allosteric three- site model for the ribosomal elongation cycle; Gnirke, Geigenmüller et al. 1989). Recently the Green group in Baltimore has published that codon-anticodon interactions in the E site can be critical for the accuracy during translation (Zaher and Green 2009).

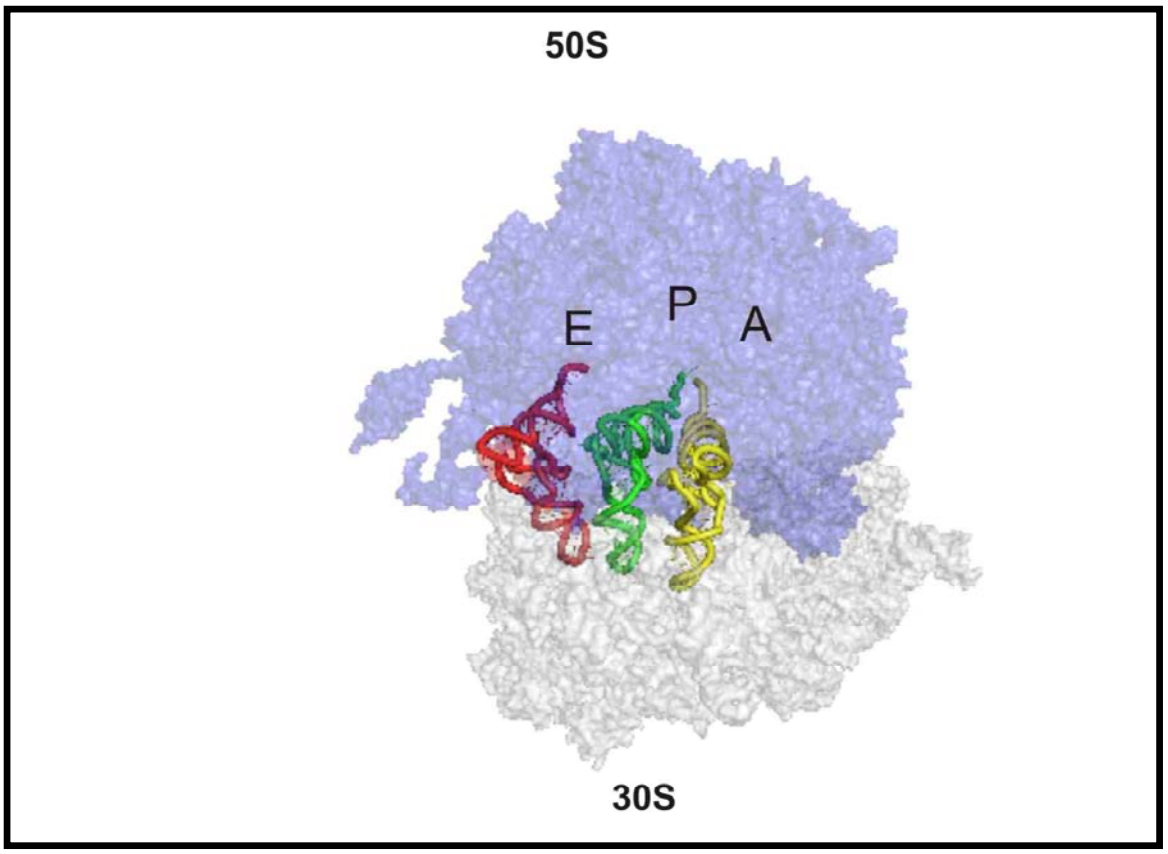

Figure 1.2 Three tRNAs on one 70S ribosome, alignment of the 70S ribosome (PDB of 30S and 50S are 2AVY and 2AW4, respectively) with 70S-bound tRNA structures obtained from PDB file 1GIX

1.4 Protein synthesis highway

The protein synthesis can be divided into four functional states: a) Initiation, b) elongation, c) termination d) recycling **Figure 1.3** is a summary of protein synthesis cycle. In each step special protein synthesis factors are involved. One sole ribosome can incorporate 20- 30 amino acids per second with a super precision of about 1 mis-incorporation per 3000 codons.

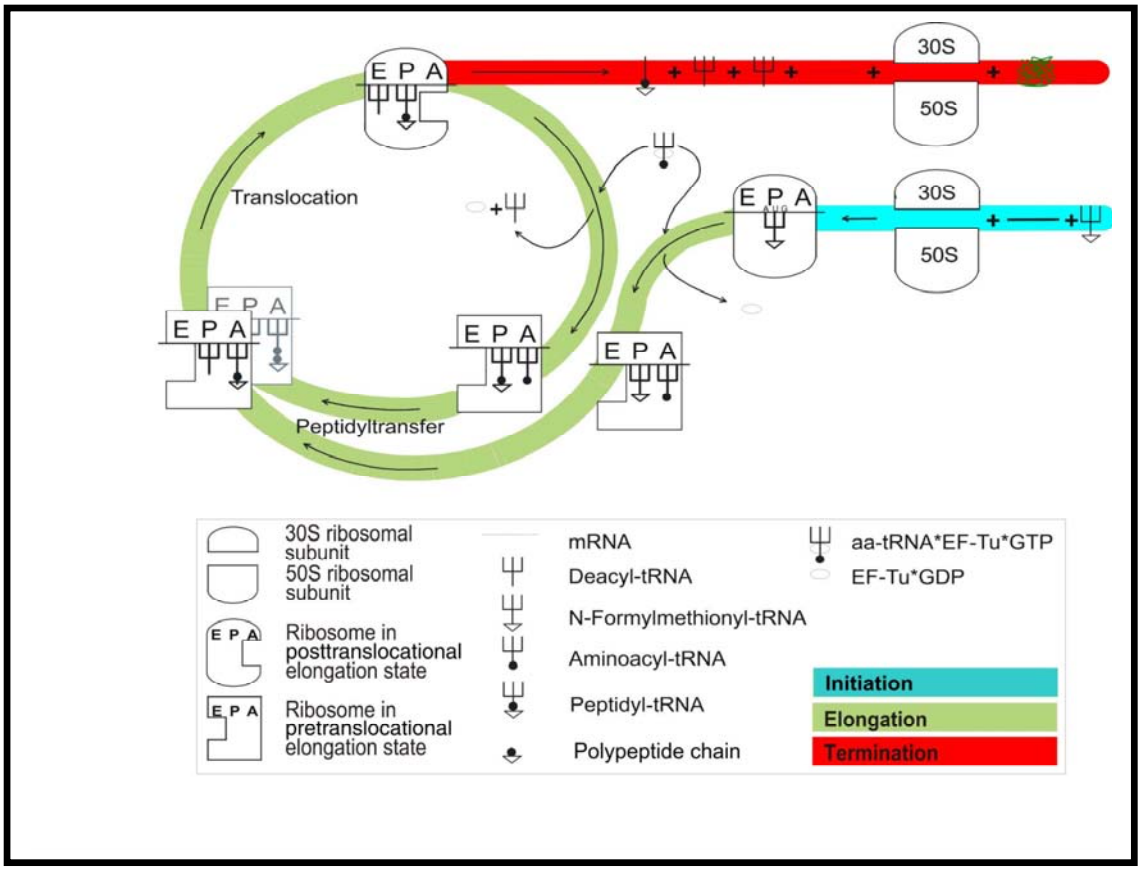

Figure 1.3 Protein synthesis cycle starting from initiation finishing with termination. The rectangular ribosomes indicate the pre-translocational (PRE) state, and the round ribosomes the post-translocational (POST) state. The gap at either A or E site indicates a low affinity state. Further details are described in the text.

1.4.1 Initiation

There are significant differences between eukaryotic and prokaryotic translation initiation, however core principles are the same; the programmed ribosome positions the initiator tRNA at the P site displaying the initiator codon AUG thus selecting the correct frame at the P site; subsequently protein synthesis starts.

In this step of bacterial translation, three highly conserved factors are involved IF1, IF2 and IF3.

IF3 stabilizes dissociated ribosomes by binding to the 30S subunits. The 30S- IF3 complex recognizes the SD (Shine-Dalgarno), which is a purin rich nucleotide stretch located upstream of the AUG codon. First Shine-Dalgarno is complementary to the 3`- end of the 16S rRNA (anti-SD sequence) (Shine and Dalgarno 1974), positions the AUG codon near the P site. This pre-initiation complex of mRNA and 30S is now ready to bind the initiator tRNA (fMet-tRNA^{fMet}), this process can occur either enzymatically in the form of a ternary complex with IF2•GTP or non-enzymatically. The role of IF1 is not yet clear, it has been reported that it stimulates the activities of

both IF2 and IF3 and stabilizes IF2 binding to the 30S reviewed by (Wilson and Nierhaus 2003), while at the same time preventing tRNA binding to the decoding center at the A site of the 30S subunit (Carter, Clemons et al. 2001). The second step is characterized by 50S joining the 30S initiation complex, IF3 is thought to be directly released since its presence inhibits subunit association (Grunberg-Manago, Dessen et al. 1975). Concerning IF1, it has been proposed that it is released after subunit association (Celano, Pawlik et al. 1988). 70S initiation complex is formed followed by release of IF2, in this stage the fMet-tRNA^{fMet} is allowed to fully accommodate at 50S P site resulting in Pi state formation: Now the ribosome is ready for the elongation cycle **(Figure 1.4)**.

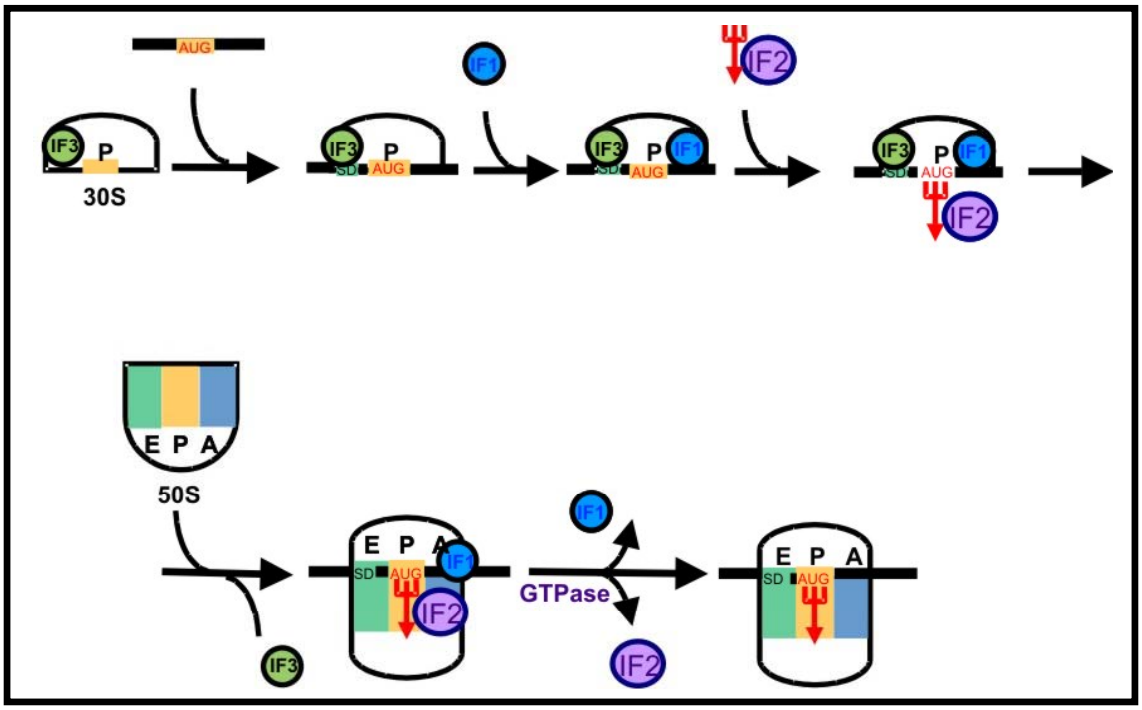

Figure 1.4 Initiation pathway.

1.4.2 Elongation cycle

The elongation cycle is a multistep process encompassing aminoacyl-tRNA selection, peptide bond formation and translocation. The highly conserved GTPases EF-Tu and EF-G drive this process.

1.4.2.1 tRNA selection pathway

The aminoacyl-tRNA is delivered to the ribosome in a ternary complex with EF-Tu and GTP, the selection of which occurs at the decoding center at the A site dictated by the codon displayed here. The decoding centre consists of the nucleotides G530

of helix 18, A1492 and A1493 of helix 44 and Ser50 of S12 (Ogle, Carter et al. 2003), which are responsible for ruling the recognition of correct Watson-Crick pairing versus non Watson-Crick base pairing (Ogle, Brodersen et al. 2001). The intricate mechanism of the selection of the correct aminoacyl-tRNA via codon-anticodon interaction is briefly described here. The first base pair (counted in the 5'→3' direction of the codon) is tested by the universally conserved A1493 of 16S rRNA (*E. coli* numbering throughout this thesis), which flips into the minor groove of this base pair and forms three sequence unspecific H-bonds, two to the 2'OH groups of both nucleotides of the base pair and one to the O2 position of the U1 of the codon (**Figure 1.5 A**). Even the latter bond is sequence unspecific, since in case of a purin in place of U1 its N3 would be at the identical position of O2. The point of decoding is now that in case of a near-cognate base-pair the spatial arrangements of the three H-bonds would be sub-optimal, and the energy difference ($\Delta\Delta G^{0'}$) to the cognate base pair is part of the discrimination energy. The same principles hold for the second (middle) base pair of codon-anticodon interaction, but here the checking is even more rigorous, involving the universal residues A1492 and G530 and Ser50 of the ribosomal protein S12 (**Figure 1.5 B**). This RNA motif involving A residues bonding into the minor groove of a Watson-Crick pair was called A minor motifs important for the stability of ribosomes, 183 of these motifs have been detected within the 50S structure (Nissen, Ippolito et al. 2001). It becomes clear that the decoding center

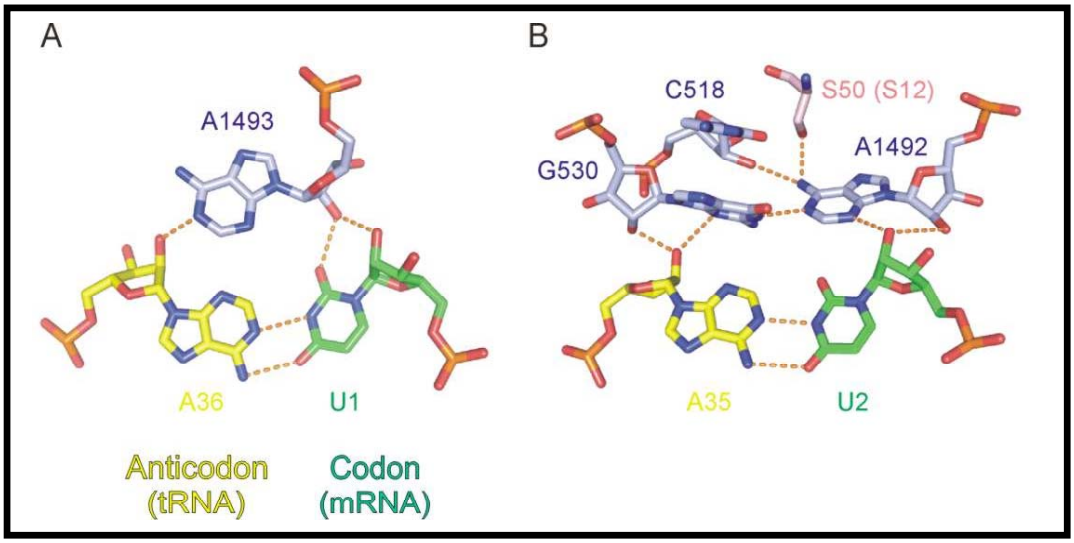

Figure 1.5 A) A minor motif typ I; the first base-pair of codon-anticodon interaction in the decoding center. B) A minor motif typ II during codon-anticodon interaction (Ogle, Brodersen et al. 2001).

does not check the stability of base pairing, base on the number of H-bonds between the bases but rather than spatial geometry and correctness of Watson-Crick. The ribosome does not rigorously check the third base pair and leaves more room for even non-canonical pairs, it is the wobble position well known not to contribute significantly to the selection process (Crick 1966; Ogle, Brodersen et al. 2001). After this selection step, the tRNA is now in a pre-accommodation stage also called A/T state, A for A site and T for EF-Tu. Codon-anticodon interaction is thought to stimulate conformational changes in EF-Tu leading to GTP hydrolysis and consequent rearrangement of the factor in the GDP conformer (Schuette, Murphy et al. 2009), subsequently it leaves the ribosome and as consequence the tRNA is fully accommodated at the A site and is ready to accept the peptidyl residue from the peptidyl tRNA at the P site, by making peptide bond formation. After peptide bond formation a deacylated tRNA is at the P site and the peptidyl tRNA is prolonged by one aminoacyl residue at the A site. The state of the ribosome is a pretranslocational state (PRE), where the tRNAs are located at A and P sites. However this state is changed directly after peptide bond formation to post translocational state (POST) from A and P sites to P and E sites, respectively, promoted by EF-G resulting in an empty A site, which makes the ribosome ready for a new cycle of elongation. Translocation of the tRNAs from A and P sites involves numerous structural rearrangements in the ribosome, however the detailed picture of the translocation remains unclear.

The ribosome makes global contacts with the A, P and E site tRNAs, and these contacts are significantly important for ribosome function and this includes contacts that have tremendous effects on ribosome motion and rearrangements of the tRNAs during translocation (Shoji, Walker et al. 2009). **Figure 1.6** shows the contact sites of the ribosome with the tRNAs at A, P and E sites.

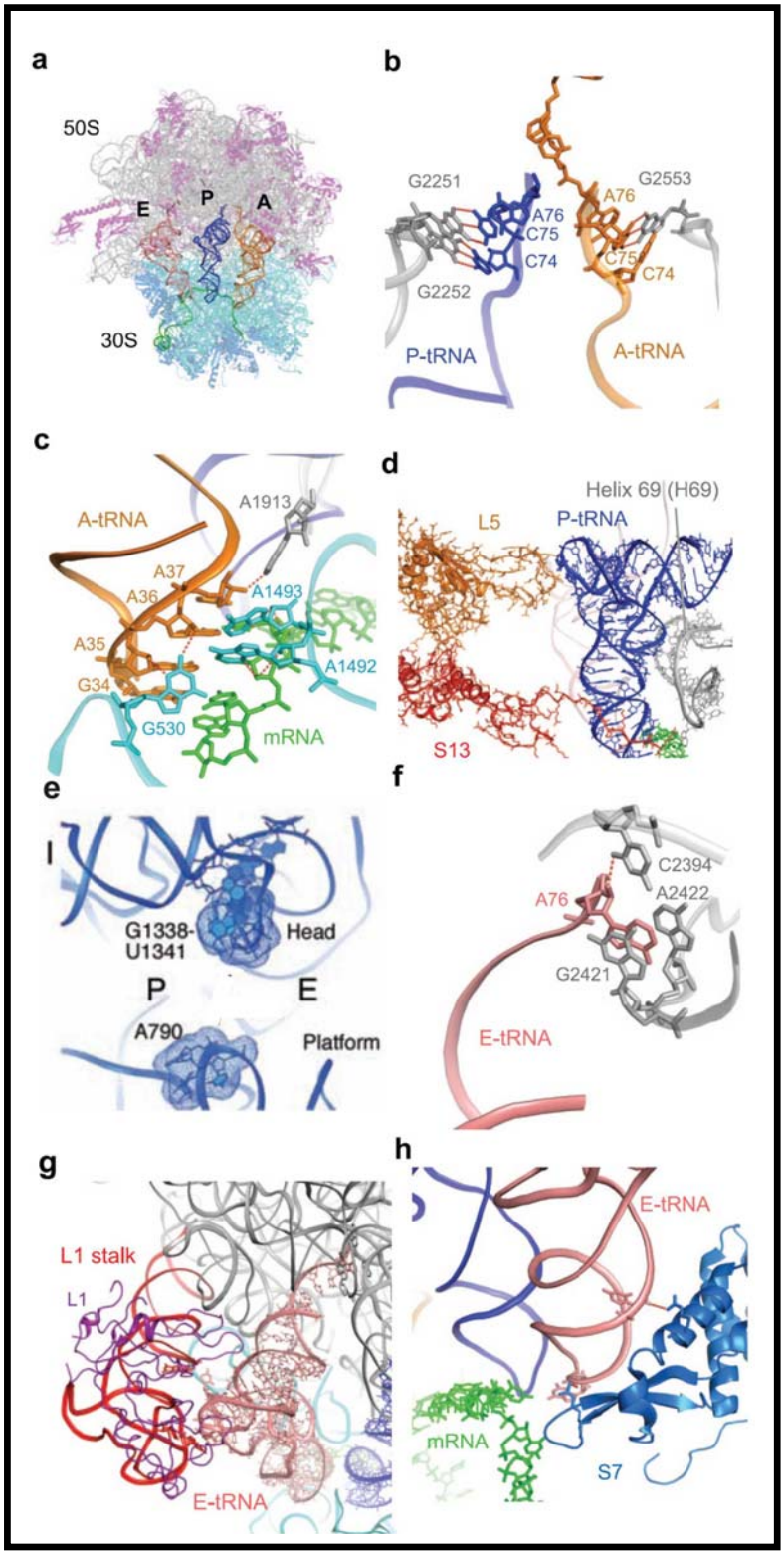

Figure 1.6 tRNA ribosome contacts. A) 70S ribosome model with 3 tRNAs and mRNA. B) Contacts at the 3'CCA of both A and P tRNA. C) Contact sites at the 30S A site. D) P site tRNA interaction with H69 of 23S rRNA and ribosomal proteins L5 and S13. E) The gate formed by A790 loop and 1338-1339 loop at 16S rRNA on the 30S P site. (Schuwirth, Borovinskaya et al. 2005) F) CCA-end contacts of E tRNA with 23S rRNA. G) L1 stalk contact with E site tRNA H) E-tRNA contact with S7 (Shoji, Walker et al. 2009).

1.4.2.2 Structural movements and dynamics of the 70S ribosome/ EF-G mediated translocation

The ribosome is a structurally adjustable platform for the movement of the $tRNA_2$•mRNA complex during the elongation cycle. Already four decades ago

Bretscher hypothesized that tRNA and mRNA movement in the ribosome might include intersubunit rearrangements (Bretscher 1968). The topic revived again when Moazed and Noller presented evidence via chemical modification experiments (footprinting) that the 3`- CCA ends of A and P site tRNAs can spontaneously move with respect to the large subunit (Moazed and Noller 1989). Cryo-EM studies supported the biochemical data and showed that EF-G in complexes with non hydrolysable GTP analogue (GDPNP) or in the presence of GTP and the antibiotic fusidic acid sampled the tRNAs at the A/P and P/E hybrid sites (nomenclature: eg. A before the slash indicates the 30S position of the aa-tRNA and P after the slash the 50S location; (Frank and Agrawal 2000)).

1.4.2.3 Hybrid states

The positioning of tRNA in hybrid states is a reversible process that can occur spontaneously or with the translocation enhancer EF-G (Moazed and Noller 1989) and shown in (**Figures 1.7 C and D**). Blanchard's group has shown that there are constant fluctuations between classical PRE state with tRNAs in A/A and P/P and two distinct hybrid states H1 (A/P P/E) and H2 (A/A and P/E) **(Figure 1.7 C)** (Munro, Altman et al. 2007). The H1 was showing to be the most transient state, fluctuates between PRE and H1 with a movement of 8 Å. Peptide bond formation is required for formation of hybrid states, while EF-G as an translocation enhancer push the process towards the POST state (Pan, Kirillov et al. 2007).

The tRNA movement in the ribosome intersubunit needs large and small scale rearrangements. Cyro-EM and x-ray crystallography input have shown a connection between ribosome mobility and tRNA movement in the intersubunit space of the ribosome (Valle, Zavialov et al. 2003; Connell, Takemoto et al. 2007; Taylor, Nilsson et al. 2007). The movement of the tRNAs are supported and pushed with help of the both subunits. However single molecular FRET (smFRET) data shows that the ribosome and tRNA movement is an uncoupled occurrence since tRNA fluctuation rate is faster than the ribosome 30S subunit movement "ratcheting" and "unratcheting" (Munro, Altman et al. 2007).

1.4.2.4 State of the art of tRNA- mRNA translocation in the 70S

Translocation is catalysed by EF-G, which accelerates the rate of translocation in comparison to spontaneous translocation (Gavrilova and Spirin 1971) by 4- 5 orders of magnitude (Bergemann and Nierhaus 1983; Cukras, Southworth et al. 2003). Cryo EM studies have shown that EF-G binds to the intersubunit space next to the A site of the ribosome with domains I and II positioned as in POST state, whereas domains III, IV and V are more mobile and accompany the movement of the tRNAS (Frank, Gao et al. 2007). Domain IV is like a door lock (Martemyanov and Gudkov 1999), which is important for positioning and movement of the tRNAs and for preventing back translocation. The positioning of deacylated tRNA at the P/E hybrid site and peptidyl tRNA at the A/P site is a consequence of the 30S subunit rotation for about ~ 6° counterclockwise with respect to the 50S subunit (Agrawal, Spahn et al. 2000; Valle, Zavialov et al. 2003; Schuwirth, Borovinskaya et al. 2005; Pan, Kirillov et al. 2007), combined with an inward movement of the L1 by about 40 Å (Cornish, Ermolenko et al. 2008) (**Figure 1.7 E**). Other movements are: (i) the A site finger (helix h38) looses the contact with S13 and makes a new one with S19 (Komoda, Sato et al. 2006). (ii) The 30S head is rotating ("swivelling") by ~ 6° coupled to an "unlocking" (Schuwirth, Borovinskaya et al. 2005) of the P site gate, which separates the P site codon from the E site codon and consists of conserved nucleotides G1338-U1341 on one site and A790, on the other. The opening width of the gate with 13 Å (**Figure 1.6 E**) does not allow a movement of the codon-anticodon complex at the P site to the E site, since a double helix has a diameter of 20 Å (Schuwirth, Borovinskaya et al. 2005). However, when EF-G is present on the ribosome the gate opens to more than 20 Å thus allowing translocation (Connell, Takemoto et al. 2007; **Figure 1.6 E**). At this stage repositioning of EF-G's domain IV in the decoding site at 30S subunit takes place, which involves a local lateral movement of the tip of the h44 with 8 Å towards the P site. This consequently inhibits back translocation of the tRNAs. The swivelling of the head also allows passage and complete translocation, from hybrid state (A/P and P/E) to classical post state (P/P and E/E site), and the L1 stalk adopts a distinct partially closed conformation in the POST state (**Figure 1.7 F**; Cornish, Ermolenko et al. 2008).

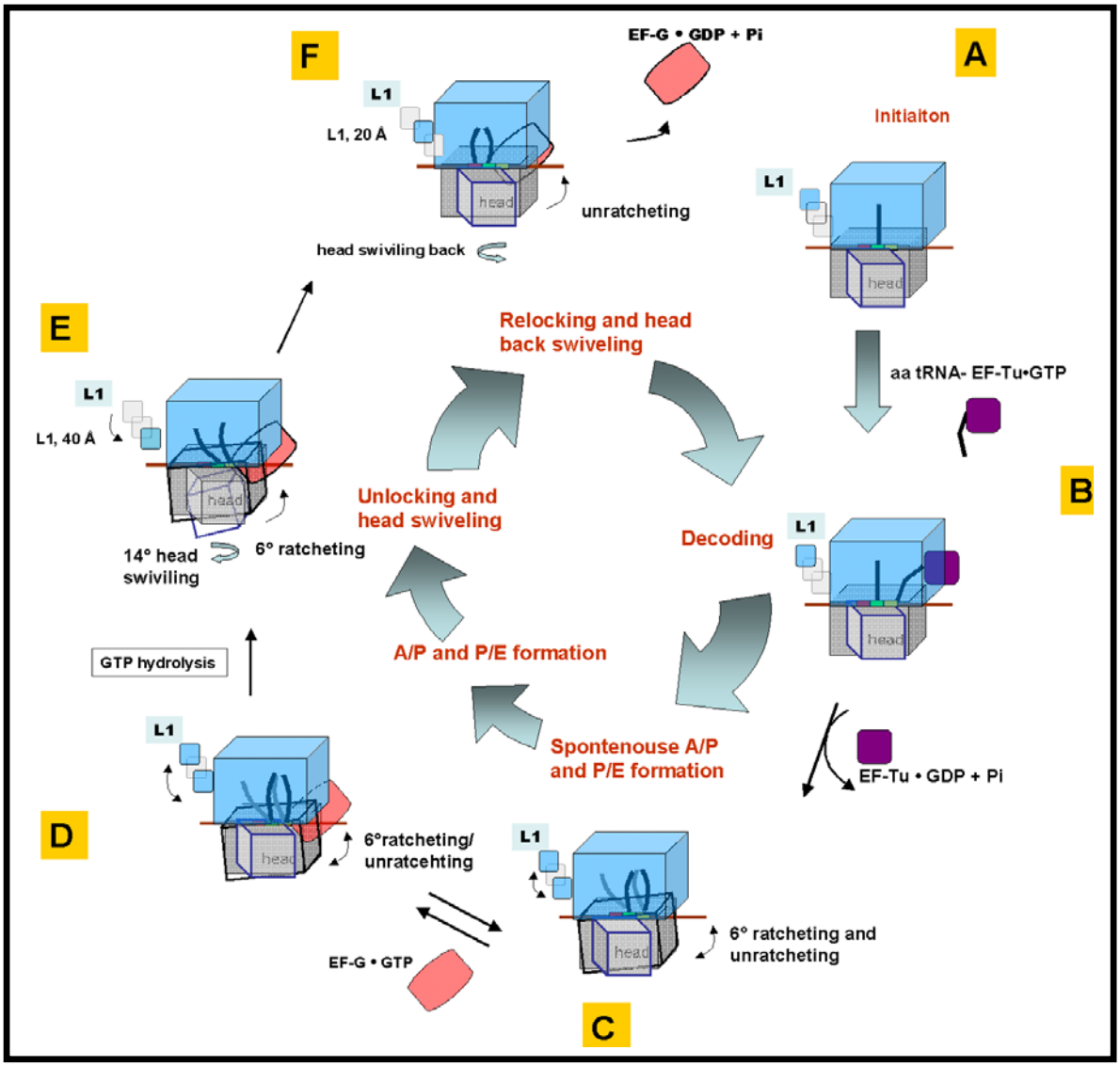

Figure 1.7 Structural dynamics of 70S ribosome in translocation, the model is explaining subunit and head motions related to tRNA translocation. L1 movements are notified.

1.4.3 Termination

Termination of protein synthesis happens through stop codon recognition by polypeptide chain release factors RF1 or RF2 (Caskey, Scolnick et al. 1969). The factors are codon-specific, RF1 recognizing UAG and UAA and RF2 recognizing UAA and UGA. They are responsible for hydrolysis of the ester bond between the polypeptide and the P-site tRNA on the ribosome leading to the release of the nascent chain. In contrast, eukaryotes have only one release one factor eRF1, which recognizes all three stop codons reviewed by (Wilson, Blaha et al. 2002). The termination is not complete unless the release factor 3, a G-protein, releases the RF1 or RF2 from the ribosome. It has been demonstrated that RF3 binds to the ribosome

with high affinity in its GDP form, on the ribosome happens the exchange GDP versus GTP, so that the ribosome takes the function of a “GDP exchange protein”, and finally the GTP hydrolysis triggers the release of RF3 (Zvialov et al., 2001). This exotic behaviour of a translational G-protein is unique. Empty of nascent chain, the ribosome is dissociated upon RRF binding with assistance of EF-G and IF3 (Hirokawa, Iwakura et al. 2008), providing the ribosomal subunits for the next round of initiation.

1.5 Elongation factor 4 previously called LepA revisited

1.5.1 EF4 (LepA)

EF4 (LepA) is the product of the first cistron of a bicistronic operon, the second gene is lepB (leader peptidase) that encodes a signal peptidase, which cleaves amino-terminal leader sequences of secreted proteins (Zwizinski and Wickner 1980). EF4 is a G-protein consisting in E. coli of 599 amino acid residues with a molecular weight of 67 kDa. EF4 has been found in mitochondria and chloroplasts but not in Archaea. It is one of the highest conserved proteins known, among bacterial homologs the amino acid identity is 55% to 68%, which ranks it as the third conserved protein among all bacterial proteins, the first two positions are taken by EF-Tu and EF-G. A recent analysis of 191 fully sequenced bacterial genomes showed that EF4 is present in practically all bacteria with only two exceptions: (i) two of twelve *Streptococcus pyogenes* strains (Margus, Remm et al. 2007) seem to contain only the C-terminus (M. Pech, personal communication). (ii). *Carsonella ruddii*, which is a γ-proteobacterium with the smallest genome of ~160,000 base pairs known. *C. ruddii* is an obligate endosymbiont of a phloem sap-feeding insects *psyllids*, and is on the way of becoming an organelle, since most of the genes for DNA replication, membrane biosynthesis, energy metabolism etc. are absent and might have been transferred to the host genome, nevertheless it contains genes for biosynthesis of essential amino acids that are required by the host (Nakabachi, Yamashita et al. 2006). Although EF4 is highly conserved, which implies an important function in the cell, a knockout strain is viable under laboratory conditions, which does not exclude an important role under distinct conditions. For example, it was reported that in *Helicobacter pylori* EF4 is required at low pH (Bijlsma, Lie et al. 2000).

EF4 has been classified as a membrane bound protein, since (March and Inouye 1985) have reported that overproduced EF4 is mainly found in the periplasmic membrane. The importance of the cell location of EF4 is addressed in this thesis.

EF4 exhibits strong similarities to EF-G, four out of five domains of EF-G have correlates in EF-4 allowing an amino acid alignment thus leading to first a structural model (Qin, Polacek et al. 2006). A cryo-EM analysis, showed EF4 bound to the ribosome, the structural contacts with the ribosome and the A-tRNA as will be described below (Connell, Topf et al. 2008).

1.5.2 Cryo-EM structure of the EF4•complex

EF-G domains I, II, III, V are strongly related to the first four EF4 domains, an exception is domain IV, which is missing in EF4. Considering the mimicry between the overall shape of EF-G and that of the ternary complex aa-tRNA•EF-Tu•GTP, the domain IV of EF-G corresponds to the tRNA anticodon stem loop region that interacts with the decoding centre at the A site of the 30S subunit. A ΔIV EF-G mutant has shown to abolish the translocation activity of EF-G. EF4 domain III is instead followed by a short sequence renamed to V'. In addition, EF4 has a specific, highly conserved, arginine and lysine rich C-terminal domain (CTD) (Connell, Topf et al. 2008; Evans, Blaha et al. 2008). **Figures 1.8 A** shows an alignment of EF4 domain structure with that of EF-G, and **Figure 1.8 B** compares the EF4 tertiary structure with that of EF-G and reveals the extreme similarity of the above-mentioned domains.

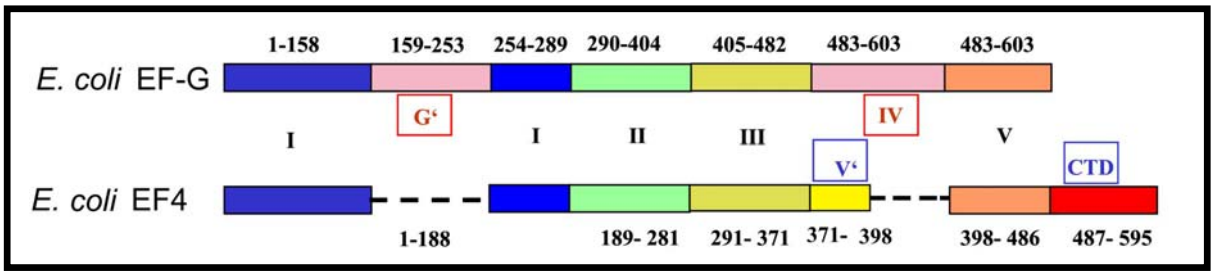

Figure 1.8 A) Alignment of Escherichia coli EF-G and EF4 domains indicated as boxes and color coded.

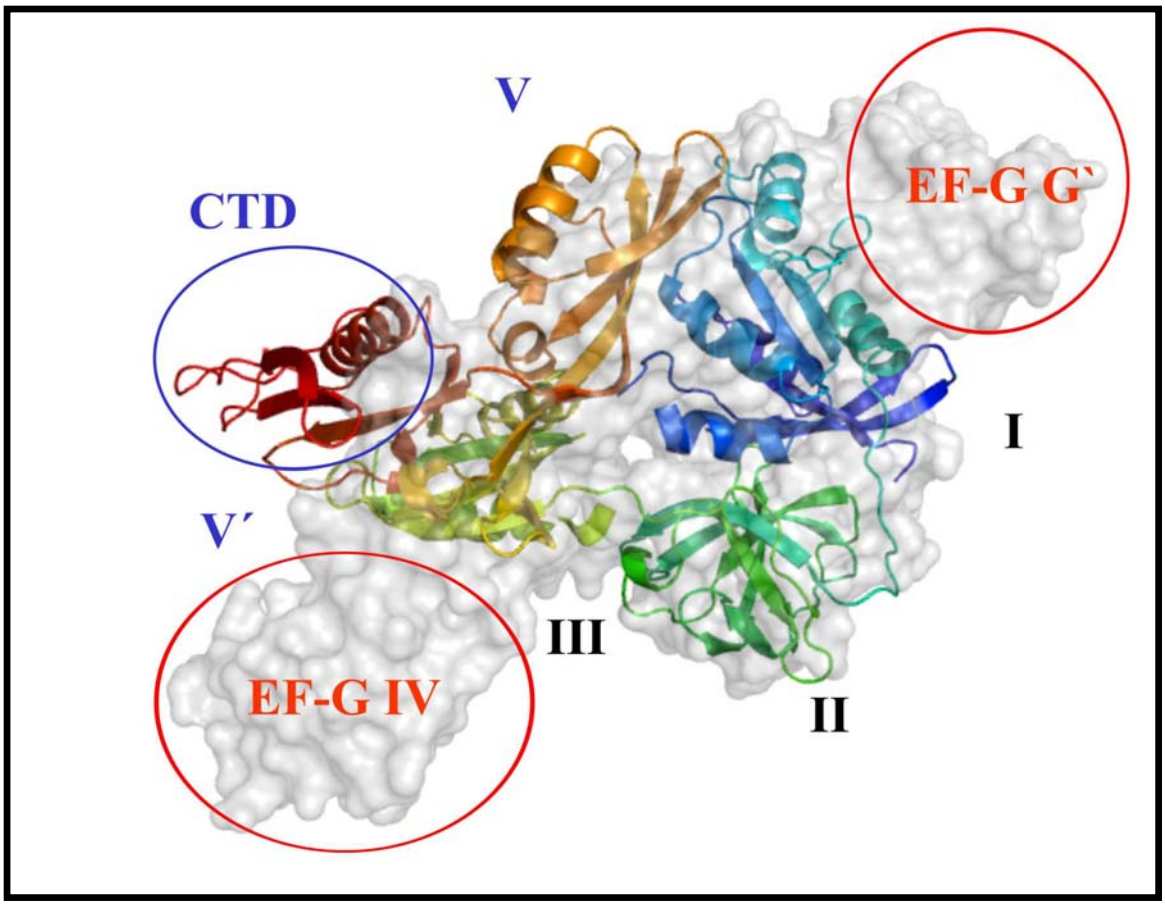

Figure 1.8 B) Comparison of the tertiary structures of EF4 and EF-G using the same color code for EF4 as in A; the structural differences are circled. The surface is a representation of EF-G. PDB files are EF4 (2AW4) and EF-G(1fnm).

1.5.3 EF4 is a ribosome back- translocator

For the first time the function of this highly conserved protein was determined in our group by five different methods, among them puromycin reaction, dipeptide formation and the toeprinting assay. The first method, tRNA binding assay with PRE and POST state formation and puromycin reaction, showed clearly that when EF4 is added to the POST state complex with Ac-Phe tRNA (an analogue of peptidyl tRNA) in the P site (positive puromycin reaction), the puromycin reaction is blocked indicating a back translocation. In the toeprinting assay, the programming mRNA carries a complementary [^{32}P]-labeled DNA primer annealed near the 3' end and located downstream of the ribosome. The primer is prolonged by reverse transcription until the polymerase clashes with the ribosome. A translocation of a PRE state shows a decrease in the length of the reverse transcript by three nucleotides, while the addition of EF4•GTP to a POST state increases the length of the transcript to that of

the PRE state again **(Figure 1.9)**, proving that EF4 is a back-translocator (Qin, Polacek et al. 2006).

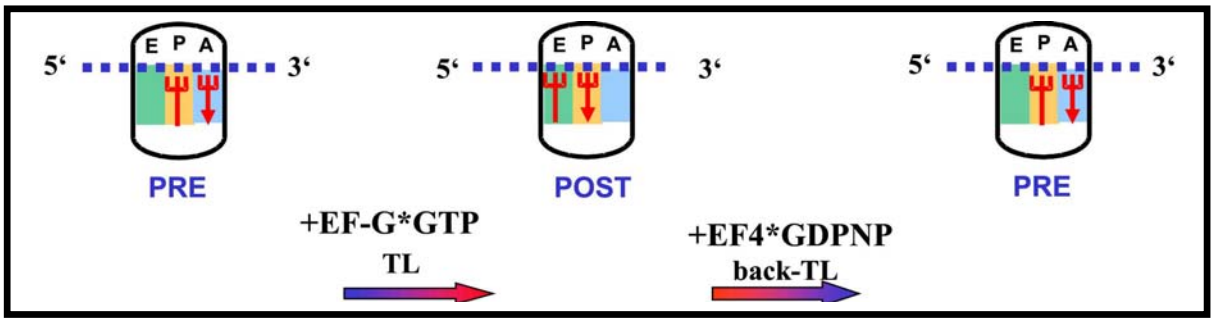

Figure 1.9 Translocation of the tRNAs from A and P sites to P and E sites, and back translocation from P and E sites to A and P sites shown with the toeprinting assay.

The function of EF4 was strongly supported by the above mentioned cryo-EM data, since the complex was initially prepared by adding EF4 to POST ribosome and the structure as depicted in (Connell, Topf et al. 2008; Evans, Blaha et al. 2008 and **Figure 1.10**). shows that EF4•complex is not in a POST state complex but rather in a PRE state. A detailed inspection showed that the peptidyl tRNA has been drawn back over the A site into a new state, the A/L state (A site / LepA bound). In contrast to the canonical PRE state, the A-tRNA is displaced by 14 Å at the T loop and the 5´ end of the tRNA by 13 Å. EF4 is making three contacts with tRNA in the A site region as shown in **Figure 1.11 and 1.11**.

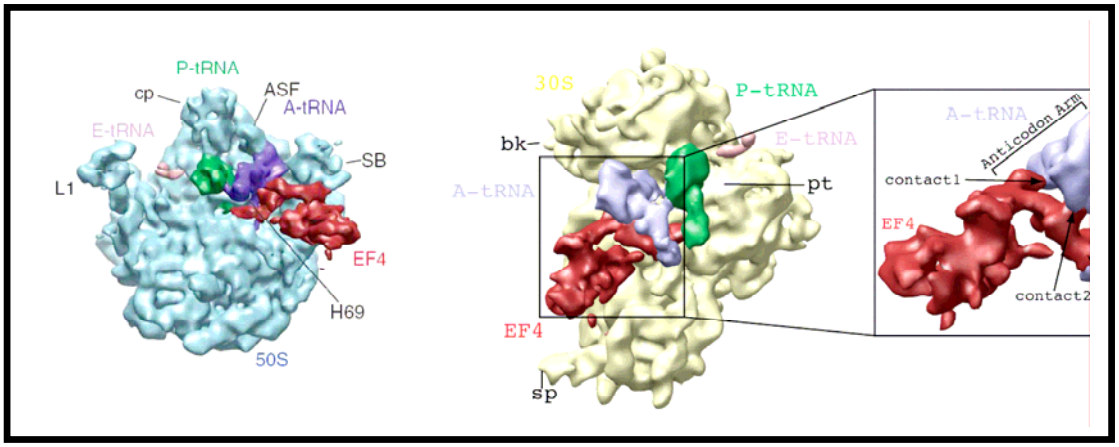

Figure 1.10 EF4 in complex with the ribosome: Left, 50S view; middle, 30S view; right, an overview of EF4 contact sites with tRNA (Connell, Topf et al. 2008; Evans).

(1) EF4 is contacting the D stem in the A/L-tRNA with the tip of V' domain (2 and 3) Contacts two and three are mediated via CTD of EF4, contact 3 interacts with the

acceptor arm of the tRNA at 3’ CCA end. One particular amino acid Arg539 has been shown to be almost 100% conserved in EF4 and might interact with RNA at contact 3 **(Figure 1.11/ contact 3)**.

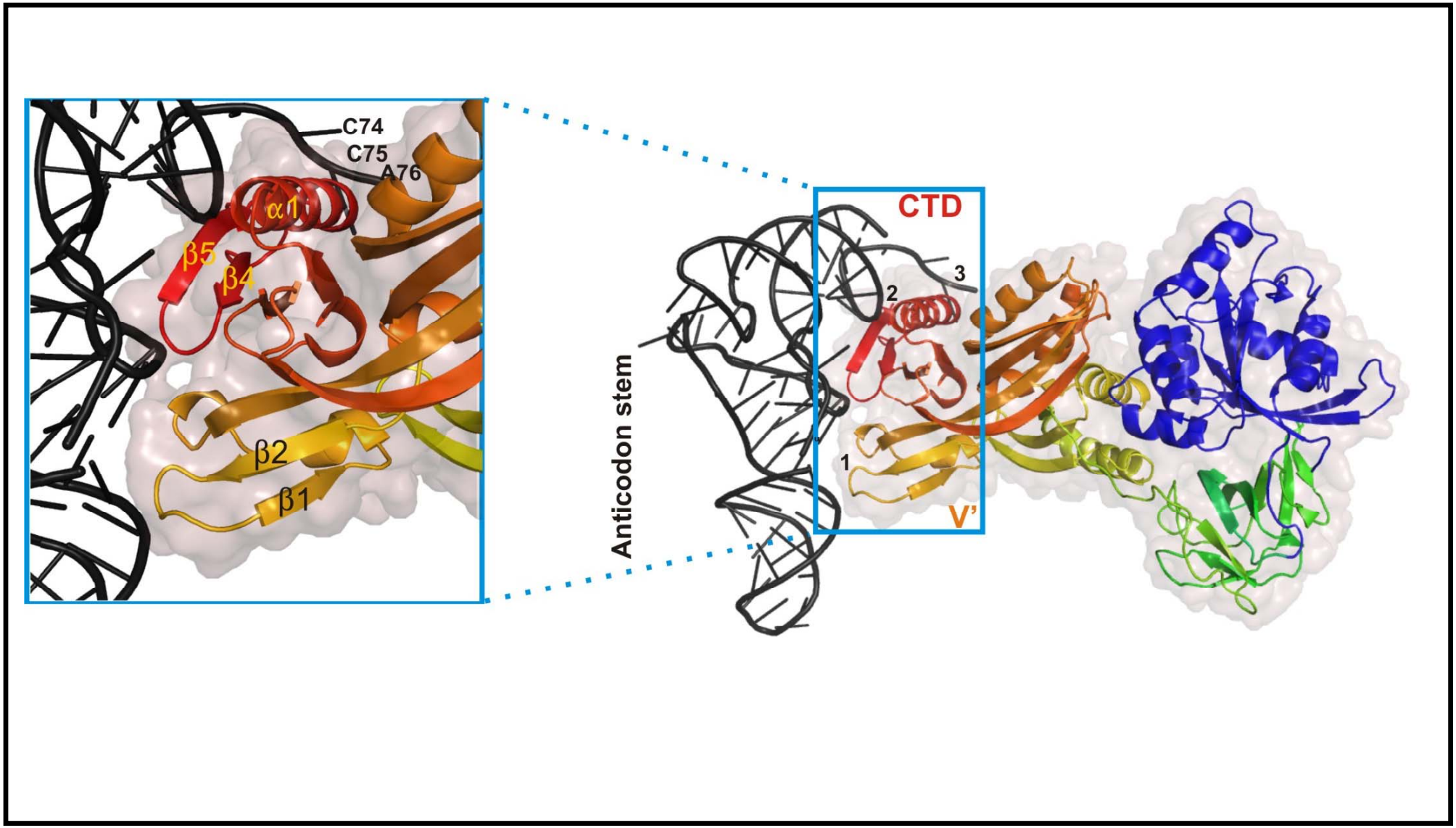

Figure 1.11 EF4 in contact with A site tRNA. The surface of EF4 is shown in light pink and the secondary structure is colour coded as in the previous figures; 3DEG. All three contact sites are numbered, and the enlarged view of the tRNA and EF4 contact sites shows details.

1.5.4 EF4 homologue GUF1

The translational apparatus of mitochondria resembles the one in bacteria, it consists of two RNAs and ~80 proteins; the rRNAs correspond to the bacterial 23S and 16S; almost half of the proteins appear to be homologues to the bacterial proteins. The elongation process in mitochondria is driven by EF-Tu_{mt} (EF-Tu homologue) and mEF1 and mEF2 (EF-G homologues), however, the translation system in mitochondria is poorly understood.

Guf1 and EF4 appear to have about 48% of amino acid identity over the complete sequence, although they had the last common ancestor about 1.5 billion years ago. This indicates a conserved function in bacteria and mitochondria.

Guf1 of yeast has been shown to be needed under suboptimal growth conditions such as non-fermentable carbon source (glycerol) and at low temperature. Moreover, an earlier in vivo experiment has confirmed the binding of Guf1 to the ribosome (Bauerschmitt, Funes et al. 2008).

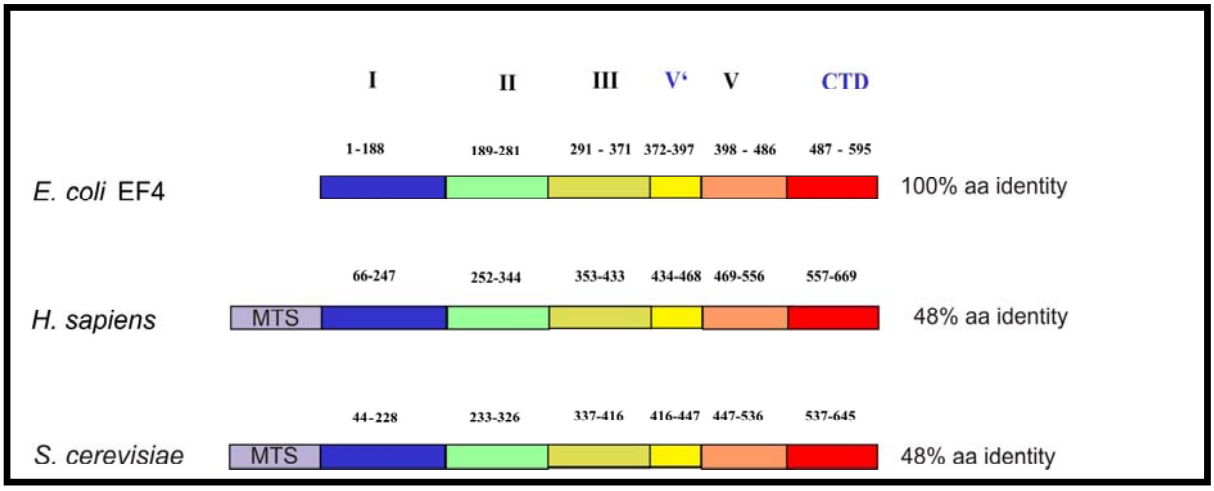

Figure 1.8 Alignment of E. coli EF4 with the mitochondrial homologues Guf1 in H. sapiens and that of S. cerevisiae. The MTS stands for the specific mitochondrial targeting sequence; aa identity is the amino acid identity to E. coli EF4 in percentage.

EF4 has been shown to be the first factor that back translocates the ribosome, and it has been speculated that its function might be prevention of errors. We are addressing this question in this thesis.

2 Materials

2.1 Materials

2.1.1 Sets of biological components

Qiagen:

Ni-NTA Spin Kit (50), (31314)

Ni-NTA Agarose (100 ml), (30 230)

Plasmid Maxi Kit (121163)

Plasmid Midi Kit (100), (12145)

QIAprep® Spin Miniprep Kit (250), (27106)

QIAquick® Gel Extraction Kit (50), (28706)

Roche:

Rapid Translation System 100, RTS 100 *E. coli* HY Kit (3 186 156)

Rapid Translation System 500, RTS 500 *E. coli* HY Kit (3 246 949)

2.1.2 Chemicals and simple biological components

Amersham:

[γ^{32}P]-Adenosine-5'-triphosphate (PB 10218)

Bovine Serum Albumine (BSA, RNase/DNase Free), (27-8914-02)

Hybond *N*-plus membrane (RPN 203N)

Poly(U), (27-444002)

Beckman:

Ready Value (Liquid Scintillation Cocktail), (PN 586602)

Ultracentrifuge tubes (Ultra-Clear) SW40 and SW28, (344060, 344058)

Biorad:

2x Laemmli Sample Buffer (161-0737)

2x Native Sample Buffer (161-0738)

Sodium-dodecyl-sulfate (SDS), (161-0301)

Calbiochem:

HEPES, Free Acid, ULTROL® Grade (391338)

Difco:

Bacto™ Agar (214010)

Bacto™ Peptone (211677)

Bacto™ Yeast Extract (212750)

Invitrogen:

Agarose Electrophoresis Grade (15510-019)

Sucrose (15503-022)

TEMED (15524-010)

Fermentas:

2x Loading Dye Solution for RNA electrophoresis (#R 0641)

6x Loading Dye Solution (#R 0611)

GeneRuler™ 1kb DNA Ladder (#SM 0311)

RNA Ladder, Low Range (#SM 0411)

T4 DNA Ligase, (#EL 0015)

Fluka:

Spermidine trihydrochloride (85578)

Spermine tetrahydrochloride (85605)

Merck:

2-Mercaptoethanol (8.05740.0250)

2-Propanol (1.09634.2500)

Acetic acid glacial 100% (1.00063.2500)

Ammonium acetate (1.01116.1000)

Ammonium chloride (1.01145.1000)

Ammonium peroxodisulfate (APS), (1.01201.1000)

Boric acid (1.00165.1000)

Chloroform (1.02445.1000)
Diethyl ether (1.00926.500)
Ethanol (1.00986.2500)
Ethidium bromide (1%), (1.11608.0030)
Formamide (1.09684.1000)
Glycerol 100% (1.05819.1000)
Glycine (1.04201.1000)
Hydrochloric acid 32% (1.00319.2500)
Magnesium acetate (1.04936.1000)
Magnesium chloride hexahydrate (1.05833.1000)
Methanol (1.06002.2500)
Potassium acetate (1.04820.1000)
Potassium chloride (1.04936.1000)
Potassium hydroxide solution 1 mol/L (1.09108.1000)
Sodium acetate trihydrate (1.06265.1000)
Sodium carbonate monohydrate (1.06386.1000)
Sodium chloride (1.06404.1000)
Sodium citrate (1.06448)
Sodium hydroxide (1.06498.1000)
Sodium hydroxide solution 1 mol/L (1.09137.1000)
Triplex III GR (EDTA), (1.08418.1000)
Tris(hydroxymethyl) aminomethane (1.08382.1000)
tri-Sodium citrate dihydrate (1.06448.1000)
Urea (1.08487.1000)

Millipore:
Filters 0.45 µm (HAW02500)

New England BioLabs:
Restriction endonucleases with buffers
T4 DNA Ligase (M0202S)

Promega: Steady-Glo® Luciferase Assay System

Roche Pharmaceuticals:

1,4-Dithiothreitol (DTT) (1 583 786)

DNase I, RNase-free (10 776 785 001)

dNTPs: dATP, dCTP, dGTP, dUTP (1 051 440, 1 051 458, 1 051 466, 1 420 470)

Roth:

1,4-Dithioerythritol (DTE), (8814.1)

IPTG 25g (2316.4)

Phenol (0040.2)

Roti-Mark STANDARD 1ml (T851.1)

Trichloroacetic acid (TCA), (8789.1)

Sodium-dodecyl-sulfate (SDS), (4360.2)

Sartorius:

Nitrocellulose filter (11306)

Schleicher and Schüll:

Glass Fiber Filters Æ23 mm (10 370 021)

Serva:

Aluminiumoxid Alcoa A-305 (12293)

Coomassie® Brilliant Blue G-250 (17524)

Coomassie® Brilliant Blue R-250 (17525)

Sigma:

3-(N-morpholino)propanesulfonic acid (MOPS), (M-1254)

Albumin, bovine (A-7906)

Dextran sulfate (D-6001)

Ficol 400 (F-4375)

Formaldehyde (F-8775)

Lysozyme (L-6876)

Polyvinylpolypyrolidone (P-6755)

ReadyMix™ Taq PCR Reaction Mix with $MgCl_2$ (P-4600)

Spectrum, Los Angeles (U.S.A)

Spectrapor dialysis membrane (MW 3500)

Non-typical laboratory machines

Wallac 1409 Liquid Scintillation Counter

RTS ProteoMaster Roche

PhosphorImager STORM 820 (Molecular Dynamics, Amersham Biosciences) and PhosphorImager cassette BAS 2325 (Fujifilm)

Luminometer Centro LB 960 (Berthold technologies, Germany)

Beckmann Coulter DU®640B Spectrophotometer

Sorvall RC 5B plus centrifufe

Beckmann L7-55 ultracentrifuge

Beckmann Coulter Optima™L-90K ultracentrifuge

New Brunswick Scientific GmbH Innova 4400 incubator shaker

Antibiotics

Ampicillin in H_2O (Roth, K029.2)

Kanamycin A (KAN) in H_2O (Roth, T832.3)

Micrococcin (MIO) in 100% ETOH

Neomycin (NEO) in H_2O (Fluka, 72133)

Paramomycin (PAR) in H_2O

Puromycin in 2% 1N KOH, pH 7.4 (Serva, 33835)

Streptomycin (STR) in H_2O (Fluka, 85880)

Thiostrepton (THIO) in 100% DMSO (Sigma, T8902-1G)

Viomycin (VIO) in H_2O

tRNA and homopolymeric mRNs

Poly(U), (27-4440-02

tRNAs, Chemical Block

tRNA bulk from E. coli MRE 600 (RNAse minus), (109550) Bohringer Mannheim

Radioactive compaunds

[γ 32P]-Adenosine-5'-triphosphate (Amerasham-Bioscience #PB 10218

[γ 32P]-Guanosine-5'-triphosphate (Amerasham-Bioscience #FP 402

L-[U-^{14}C]-Phenylalanin (Amerasham-Bioscience #TRK583

L[U-^{3}H- Leucine (Amerasham- Bioscinece) #TRK170

Software

Image Qunat 5.2

PyMol v1.1

CorelDRAW X3

Pico Log Recorder (Software for Pico ADC-16 module)

2.1.3 Buffers and solutions

2.1.3.1 Buffers for electrophoresis solutions

Agarose gel	10X TBE	10 ml
	Agarose	1-2%
	Ethidium Bromide 1%	5 µl
	MQ- H_2O	Add 100 ml
10X TBE	Tris	89 mM
	Boric Acid	89 mM
	EDTA	2 mM
1X TBE	10X TBE	100 ml
	MQ- H_2O	ad 1000 ml
10X TAE	Tris	48.4 g
	Glacial acetic acid	11.4 ml
	EDTA	3.7 g
	MQ- H_2O	ad 1000 ml
1X TAE	10X TAE	100 ml
	MQ- H_2O	ad 1000 ml
APS solution 10%	Ammonium peroxodisulfate	10% (w/v)
Polyacrylamide gel 10% (separating gel)	1.5 M Tris solution, pH 8.8	5 ml
	Rotiphorese®Gel 30 (37, 5:1)	6.8 ml
	APS solution 10%	
	TEMED	100 µl
	MQ- H_2O	10 µl
		add 20 ml
Polyacrylamide gel 5% for protein electrophoresis (stacking gel)	0.5 M Tris solution, pH 6.8	2.5 ml
	Rotiphoreses® Gel 30 (37, 5:1)	1.3 ml
	APS solution 10%	100 µl
	TEMED	10 µl
	MQ- H_2O	Ad 10 ml

SDS-PAGE separation buffer pH 8.8	Tris	90.86 g
	SDS	1 g
	MQ- H_2O	Add 250 ml
SDS-PAGE stacking buffer pH 6.8	Tris	6.1 g
	SDS	0.4
	MQ- H_2O	Add 100 ml
Coomasie staining solution	Coomassie blue R-250	0.25 % w/v
	Methanol	50% v/v
	Glacial Acetic acid	10% v/v
Coomassie gels destaining solutions	Methanol	50% v/v
	Glacial acetic acid	10% v/v
	Bromophenol blue	0.05% w/v
	Xylencyanol	0.05% w/v

2.1.3.2 Buffers for microbiological purposes

Luria-Bertani (LB) medium	Bacto™ Peptone	1% (w/v)
	Bacto™ Yeast Extract	0.5% (w/v)
	Sodium chloride (NaCl)	1% (w/v)
Luria-Bertani (LB) solid medium	Bacto™ Peptone	1% (w/v)
	Bacto™ Yeast Extract	0.5% (w/v)
	Sodium chloride (NaCl)	1% (w/v)
	Bacto™ Agar	1.5% (w/v)
Luria-Bertani (LB) medium For competent cell preparation	Bacto™ Peptone	1% (w/v)
	Bacto™ Yeast Extract	0.5% (w/v)
	Sodium chloride (NaCl)	0.5% (w/v)

2.1.3.3 M9 medium with various pHs

M9 medium with various pHs according to the Sørensen buffer (Geigy, 1960, buffer 19) and http://www.aeisner.de/rezepte/puffer2.html

Reagents	**pH 5**	**pH 5.6**	**pH 6**	**pH 6.6**	**pH 7**	**pH 7.6**	**pH 8**
1x 1/3 M KH_2PO_4	98.8 ml	94.8 ml	87.7 ml	62.7 ml	39.2 ml	13.2 ml	5.5 ml
1x1/3 M Na_2HPO_4	1.2 ml	5.2 ml	12.3 ml	37.3 ml	60.8 ml	86.8 ml	94.5 ml
NaCl	0.1 g	0.1 g	0.1 g	0.1 g	0.1 g	0.1 g	0.1 g
NH_4Cl	0.1 g	0.1 g	0.1 g	0.1 g	0.1 g	0.1 g	0.1 g
$MgSO_4$- 1 M	100 µl	100 µl	100 µl	100 µl	100 µl	100 µl	100 µl
$CaCl_2$- 1M	10 µl	10 µl	10 µl	10 µl	10 µl	10 µl	10 µl
Glucose (40%)	1ml f. c. 0.4%						
Thiamine (1 g/ ml)	100 µg per ml						
Total Volume	100 ml						

2.1.3.4 Buffers for EF4 distribution between membrane and cytosol

Standard buffer for EF4 distribution between cytosol and membrane	Hepes-KOH pH 7.5 $MgCl_2$ NH_4^+ Spermine Spermidine	20 mM 6 mM 150 mM 0.2 mM 2 mM
Lysis buffer for distribution assay	Hepes-KOH pH 7.8 NaCl Sucrose EDTA Lysozym	20 mM 100 mM 0,5 M 2 mM 200 µg/ ml

Urea- SDS buffer	0.5 M Tris pH 6.8 β-Merceaptoethanol Urea Bromophenolblue 40%	25 ml 500 µM 18.5 g 250.µl ad 50 ml
7x Protease inhibitor cocktail mini tablets	Protease inhibitor tablet MQ- H_2O	1 tablet ad 2 ml

2.1.3.5 Buffers for Western blotting

Transfer buffer	Tris base	25 mM
	Glycine	192 mM
	Methanol	20 %
		pH adjusted to 8.1 –8.4
5X PBS (Phosphate buffered saline)	Na_2HPO_4	57.5 g
	NaH_2PO_4	14.8 g
	NaCl	29.2 g
	MQ- H_2O	pH adjusted to 7.1
		ad 1000 ml
1X PBS-T (1x PBS and Tween 20)	5x PBS	50 ml
	Tween 20	100 µl
	MQ- H_2O	200 ml
Blocking buffer 5%	1x PBS-T	50 ml
	Milk powder (fat free)	2.5 g

2.1.3.6 Buffers for Watanabe assay

Binding buffer	Hepes-KOH, pH 7.5	20 mM
$H_{20}M_{4.5}K_{150}SH_4Spd_2Spm_{0.05}$	Mg-Acetate	4.5 mM
	K-Acetate	150 mM
	ß-Mercaptoethanol	4 mM
	Spermidine	2 mM
	Spermine	0.05 mM

HMK Buffer	Hepes-KOH, pH 7.5	20 mM
$H_{20}M_6K_{150}SH_4$	Mg-Acetate KCl	6 mM
	ß-Mercaptoethanol	150 mM
		4 mM
Mix I	Hepes-KOH, pH 7.5	60 mM
$H_{60}M_{10.5}K_{690}SH_{12}Spd_{10}Spm_{0.25}$	Mg-Acetate KAc	10.5 mM
	ß-Mercaptoethanol	690 mM
	Spermidine	12 mM
	Spermine	10 mM
		0.25 mM
Mix II	Hepes-KOH, pH 7.5	100 mM
$H_{100}M_{22.5}K_{750}SH_{20}Spd_{10}Spm_{0.25}$	Mg-Acetate	22.5 mM
(Watanabe Ion mix II for tRNA non-	K-Acetate	750 mM
enzymatic A site binding)	ß-Mercaptoethanol	20 mM
	Spermidine	10 mM
	Spermine	0.25 mM
Mix IIe	Hepes-KOH, pH 7.5	40 mM
$H_{40}M_{8.3}K_{300}SH_8Spd_5Spm_{0.125}$	Mg-Acetate	8.3 mM
(Watanabe ion mix II for	KAc-Acetate	300 mM
enzymatic A site binding)	ß-Mercaptoethanol	8 mM
	Spermidine	5 mM
	Spermine	0.125 mM
Mix III	Hepes-KOH, pH 7.5	66.7 mM
$H_{66.7}M_{12.6}K_{500}SH_{13.4}Spd_{9.96}Spm_{0.26}$	Mg-Acetate	12.6 mM
	K-Acetate	500 mM
	ß-Mercaptoethanol	13.4 mM
	Spermidine	9.96 mM
	Spermine	0.26 mM
Tico	Hepes-KOH, pH 7.5	20 mM
$H_{20}M_6K_{30}SH_4$	Mg-Acetate	6 mM
	K-Acetate	30 mM
	ß-Mercaptoethanol	4 mM

2.1.3.7 Buffers for poly(U) dependant poly(Phe) synthesis assay

Mix I	Hepes-KOH pH 7.5	100 mM
$H_{100}M_{21}K_{870}SH_{20}Spd_{12}Spm_{0.3}$	Mg-Acetate	21 mM
	K-Acetate	870 mM
	ß-Mercaptoethanol	20 mM
	Spermidine	12 mM
	Spermine	0.3 mM
Mix II/Charging Mix	Hepes-KOH pH 7.5	80 mM
$H_{80}M_{15}K_{840}SH_{16}Spd_{12}Spm_{0.3}$	Mg-Acetate	15 mM
	K-Acetate	840 mM
	ß-Mercaptoethanol	16 mM
	Spermidine	12 mM
	Spermine	0.3 mM
Mix E	ATP	45 mM
$ATP_{45}GTP_{22.5}(AcPO_4)_{75}$	GTP	22.5 mM
	Acetyl phosphate	75 mM
	KOH	360 mM

2.1.3.8 Buffers for polysomes

10x polysome lysis buffer	Hepes-KOH pH 7.5	200 mM
	Mg-Acetate	45 mM
	NH_4Ac	1500 mM
	ß-Mercaptoethanol	60 mM
	Spermidine	20 mM
	Lysozyme	4 mg/ml

10x binding buffer	Hepes-KOH pH 7.5	200 mM
	Mg-Acetate	45 mM
	K-Acetate	1,500 mM
	ß-Mercaptoethanol	40 mM
	Spermidine	20 mM
	Spermine	0.5 mM
1x Binding buffer($H_{20}M_{4.5}K_{150}SH_4Spd_2Spm_{0.05}$)	Hepes-KOH, pH 7.5	20 mM
	Mg-Acetate	4.5 mM
	K-Acetate	150 mM
	ß-Mercaptoethanol	4 mM
	Spermidine	2 mM
	Spermine	0.05 mM
30% Sucrose in binding buffer	Sucrose	30 g
	binding buffer	ad 100 ml
10% Sucrose in binding buffer	Sucrose	10 g
	binding buffer	ad 100 ml

2.1.3.9 Buffers for EF4 purification

Buffer A (Ni-NTA) pH 8.0	Na_2HPO_4	46.6 mM
	NaH_2PO4	3.4 mM
	NaCl	300 mM
Buffer B_1 (MonoS) pH 7.6	Hepes- KOH	20 mM
Buffer B_2 (MonoS) pH 7.6	Hepes-KOH	20 mM
	K-Acetate	1 M

Buffer A (Ni-NTA) pH 8.0	Na_2HPO_4	46.6 mM
	NaH_2PO4	3.4 mM
	NaCl	300 mM
Buffer B_1 (MonoS) pH 7.6	Hepes- KOH	20 mM
Buffer B_2 (MonoS)	Hepes-KOH	20 mM
pH 7.6	K-Acetate	1 M
Buffer C (storage buffer)	Hepes-KOH pH 7.6	20 mM
	K- Acetate	500 mM
	BME	4 mM
	Glycerol	10%
EF4 AB buffer	Hepes-KOH pH 7.6	20 mM
(Adjustment buffer)	Mg-Acetate	6 mM
	ß-Mercaptoethanol	30 mM
	Spermidine	2.7 mM
	Spermine	0.07 mM

2.1.3.10. Analytical methods

The concentration of 70S ribosomes, 30S and 50S ribosomal subunits was determined measuring the absorption at 260 nm.

70S 1 A_{260} unit = 24 pmol

50S 1 A_{260} unit = 36 pmol

30S 1 A_{260} unit = 72 pmol

Conversion factors for the quantification of DNA and RNA

1 base pair in double stranded DNA	660 g/mol
1 A_{260} unit of double stranded DNA	50 µg
1 A_{260} unit single stranded DNA or RNA (more than 100 bases)	40 µg

1 A_{260} unit of single stranded DNA (less than 25 bases)	20 µg
1 A_{260} unit of single stranded DNA (30-100 bases)	30 µg
A_{260}/A_{280} ratio for pure DNA	1.8
A_{260}/A_{280} ratio for pure RNA	2.0
1 triplet (codon) of RNA	~1000 g/mol

2.1.3.11 Radioactivity

Radioactivity calculations

The purchased radioactive ligand, is supplied with information about the specific activity as Curies/ mol (µCi/ µmol) since our measurement are done per minute (dpm). It is more useful to convert the Ci/ mol to dpm.

1 µCi = 2.22 x 10^6 dpm

$$\frac{\mu Ci}{\mu mol} = 2.22x10^6 \frac{dpm}{\mu mol} = 2.22 \frac{dpm}{pmol}$$

Radioactive decay

Radioactivity decay follows an exponential decay, and each radioactive isotope has a different half-live.

2.1.3.12 *E. coli* strains

XL-1 Blue: recA1 endA1 gyrA96 thi-1 hsdR17 supE44 relA1 lac [F' proAB $lacI^qZ\Delta M15$ Tn10 (Tet^r)]

BL21(DE3): F^- dcm ompT hsdS(r_{B-} m_{B-}) gal λ(DE3)

CAN20-12E: derived from *E. coli* K12, which is deficient in RNases BN, II, D (Deutscher, Marlor et al. 1984)

K12: *F´proA$^+$B$^+$ lacI^q Δ(lacZ)M15 zzf::Tn*10(Tet^R)*/ fhuA2 glnV Δ(lac-proAB) thi-1 Δ(hsdS-mcrB)5.*

MG1655: The *E. coli* strain MG1655 was sequenced by Blattner laboratory, it has minimal genetic manipulation, F- lambda- ilvG- rfb-50 rph-1 (Blattner FR 1997).

BW25113: BW25113 strain was used to make the Keio Collection of single-gene knockouts (Baba, Ara et al. 2006).The genotype for this strain is Δ*(araD-araB)567*, Δ*lacZ4787*(::rrnB-3), lambda⁻, *rph-1*, Δ*(rhaD-rhaB)568*, *hsdR514* (Baba, Ara et al. 2006),

JW2553: This strain is carrying a kanamycin resistance gene instead of *lepA* gene. The deletion of *lepA* gene is done according to Keio collection; one step single gene knockout method which is illustrated in (**Figure 2.1**).

MDEF4: MDEF4 (mutant defective in EF4) is a *lepA* gene deletion strain of BW25113 strain. The already deleted *lepA* gene replaced by kanamycin gene from BW2553 is reintroduced into a single colony purified BW25113 strain with P1kc transduction.

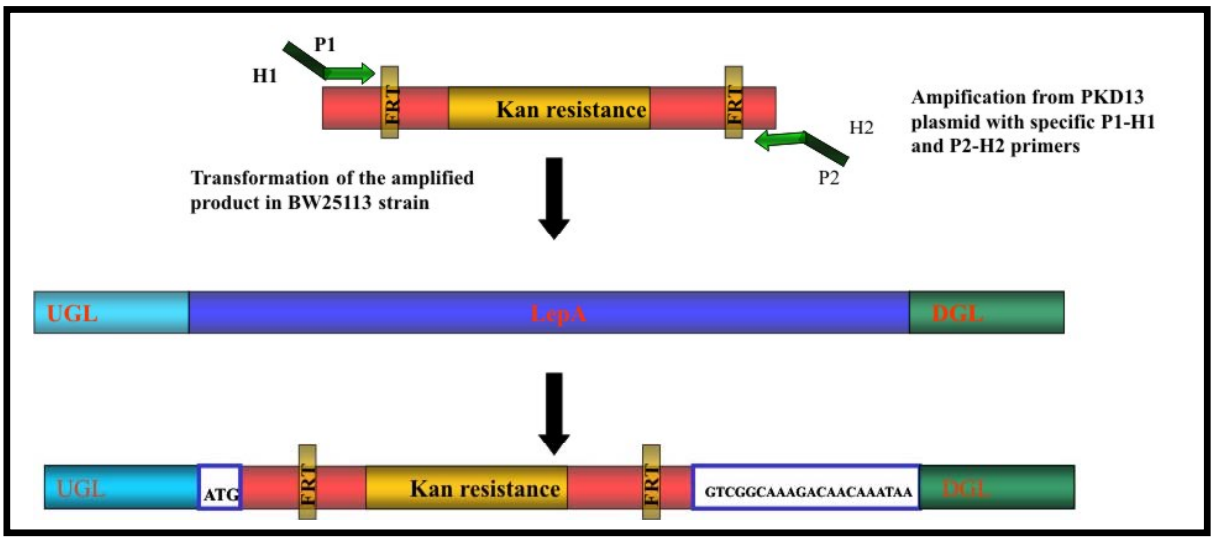

Figure 2.1: One-step lepA gene knockout made by Keio collection. Primer designed P1-H1 has 20-nt 3' ends for priming upstream (P1) downstream (P2) of the FRT(Flippase recognition target for the enzyme Flippase that recombinate the FRT sites and remove the gene between the FRTs) sites flanking the kanamycin resistance gene in pKD13. H1 includes a sequence part from the upstream gene and the lepA initiation codon. H2 includes codons of the six final C-terminal residues, the stop codon, and 29-nt downstream. Then the construct is checked by PCR using K1 and K2, D1 and D2 primers followed by PCR from primers that are located in the neighboring genes followed be DNA sequencing This construct can be altered by further modifications, e.g. by removing the kanamycin gene. For convenience, the

Keio collection retains the resistance marker. UGL (upstream gene), DGL (downstream gene).

2.1.3.13 Plasmids

pET-28a (+): The pET- 28a is developed for the cloning and expression of recombinant proteins in *E. coli*. Target genes are cloned in pET plasmids under control of a strong T7 promoter. The pET-28a vectors carry an N-terminal His-Tag®/thrombin/T7-Tag® configuration plus an optional C-terminal His-Tag sequence.

pET-28a –EF4 The *lepA* gene was cloned via NdeI and EcoRI in pET- 28a, has N-terminal His-tag.

PZS*24-MCS-1: Plasmid pZS24-MCS1 contains the low-copy modified pSC101 ori, which is derived from another plasmid pMPP6. It caries a kanamycin resistant gene and has a promoter (Plac/ara-1), which is regulatable over an ~1800-fold (Lutz and Bujard 1997) range and when fully induced with arabinose and IPTG, it exceeds the *in vivo* strength of Plac 6-fold.hus it is a strong and highly regulatable promoter, The fine-tuning of Plac/ara-1 is facilitated by a two step mechanism: increasing the IPTG concentration in the medium up to 0.2 mM leads to an ~100-fold induction, which can be enhanced 15–20-fold by adding arabinose to a final concentration of 0.03% (Manen, Xia et al. 1994; Lutz and Bujard 1997).

PZS*EF4 l*epA* gene cloned in the low copy plasmid PZS*24-MCS-1 with restriction sites KpnI and MluI.

PZS*HsmEF4 Homosapiens mitochondrial lepA (HsmEF4) homologue gene *Guf1* is cloned into PZS*24-MCS-1 with restriction sites KpnI and ClaI

pQE70: An expression vector, originally from Qiagen, with C-terminal His- tag and T5 promoter / lac operator.

2. 2 Methods

2.2.1 Microbiology and molecular genetics methods

2.2.1.1 Transformation of cells with high-voltage method (electroporation)

Electroporation is one of the most efficient methods for transformation of bacterial cells with plasmids. The permeability of the cell plasma membrane is cause by an externally applied electrical field. The settings for cell transformation were: current - 1.5 kV (for 0.5 mm cuvette), electrical capacity - 40 μF, resistance - 412 Ω mode - one pulse.40 μl competent cells were thawed on ice and transformed with current plasmid 5 ng then incubated on ice for 1-2 min. Electroporated by electroporation chamber by applying the current described above. A succeeded electroporation with our current setting must be between 3-5 ms. The newly electroporated cells are mixed with 1 ml cold LB medium and incubated at 37 °C for 1 hour in 2 ml Eppendorf tube. Finally, the cells were plated out on LB plates with proper antibiotic as a selection marker and incubated overnight at 37 °C for 14-16 hours.

2.2.1.2 Restriction digestion of DNA

Restriction enzymes are naturally occurring endonucleases that recognize a specific palindromic sequence (4-12 bp) and cut the double strand phosphate backbone of DNA within or near the recognition sequence. Producing different DNA restriction ends; sticky ends with either 3' or 5' tail and blunt- ends. Restriction enzymes are widely used to manipulate DNA for different scientific applications. They are used to assist insertion of genes into plasmids in gene cloning. Usually plasmids are designed to contain a short polylinker sequence called multi cloning site, which is rich in restriction enzyme sites. Normally both the plasmid and the gene are digested with the same restriction enzymes. The activity of endonuclases is defined as unit; which is amount of enzyme needed to digest 1 μg bacteriophage lambda DNA to completion in an hour.

A restriction enzyme reaction contains: 1) 1-10 μg of DNA product e.g. PCR product. 2) A buffer that is suitable with the used restriction enzyme 3) Restriction enzyme in required concentration. The reaction is incubated for 1-2 hours at 37 °C.

2.2.1.3 Ligase reaction: DNA ligation into a plasmid (vector)

The mechanism of DNA ligase is to form two for covalent phosphodiester bond between 3' hydroxyl ends of one nucleotide with the 5' phosphate end of another nucleotide in the presence of ATP this is done by the enzyme T4 DNA ligase This reaction allows incorporation of genes in a vector or in the chromosomal DNA.

The DNA fragment and the vector that are digested by specific restriction enzymes are then purified from agarose gel with gel extraction kit or with phenol extraction and ethanol precipitation method.

The ligase reactions were done according to manufacture's guide (Fermentas). The ratio between plasmid and insert are used in 1:1 and 1:4 in a total volume of 20 µl. To the reaction was usually taken 60-100 ng of DNA and sufficient amount of insert. The reaction is incubated at 16°C for 16 hours. Finally the ligated product is dialyzed with Nitrocellulose- filter against MQ- water for 20 min and then transformed into competent cells.

Two equations which allow convert weight mass of DNA to its molar mass and vice versa are listed below

a) to convert pmol to µg:

$$pmol \cdot N \cdot \frac{660\,pg}{pmol} \cdot \frac{1\mu g}{10^6\,pg} = \mu g$$

b) to convert µg to pmol:

$$\mu g \cdot \frac{10^6\,pg}{1\mu g} \cdot \frac{pmol}{660\,pg} \cdot \frac{1}{N} = pmol$$

Where N is the number of nucleotide pairs and 660 pg/pmol is the average MW of a nucleotide pair.

2.2.1.4 Extraction and ethanol precipitation of DNA

2-3 volumes of 100% ethanol is added in the DNA sample, followed by addition of 1/10 volume 3 M sodium acetate, pH 5.2 mixed and kept in –20 °C overnight or –80 °C for 1 hour. Spin at full speed in a standard microcentrifuge for 30 min. Carefully decant the supernatant and wash the DNA pellet with 70% ethanol, spun at full speed for 30 minutes. The DNA is air dried and dissolved in H_2O

2.2.1.5 Elution of DNA or RNA from agarose gels

DNA was eluted from agarose gel with either Invitek gel extraction kit or Qiagen QIAquick Extraction kit and the procedures were followed as described in the companies' manuals.

2.2.2 Cloning strategy

1. Primer design with appropriate melting temperature (Tm)
2. PCR amplification of the wanted gene to be cloned from K12 genome or another vector. PCR product purification with Invitek PCR purification kit
3 Plasmid preparation with Quiagen Miniprep kit which gives a yield of 50-450 ng/µl
4 Digestion of the target plasmid and the PCR product, followed by gel extraction.
5. Estimation of amount of purified plasmid and insert
6. Ligation either 30 min at room temperature or overnight at 4°C
7. Transformation into appropriate strain.

2.2.2.1 Genes of both bacterial EF4 and human mitochondrial EF4 homologue inserted into pZS*24-MCS-1 plasmid

E. coli lepA gene was amplified with PCR from pET28a_*lepA* DNA using specific primers that emerged restriction sites for KpnI and ClaI. The human mito EF4 was cloned from cDNA of following tissues esophagus, sk. Muscle, brain. The restriction sites KpnI and MluI were chosen for cloning into pZS*24-MCS-1.

2.2.2.2. Inserting the EF-G gene into pET-28a

fusA gene, which encodes for the EF-G protein was originally cloned into pQE70 that have a C-terminal His-tag. From this plasmid the *fusA* gene was amplified and cloned into pET-28a, where we allowed an N terminus His-tag and this clone was used for toxicity experiments.

2.2.3 Propagation of P1kc lysates

A 1/100 portion of an overnight culture of cells containing the appropriate antibiotic (Kan) was transferred to a fresh LB medium containing 5 mM $CaCl_2$ and grown at 37

^{o}C until the OD_{600} was ~0.6. The P1kc lysate was mixed with 0.5 ml of the culture and the phage was allowed to adsorb for 20 min with gentle shaking. The mixture was spread on LC plates together with 3 ml of pre-warmed top agar and incubated at 37 ^{o}C overnight for lysis to occur. The top agar was scraped the following day using a sterile spatula into a test tube containing about 50 µl chloroform; the plate was washed with 1 ml of LB medium and the medium combined to the top agar in the tube. The contents were mixed by vortexing followed by centrifugation at 3,000 rpm for 10 min. The supernatant was collected in to a new tube containing 50 µl chloroform, mixed and refrigerated. Transduction was done by our colleague Dr. Madoka Kitakawa in Kobe in the following way. An overnight culture of the recipient was diluted 50-fold with fresh LB medium and shaken at 37 ^{o}C until the OD_{600} reached ~0.7. Cells were collected by centrifugation and re-suspended in 1/10 volume of tryptone solution (1% Bacto-tryptone). One volume of cells was mixed with equal volume of 2x ADS buffer and two volumes of P1 lysate propagated in donor strain and appropriately diluted with 1x ADS buffer (usually 1:20 dilution). 1x ADS buffer contains 5 mM $CaCl_2$ and 10 mM $MgSO_4$. After 20 minutes incubation at 37 ºC, four volumes of 1 M sodium citrate solution was added to inhibit re-adsorption of P1 phage to transductants. Aliquots (0.1~0.2 ml/plate) were spread directly on LB plate containing the antibiotic used for selection (40 µg/ml Kan). Plates were incubated at 37 ºC overnight and the resulting transductants were streaked to obtain single colonies (**Figure 2.1)**.

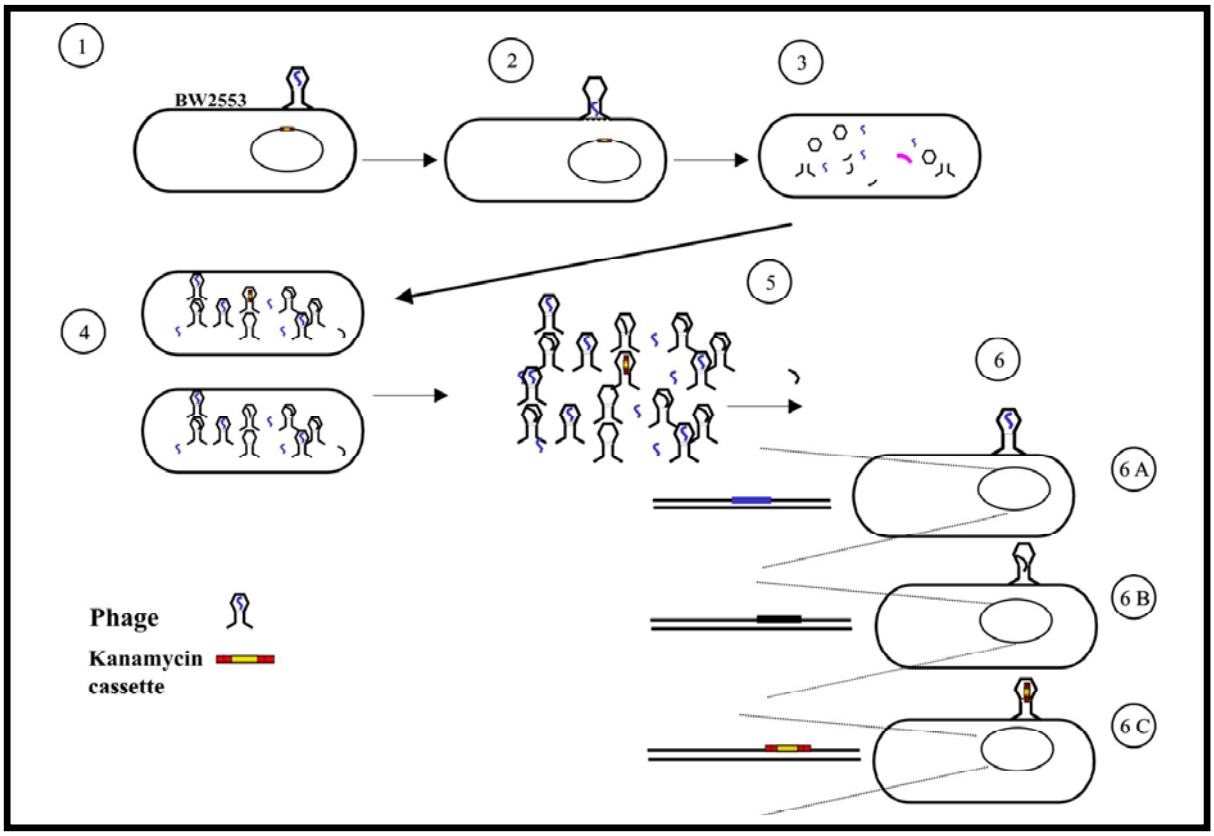

Figure 2.1: Scheme of P1 transduction of EF4 gene. 1) Phage attaches the host and 2) injects its DNA into the host. 3) Phage uses the host enzymes and replicates phage DNA, expresses phage protein and chops the host genome. 4) Phage packs the DNAs including the host DNA, 5) lyses the cells and 6) infects new host cells.
6A, Phage contains its own DNA (most likely case). 6B, phage contains part of the host gene. 6C, phage contains the kanamycin resistant cassette after homologous recombination with the corresponding chromosomal gene making the cell Kan resistant.

2.2.4.1 Agarose gel electrophoresis of DNA and RNA

The principle of this method is; the pool of DNA/RNA with different sizes are migrating according to their length shorter fragments are migrating faster through the gel and the molecules are visualized with ethidium bromide which is an intercalating agent when exposed to UV light it fluoresce orange colored light.

It is a technique used for both analytical and preparative purpose for plasmid DNA, bacterial genome, restriction analysis, PCR, and cloning. For RNA this method is used for qualitative purposes of rRNAs from 70S ribosome, 50S, 30S ribosomal subunits. Standard agarose gel electrophoresis of DNA, 0.8-2% concentrations were used depending on the length of the DNA or if it is RNA to be run. The proper amount

of agarose was dissolved in TAE by boiling it in a microwave for about 2-3 minutes, then ethidium bromide is added to a final concentration of 0.04%. When the solution reaches 50- 60 °C it is poured in the electrophoresis chamber where the correct size of comb are put in order to generate the wells, wait until the gel becomes solid. Since RNA has an ability to form secondary structures a denaturing agent has to be added in the agarose gel as formaldehyde to a final concentration of 2 %. And the RNA samples are mixed with 2X loading RNA buffer containing formaldehyde. The samples DNA/RNA are then run about 1 hour at 60 V (20 mA) in 1X TAE buffer. In addition 1kb DNA marker/ or RNA marker with known molecular weight were loaded in order to estimate the correct size of the samples.

2.2.4.2 Plasmid purification with Qiagen kits

The Qiagen company provides different plasmid purification kits mini, midi, maxi and giga Based on amount of required plasmids the kit is chosen. The principle of the plasmid purification of Qiagen is alkaline lysis method where the DNA in the lysated cell is caught with either silica gel columns mini prep or anionic exchange columns for midi and maxi prep. The columns are washed extensively in order to get rid of unbound DNA or RNA fragments. The elution step is carried out with H_2O for mini prep and with high salt buffer in midi prep, in the latter prep requires precipitation since the eluted sample is in a bigger volume. The use of Rnase in our DNA lysis buffer form Qiagen is omitted due to high risk of contamination of our lab equipments,which might lead to unfunctional RNA compounds such as ribosomes. Beside the mentioned changes the Qiagen protocols are exactly followed in this thesis.

2.2.5 PCR

2.2.5.1 PCR (Polymerase Chain Reaction) *in vitro* amplification of DNA fragments

PCR is one of the most used techniques in molecular biology; DNA fragments are amplified many times in an exponential manner. Two oligonucleotides are usually used as primers that have different sequences and are complementary to the template on both 3’ and 5’ sides.

First the DNA template is denatured at 95 °C in the reaction mix including primers and dNTPs, then the temperature is lowered so the oligos anneal to the DNA template. In the reaction mix Taq DNA polymerase is included, which amplifies the DNA template. This is repeated in cycles many times. The (Table 2.2) shows ReadyMix™ Taq PCR reaction mix with $MgCl_2$, which is frequently used for e.g. colony PCR.

2.2.5.2. Colony PCR

Colony PCR is a rapid way of screening correct plasmid construct or for confirmation of a gene knockout directly from bacterial colonies.

Here colony PCR is performed in order to confirm the lack of the lepA gene. For that purpose cells were streaked out on plates and incubated for ~16 h at 37 °C then colonies with a tip are inoculated and dabbed in to the PCR buffer (ReadyMix™ Taq PCR reaction mix with $MgCl_2$). The PCR reaction consisted of the reagents listed in (Table 2.2) and the primers were ordered from AGOWA (Appendix II). The PCR reaction was performed according to the PCR program seen in (Table 2.3), with proper annealing temperature. Finally the amplified products are analysed in 1% agarose gel at 70 V for ~ 1 hour.

Table 2.2 ReadyMix™ Taq PCR reaction mix with $MgCl_2$

Reagents	Volume total (10 µl)	Final Concentration
2X ReadyMix Taq PCR Reagent Mix	5 µl	1x ReadyMix Taq PCR Reagent Mix
Forward primer	1 µl	0.1-1 µM (15-30 bases in length)
Reverse Primer	1 µl	0.1-1 µM (15-30 bases in length)
Water	3 µl	

Table 2.3 The PCR cycle parameter

Cycling parameter	Temperature	Time
. Pre-Denaturation	94°C	5 min
Denaturation	94°C	30 sec
Primer Annealing	x°C	30 sec
Polymerase reactio Extension	72 °C	3 min
Amplification 30 cycles, go to Denaturtion step		
Final extension	72 °C	10 min
Cooling	4 °C	~15 min

2.3. Growth Curves

E. coli growth is an increase of cells exponentially in an asexual reproduction process called binary fission or cell division. Bacterial growth can be divided into 4 phases per cycle:

1. Lag phase cells. Immediately after inoculation of bacterial cells into fresh medium, no growth is noted, here cells are increasing in mass and volume (**Figure 2.2 A**)
2. Exponential (log) phase cells, this is the period of cell doubling at constant rate, if the growth is not inhibited by e.g. stress factors (**Figure 2.2 B).**

3. Stationary phase cells. Usually reached in closed systems, the growth is then limited by depletion of nutrients, accumulation of waste products, lack of space. The cells starts to stop growing and dividing (**Figure 2.2 C**).
4. Death phase cells. Continues incubation of cells after stationary leads to cell death so the viable cells are dying in an exponential manner as the log phase.

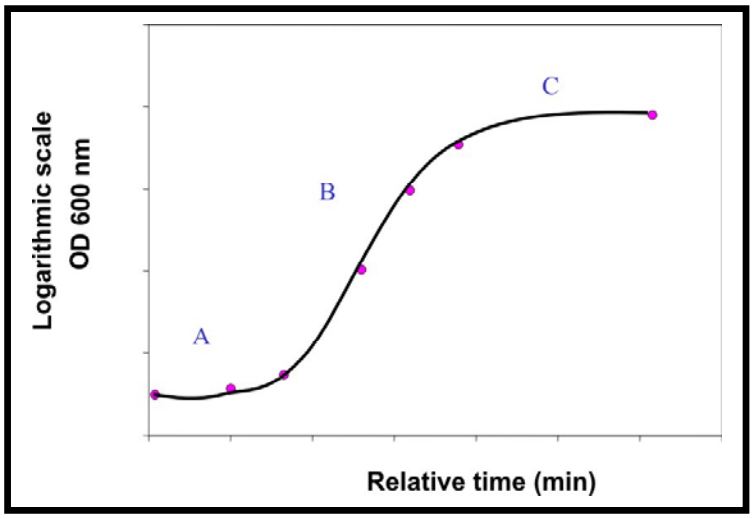

Figure 2.2. Growth curve pattern of bacteria. Growth graphs are usually plotted in logarithmic scale since bacteria increases in amount exponentially. The life cycle of bacteria can be divided in three phases: A) lag- phase, B) log- phase, and C) stationary- phase.

2.3.1 Growth curve procedure

Single colonies were inoculated in 5 ml LB medium and grown overnight, which was then diluted 1:100 in fresh M9 medium with various pHs at 3 °C or lower temperature and, where indicated, in the presence of high concentrations of various salts **(Table 2.4).** The cultures were grown in a shaker incubator with 180 rpm. The growth curves are obtained from OD_{580} measurement at a constant time rate, until reaching stationary phase; then the cultures are diluted 1:10 and growth measurement continued as described before.

Table 2.4. Stress condition parameters

Stress conditions
pH 7 100 mM $MgCl_2$
pH 7 200 mM KCl
pH 6
pH 6 100 mM $MgCl_2$
pH 6 200 mM $MgCl_2$
42°C
35°C
25°C
16°C

2.3.2 Growth curves done with ELISA reader for EF4 toxicity determination

The plasmids PZS*24-MCS-1-lepA, PZS*24-MCS-1-Guf1 and the empty plasmid PZS*24-MCS-1 were transformed to DH5α strain. Plated on LB supplemented with 50 µg/ ml kanamycin and the plates were incubated overnight. The main culture was made by dilution of the overnight culture 1:100 in 96 wells ELISA plate containing fresh LB medium. After that the cultures density reached ~0.2, were induced with 5 mM IPTG and 0.05 % arabinose. After one generation, sample was withdrawn for SDS page gel analysis to detect amount of expressed EF4. The cells were diluted 1:10 and grown in fresh LB medium plus 5 mM IPTG and 0.05 % arabinose and grown to OD_{600} ~1. Also cells were withdrawn before 1:10 dilution. For each condition triple determinations were performed with 2 times repetitions.

2.3.3 Growth competition

Growth competition is an sensitive assay that shows the ability of a mutant to grow in competition with a wild type over the whole range of growth cycle from stationary phase to lag phase and log phase back to stationary phase. This assay is usually used when the individual growth rates of wild type and a mutant is indistinguishable (Gutgsell, Deutscher et al. 2005).

After confirmation of the EF4 gene deletion by colony PCR, where half of the colony is taken for PCR and the other half for making an overnight culture in 5 ml fresh LB medium. Main culture was started by mixing wildtype and mutant in equal amount to a final OD_{600} of 0.01 in a total volume of 5 ml, and then the mixed culture was incubated at 37 °C with shaking. Samples were withdrawn every 4 hours interval up to 24 hours then 1:100 dilution of the cells was done every 24 hours up to 72 hours. For every withdrawn sample, OD_{600} was measured and serial dilution was performed at 10^{-3}, 10^{-6}, 10^{-7} . From each diluted sample 250 µl was plated in duplicates both on LB plates and LB with 50 µg/ ml kanamycin and incubated for 12-16 hours. The numbers of colonies were counted on both plates and percentage of mutant was estimated **(Figure 2.3)**. A graph is made with calculation of total generations based on the equation below and the estimated percentage of mutant cells is plotted as a function of number of generations.

$$\frac{\ln OD_{600} - \ln 0.01}{\ln 2}$$

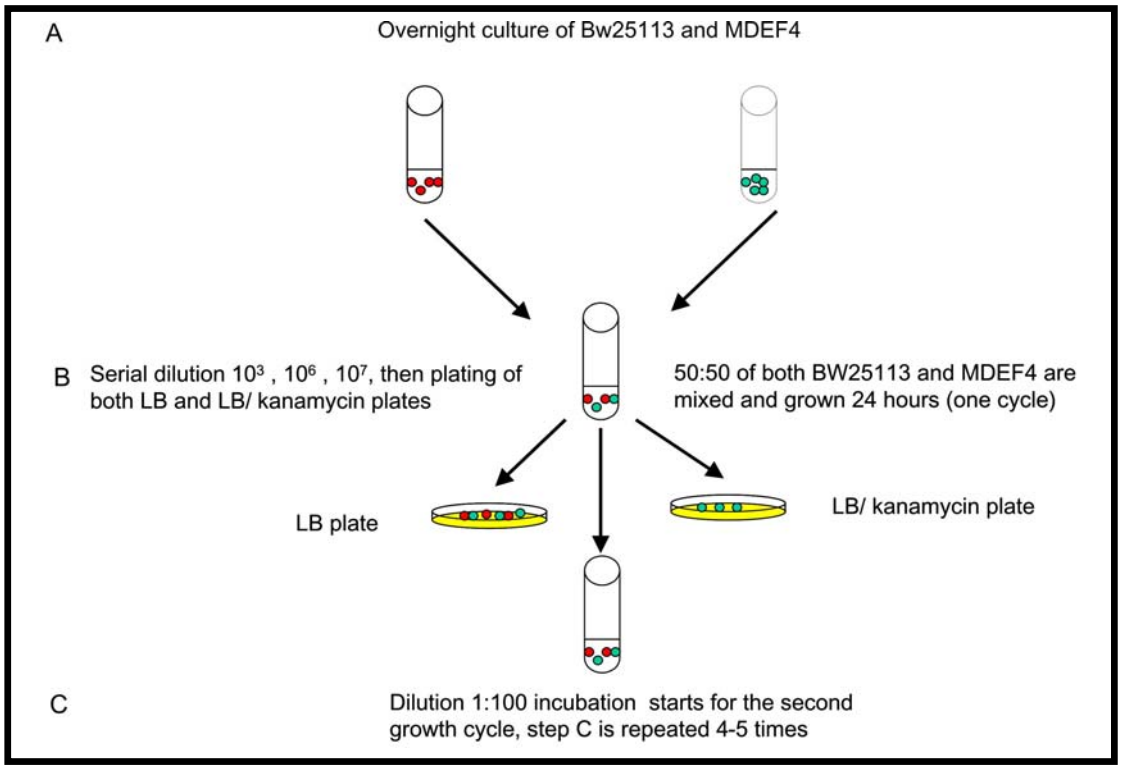

Figure 2.3 Schematic presentation of growth competition.

2.4 Electron Microscope (EM) analysis of *E. coli* strains BW25113, JW2553, MDEF4

Electron microscope is a tool for visualization and enlargement of an object. The electron microscope higher resolution and magnification is due to the electron wavelength that is much smaller than a light photon electromagnetic radiation.

2.4.1. Sample preparation for EM

The current method that was used to prepare the *E. coli* samples for EM is according to (Steven, Trus et al. 1988). First a thin carbon layer was prepared, then the wanted size of the carbon sheet is cut off and placed on a buffer solution 0.2 % Am (ammonium molybdate) and let it to float for a few seconds then the carbon is pressed into a piece of parafilm. The specimen (bacterial cells) are pressed between the parafilm and the carbon so the carbon is floating and incubated for 60 s during this time the cells are adsorbed to the underside of the carbon film. The carbon film is then lifted and placed on a copper grid, the negatively stained cells were visualized with the electron microscope. With the current software of the EM we could measure the size of each *E. coli* cells. The cells width and length were measured and an average value was calculated for each pictured cell.

2.5 Cell growth and fractionation of cytosol and membranes for Western blotting

Wild type strain BW25113 and the mutant MDEF4 were grown overnight in 5 ml LB medium at pH 7. The overnight culture was then diluted 1:100 in 100 ml LB medium at different stress conditions shown in the (Table 2.4) to an OD_{600} of ~0.6 then the culture was aliquotized to 10 ml/ aliquot and pelleted at (3,000xg for 15 min) then flash frozen and stored in –80 freezer. For the cytosol and membrane fractionation one aliquot of cells was thawed and resuspended in 400 µl standard buffer, a fraction of 100 µl is separated and is used as total cell extract. The remaining cell solution is pelleted at (3,000xg for 15 min) and carefully the supernatant is removed with a pipette, then the cells were diluted in 250 µl lysis buffer incubated on ice for 5 min and 2.5 µl Mg^{2+} is added to a final concentration of 10 mM. Directly subjected for freezing at –20°C and subsequent thawing on ice for 3 cycles. After the cells completely lysated, then were centrifuged (51,000xg for 60 min), and the supernatant was removed carefully and kept on ice, while the pellet, which consisted of the total membrane fraction, was dissolved in 250 µl of Urea-SDS buffer. In the supernatant fraction, which is the cytosol fraction, SDS loading dye was added in a 1:1 ratio and the total cell extract fraction is dissolved in Urea-SDS buffer. All the samples are denatured for 5 min at 95 °C, briefly vortexed and spun shortly. Equal volumes are loaded on 12.5% SDS- PAGE gel, run with 1x SDS-PAGE running **(Figure 2.4)** shows a schematic view of cytosol and membrane separation.

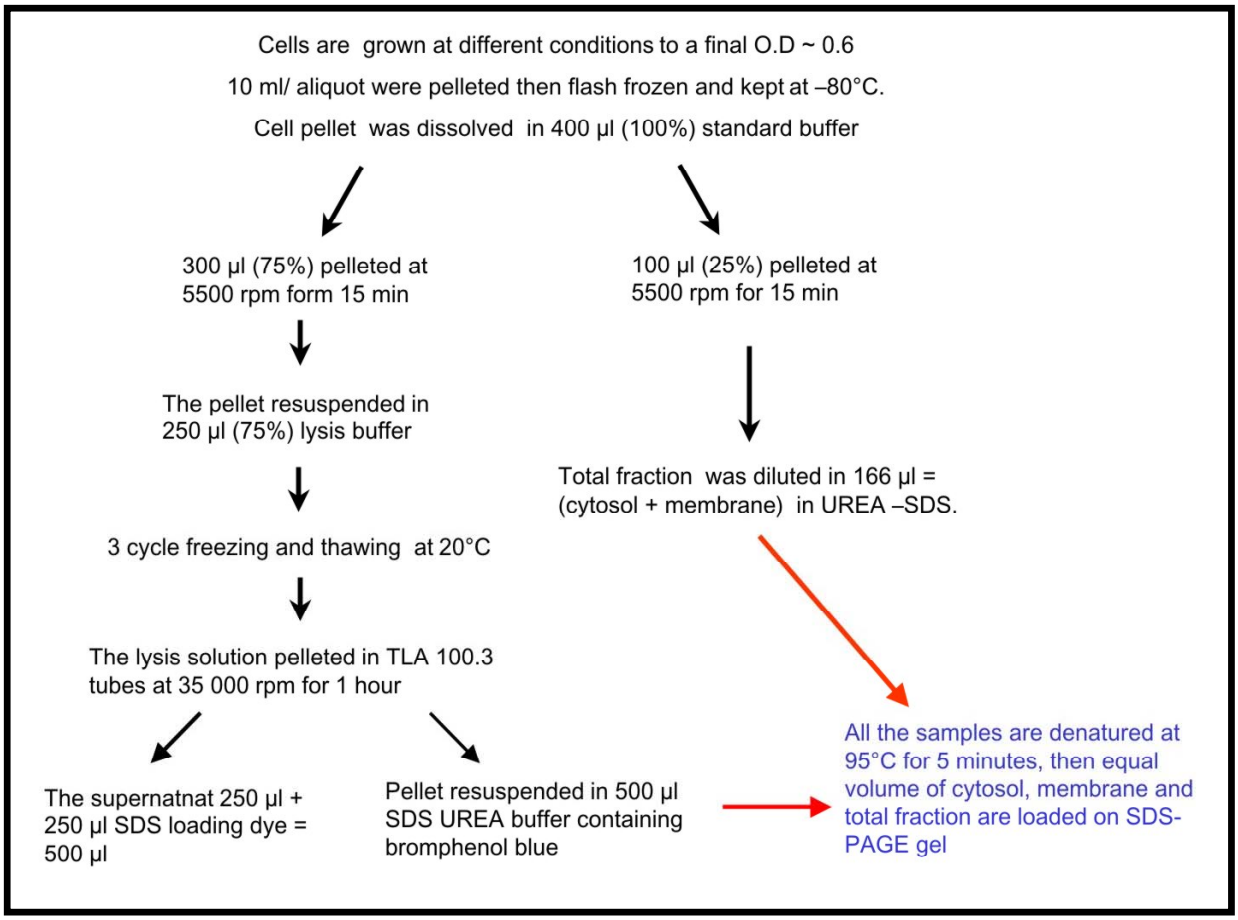

Figure 2.4. Scheme describing separation of cytosol and membrane.

2.6 Western blotting procedure

Western blotting or immunoblotting is an analytical method that involves the immobilization of proteins on membranes, which enable us to determine with primary antibody the relative amount of protein present in different samples. Samples and controls, prestained markers are loaded on 10-12% PAA SDS gel and run at 70 V for 10 min until the samples passes the upper gel, then the voltage is increased to 120 – 130 V for 1-2 h depending on the separation efficiency of the gel, which can be monitored by the prestained marker.

2.6.1 PVDF membrane preparation

The membrane is soaked in methanol for a few seconds and diluted the methanol by incubating it in MQ water for 5 min and stored in transfer buffer until use.

2.6.2 Protein transfer from gel to membrane

The procedure was done according to (**Figure 2.5**), the protein transfer apparatus obtained from Bio-Rad. The cassette has 2 color codes black for katode and white for anode, the so called sandwich assembly starts with placing the pads on the black side and 2 pieces of Wattman paper on top of it followed by placing the SDS gel and smooth out with a glass cylinder ruler to remove bubbles. The membrane is then placed on top of the gel in a precise way that covers the whole gel and the membrane should be kept unmovable since the protein transfer starts right away. 2 additional Wattman papers are placed on top of the membrane followed by one pad then the cassette is clamped together and run in transfer buffer at 200 V, 4 °C for 60 min.

2.6.3 Blocking

An important step in order to prevent interaction of the membrane with the antibody this is done in PBS-T 5% non- fat milk for half an hour or overnight. Followed by rinsing with PBS-T buffer.

2.6.4 Primary antibody hybridisation.

The primary antibody e.g. anti EF4 was diluted 1:10,000 in PBS-T containing 5% milk, then incubated at room temperature for 90 min with mild shaking.

2.6.5 Secondary antibody hybridisation

The membrane is washed 3X with 50 ml PBS-T to remove unbound antibody then the secondary antibody HRP-conjugated goat anti rabbit was diluted 1:15,000 in PBS-T with 5% milk and added to the membrane incubated at room temperature for 90 min with mild shaking. The next step of washing is more important since appropriate washing with PBS-T decreases the background, the washing is increased to 5X 50 ml 7 min each wash.

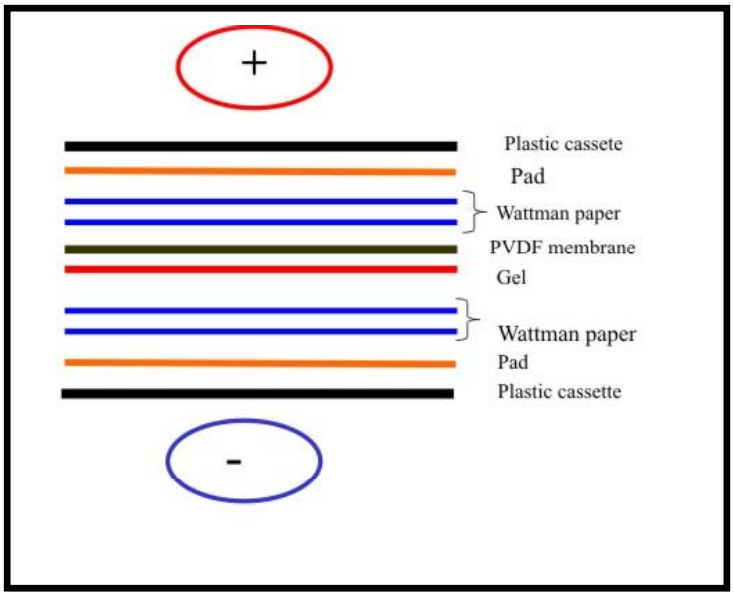

Figure 2.5. A cartoon representation of Western blotting, assembly system for protein transfer from the gel to the membrane.

2.6.6 Detection methods

Chemoluminiscence substrate ECL kit was kept at 4 °C in order to prevent oxidation of the chemicals. Before usage one aliquot of ECL solution was kept at room temperature while the blot was prepared for detection, this is done by removing access of buffer with angling the blot try and tipping out the buffer. The ECL reagent is prepared with 1:1 dilution then ca 300 µl ECL mix is applied on the blot and incubated for 5 min then the access of the reagent is drained and the blot is kept in small plastic bag, this was subjected for detection with either classical way of detection with x ray film and development or with LAS 1000. The Fujifilm *LAS-1000* is a high sensitivity imaging system for chemoluminiscence and fluorescence. This way of development is simpler, more sensitive and directly saved on the computer as image, which is easier to quantify each band without a high background.

Table 2.5 Summary of all primary and secondary antibodies that are used in the experiments

Primary Antibody	Dilution factor
EF4 polyclonal from rabbit	1:10,000
EFP polyclonal from rabbit	1:10,000
S8 polyclonal from sheep	1:5,000
L2 polyclonal from sheep	1:5,000
S7 polyclonal from sheep	1:3,000
L22 polyclonal from sheep	1:2,500

Secondary Antibody	Dilution factor
Goat anti rabbit	1:15,000
Rabbit anti sheep	1:10,000

2.6.7 ImageQuant 5.2 software used for quantification of Western blotting

ImageQuant software is an analytical program, which enables us to quantify the immunoblotting results by determining the width and the length of the selected object in the image. Moreover the background can be corrected and this is completed by pixel calculation.

2.6.8 EF4 concentration estimation *in vivo* procedure

EF4 amount was estimated and also the ratio to the ribosomal protein in the total cell extract under optimal condition. BW25113 cells were grown overnight and then diluted 1:100 culture grown until OD ~0.6. The pelleted cells were resuspended in 1.5 ml SDS loading dye followed by protein denaturation at 95°C for 5 min. Samples from the total cell extract were loaded in different volumes 5 µl and 10 µl, where 5 pmol 70S ribosome and 0.5 pmol purified EF4 was used as controls. The software Image-Quant was utilized to estimate EF4 concentration *in vivo* and in relativity to ribosome.

2.7 Polysome preparation

2.7.1 Polysome preparation for Western blotting

A preculture of BW25113 in 5 ml LB medium was made from one single colony. Then the preculture was diluted in 100 ml LB to reach an OD_{600} up to 0.05 and let grow to

OD_{600} ~0.5. Then the main culture was set in 200 ml LB pH 7, pH 6 100 mM $MgCl_2$ and then grown at 37°C or at 16°C to a final OD_{600} of 0.4-0.5. Half of the culture was quickly mixed with the same amount of ice in a prechilled tube then speed cooling of the culture in dry ice/ acetone mixture followed by direct centrifugation at 5,000 rpm for 5 min in GSA 250 ml tubes. The supernatant was afterwards decanted and the last bit of left LB medium is removed with pipette. All the steps are done at 0°C. The pellet is resuspended in 400 µl polysome lysis buffer. The suspension is then transferred to a 2 ml Eppendorf tube and 5 µl DNase (RNase free; 10 U/ µl) was added, shock froze in liquid nitrogen and stored at –80°C minimum overnight. The second half of the culture is divided in 250 ml and centrifuged down at 5,000 rpm for 15 min then shock frozen and kept in –80°C freezer. These samples are used as internal control for distribution of EF4 between the membrane and cytosol fraction. After thawing the lysate is centrifuged 5 min at 10,000 rpm (4 °C, Eppendorf table top centrifuge), the A_{260} is monitored and 1 A_{260} is taken for analytical polysome profiling. This is performed in an SW60 rotor with a sucrose gradient (10% - 30% (w/v) in binding buffer) then run for 2 h at 38,000 rpm.

2.7.2 TCA precipitation of polysomes for Western blotting

A large batch polysome profiling is performed in order to have enough material for Western blotting. 10 A_{260} / growth condition is overlaid on the top of sucrose density gradient 10% to 30% in Ultra-Clear tubes (14 x 95 mm Beckman) and run in SW40 for 18,000 rpm for 18 hours. Then the samples are obtained from fractionation of sucrose gradient, and it is done via fraction collector, which enables us to collect constant volume of samples of definite size. The polysomes were pooled as one sample, while keeping 70S fractions and 50S, 30S fractions separately. To the fractions 1x BB (1:1 v/v) is added, TCA was then added to a final concentration of 10% and incubated on ice for 1 hour, then centrifuged at 14,000 rpm for 45 min at 4°C. The supernatant is decanted very slowly and the pellet is washed with 1.5 volume acetone and centrifuged again at 14,000 rpm. Carefully the supernatant is decanted and the pellet is dried at 37 °C incubator or at room temperature. The pellet, which appears white due to the TCA and acetone, were suspended in SDS loading dye, which had pH ~9 in order to neutralize the pH of the pellet since the TCA is acidic and this disturb the migration of the protein. The samples are then

denatured at 95 °C for 5 min, mixed and spun shortly, then loaded on the SDS-PAGE gel for further analysis by Western blotting.

2.8 Analytical sucrose gradient centrifugation

Sucrose gradient centrifugation is a technique that allows the separation of complexes based on the sedimentation coefficient (S). This technique can be used to separate polysomes, 70S, 50S and 30S ribosomal subunits.

A sucrose gradient (10-30% (w/v) in binding buffer) was prepared in an Ultra-Clear or polyallomer tubes (14 x 95 mm Beckman). The reaction mix (10 A_{260}) was overlaid on the gradient and centrifugation was performed in SW 40 rotors (Beckmann). In the SW 40 up to 10 A_{260} of polysomes, pure ribosomes or ribosomal subunits per tube can be loaded. The centrifugation was performed at 18,000 rpm for 18 h, 4 °C. After centrifugation the gradient was fractionated while monitoring the absorbance at 260 nm.

2.9 EF4 protein purification procedure

The *lepA* gene was cloned via NdeI and EcoRI in pET- 28a and transformed into *E. coli* BL21 (DE3) strain then plated on LB + Kan (50 µg/ ml). One single colony was inoculated into 200 ml LB + KAN (50 µg/ ml) incubated at 37 °C with 170 rpm overnight. The Main culture was prepared by inoculating 8 l of LB medium + KAN (50 µg/ ml) with 1:100 dilution of the preculture then the culture was incubated until it reached OD_{600} 0.4 and induced with 1 mM IPTG, followed by additional incubation for 2 hours. The cells are then harvested by centrifugation at 6,000 rpm for 10 min at 4 °C and resuspended in buffer A. The cells were then disrupted with 3 passages through the microfluidizer to lysate the cells. Subsequently the cell lysate was centrifuged at 35,000 rpm for 1 hour at 4 °C to separate the supernatant from the cell debris and prepared for NiNTA-agarose. 4.5 ml of the NiNTA was used in polypropylene columns, and the column was equilibrated with buffer A by washing with 2 X column volume (CV). The supernatant was applied on the column and washed with 6x CV buffer A+ 10 mM imidazole. The protein is then eluted with using buffer A with different imidazole concentrations (100 mM, 200 mM, 300 mM). The fractions where the protein is eluted is pooled and then subjected to FPLC where further purified with cationic exchange chromatography. The samples are diluted 2:3 with buffer B1 **(see section 2.1.2.9)**, this gives a final concentration of 200 mM K^+. The protein is then eluted via a linear gradient from 200 mM K^+ to 1000 mM K^+. The

pooled fractions are concentrated to up to 3 mg/ml finally the buffer is exchanged by using a desalting columns to a final storage buffer C, shock freeze the protein in small aliquots and store at –80 °C.

2.10 Poly(U) dependent poly(Phe) synthesis

Poly(U) dependent poly(Phe) synthesis is a cell free system that was developed for the first time by (Barondes and Nirenberg 1962) and later improved by (Traub and Nomura 1969). The poly(Phe) chain is synthesized in a binding buffer condition ($H_{20}M_{4.5}K_{150}SH_4Spd_2Sp_{0.05}$), in a total volume of 15 µl. The compounds are written in the table below **(Table 2.5).** The reaction mixture is then incubated at 37 °C for 1 hour then cooled on ice. The reaction is then precipitated with hot 5% TCA. The phenylalanine incorporation is then calculated as Phe per 70S ribosome.

This assay was used at different Mg^{2+} concentration by changing the H_2O module in the protocol. In all our Poly(U) dependent poly(Phe) synthesis, EF4 concentration was standardized to 2 times over the 70S ribosomes.

Organic compounds	**Energy**	**Ions, polyamines**
Phenylalanine, 450 µM [^{14}C]Phe, spec. act, 10 dpm/pmol tRNA^{Phe}, 2.5 µM S-100 enzymes, ca. 2 µl/15 µl 70S reassociated, 2 to 4 pmol ribosomes per 15 µl poly(U), 2 µg	ATP, 3 mM GTP, 1.5 mM Ac-P, 5 15 µM	Mg-Acetate, 4.5 mM K-Acetate, 150 mM Spermidine, 2 mM Spermine, 0.05 mM

Table 2.5 a collection of all compounds that are used in the poly(U) dependent poly(Phe) synthesis

2.11 Misincorporation assay performed in poly(U) dependent poly (Phe) synthesis

The poly(U) dependent poly(Phe) synthesis is performed as described in section above. In addition incorporation of near-cognate tRNA leucine, 10 µM [^{3}H] Leu, specific activity, 3,000 dpm/ pmol) and 200 mM tRNA bulk was added to the assay and proceeded as normal poly(U) dependent poly(Phe) synthesis. The mis-incorporation was monitored by counting the radioactivity of both [^{14}C]Phe and [^{3}H]Leu and the number of Leu mis-incorporation was estimated.

2.12 Watanabe assay: site specific binding of tRNA to ribosomes, translocation and puromycin reaction

The functional states (Pi, PRE and POST states) of the ribosome in the elongation cycle were first studied with the novel method that was described by Watanabe (Watanabe, 1972). In our lab this methodology has been modified and optimised to a near *in vivo* condition buffer compounds. The Watanabe assay allows in detail monitoring the stepwise reactions that happens in the ribosome elongation cycle **(Figure 5.6)**. In the **first step** a 70S-mRNA-tRNA complex is formed, in which the tRNA is located in the ribosomal P-site. If N-acetylated- tRNA (e.g., N-Acetyl-Phe-tRNA^{Phe}) or N-formylated-Met-tRNA is used in the first step, an initiation complex is simulated (Pi-complex, I for initiation). In the **second step** the A site can be filled with the corresponding cognate tRNA either enzymatically (with EF-Tu) or non-enzymatically (without EF-Tu) forming a pretranslocational complexes (PRE complex). In the **third step**, PRE-complexes containing tRNAs in P and A sites are translocated to the E and P sites respectively (POST-complexes) upon addition of elongation factor G (EF-G) and GTP. The effectiveness of the translocation reaction and /or the binding state of the tRNAs is determined in a fourth step taking advantage of the antibiotic puromycin (analogue of the 3' aminoacylated end of a tRNA). This antibiotic reacts specifically with the P-site bound acyl-tRNA, if the ribosomal A site is free, forming an acyl-puromycin derivative (Allen and Zamecnik 1962). The puromycin reaction defines the location of a charged tRNA on the ribosome, i.e., if the P-site binds a peptidyl-tRNA, the puromycin reaction will be positive, whereas if the aminoacyl or peptidyl bound tRNA is present at the A site, the puromycin will not react (Traut and Monro 1964). In any case, after the addition of EF-G that does not affect the binding state, the puromycin reactivity of a P site bound aminoacyl- or

peptidyl-tRNA will be positive, while the A site bound species should show a translocation factor-dependent puromycin reaction. The final ionic condition used in

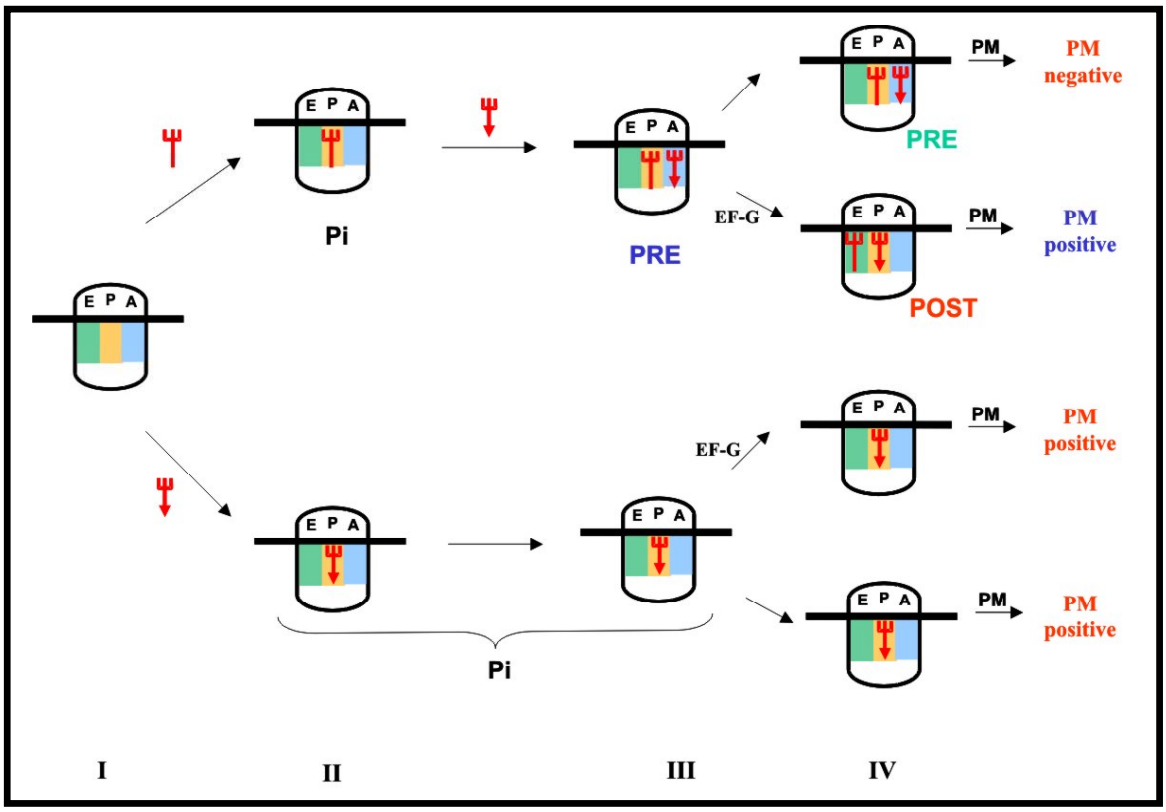

this experimental scheme were $H_{20}M_{4.5}K_{150}SH_4Sd_2Sp_{0.05}$ pH 7.5, the same as the poly(Phe) synthesis. A typical experiment was conducted as follows:

Figure 2.7. Watanabe assay. General picture of non-enzymatic A-site binding. (I) 70S programmed ribosome with mRNA. (II) P site is occupied by deacylated tRNA (upper row) or with acetylated tRNA (lower row) - Pi complex formation. (III) Pre-translocational complex formation after addition of acetylated tRNA (upper row). (IV) EF-G dependent translocation (the proper translocation can be only observed after A-site occupation: see upper row). (V) Puromycin reaction.

First step: P site binding or Pi complex formation

Pi complexes were prepared with 3-5 pmol of re-associated ribosomes in a volume of 12.5 µl incubated with: 25 µg of homo-polymeric mRNA (e.g., poly(U)) or 8-fold molar excess of a natural or hetero-polymeric mRNA over ribosomes and 1.5-2-fold excess of labeled N-Acetyl-Phe-$tRNA^{Phe}$ or N-formyl-Met-$tRNA^{fMet}$, respectively. The first step was incubated for 15 min at 37 °C. For P-site blockage with deacylated tRNA, programmed ribosomes were primed with 1.5-2-fold of deacylated-tRNA (sometimes

5' labeled with γ-[^{32}P] keeping constant the same size aliquots and the ionic binding conditions.

Second step: A site binding and/or PRE complex formation

Keeping constant the ionic conditions (binding buffer), the volume of reaction was increased to 25 µl per single determination. Non-enzymatic A site occupation was carried out (PRE complex formation) adding 0.8 to 1.5 molar excess of N-acetyl-

aminoacyl-tRNA ([^{3}H] or [^{14}C] labeled) to ribosomes, whose P site was pre-occupied with deacylated tRNA in the first step. The mix was incubated for 30 min at 37°C. The binding was measured with double determination by nitrocellulose filtration.

Third step: Translocation reaction

At this step, a GTP-mix (5 µl per aliquot) was added to Pi or PRE complexes maintaining constant the binding ionic conditions (H20M4.5K150SH4Sd2Spm0.05). Samples were split in 30 µl aliquots and 2.5 µl of EF-G was added to each (0.1-0.4-fold EF-G per ribosome). Control aliquots contained binding buffer instead of EF-G. After the addition of EF-G the aliquots were incubated for 10 min at 37°C.

Fourth step: puromycin reaction

Four aliquots from the binding assay containing EF-G and four without EF-G, were processed in the following way: 2.5 µl of puromycin stock solution in binding buffer (final concentration = 0.7 mM) were added to two aliquots from every group (± EF-G), while the other two received 2.5 µl of binding buffer. After these additions the samples were incubated at 37 °C for 5 min and the reaction was stopped adding 32.5 µl of 0.3 M sodium acetate, pH 5.5, saturated with $MgSO_4$. The amount acyl-puromycin formed was determined by extraction with 1 ml of ethyl acetate. After the addition of the organic solvent, the samples were strongly vortexed for 1 min, left 10 min on ice and centrifuged for 30 seconds at 15,000 x g in order to achieve complete phase separation. 800 µl of the organic phase was withdrawn and counted. The radioactivity extracted in the controls (minus puromycin) was subtracted from that plus puromycin in order to calculate the amount of acyl-puromycin formed. A successful puromycin reaction depends critically in the way in which the puromycin solution is prepared and handled. Two basic rules for the preparation of the puromycin stock solution with the maximal activity should be observed: The pH of the solution must be neutral. Since the puromycin is obtained commercially as

hydrochloride, the pH of the solution had to be neutralised adding 1 M KOH (1/100 of the reaction volume). The puromycin stock solution must be maintained at room temperature (otherwise it precipitates lowering the effective concentration). Under these conditions the stock solution retained its maximum activity for about one hour.

However, one can prepare a larger stock of puromycin solution that if aliquotized and flash-frozen in liquid nitrogen keeps its activity for months. Binding assays without ribosomes were included in all the experiments as standard controls in order to determine the background of radioactivity adsorbed to the filters. This background was normally low (below 10% of the binding signal) and directly proportional to the concentration of the radioactive component in the assay. Controls without mRNA plus ribosomes were also included when needed (e.g. the test a new heteropolymeric mRNAs).

2.13 tRNA binding assay modified Watanabe system, Puromycin reaction and poly(Phe) synthesis without S100 at 4.5 and 14 mM Mg-Acetate.

The tRNA binding at the P site and A site was monitored as described before in Watanabe assay, in addition, the binding affinity was determined at different Mg^{2+} concentrations in the presence and absence of 1:3 of 70S:EF4. The complex were subjected to poly(U) dependent poly(Phe) synthesis, where instead of S100, the purified factors as EF-Tu (45 pmol), EF-Ts (45 pmol) were added plus GTP (3 mM), the reaction was monitored in binding buffer with different Mg^{2+} concentrations.

2.14 GTPase assay

Is used to monitor the GTPase activity of EF-G and EF4 by using [γ ^{32}P] GTP and measuring [γ ^{32}Pi] release means monitoring the hydrolysis of GTP to GDP presence of the ribosome. The buffer condition were maintained in final binding buffer condition by 20% Mix I, 40% Tico, 40% H_2O. The assay contains 3-5 pmol ribosomes, which are diluted in Tico buffer and the [γ-^{32}P] GTP was diluted in a total volume of 160 µl that contains 2.5 mM cold GTP. The final concentration of [γ-^{32}P] GTP is 50 µM, which usually has (10- 40) dpm/ pmol. The factor module, where either EF-G or EF4

is added, is as well prepared in binding buffer. The reaction mixture performed on ice, after [γ-^{32}P] GTP addition, directly the reaction mixture is incubated at 37 °C for 5-10 min according to the requested incubation time, then the reaction is stopped by addition of the stop solution (120 µl 0.5 M H_2SO_4, 1.5 mM NaH_2PO_4), then addition of 30 µl 200 mM $MoNaO_4$. To this mixture, H_2O saturated 2-butanol is added and then vortexed for 1 min, followed by centrifugation for 10 min. The molybdate in complex with [γ ^{32}Pi] is then in the organic phase, which is subjected to counting of radioactivity dpm after addition of Liquid *Scintillation* Counter.

2.15 RTS 100 High Yield E. coli Kit

The Roche batch system was adjusted to 10 µl volume instead of 50µl suggested by Roche. According to the protocol, the contents of the kit were reconstituted with a supplied Reconstitution buffer. The reaction mixes were prepared according to the Table 2.6 and 8 µl were distributed to separate vials, DNA template was added after this. Standard incubation temperature was 30°C. Samples were introduced into ProteoMaster instrument and incubated for 6 h at 900rpm. Then the machine will automatically stop and deduce the temperature to 8°C for the maturation of the reporter protein GFP for 20 h. To quantify the translation fidelity (active fraction) from each 10 µl reaction, 1.5 µl was analysed on a 15% PAGE, under denaturing conditions with 2% SDS according to (Laemmli and Favre, 1973) or after a maturation period of about 16 h at 4°C under native conditions (Maniatis et al., 1982). On each gel, reference lanes were included with a known amount of pure and active GFP protein (Roche). The denaturing gels were run for 3 h at 150 V, which enabled good separation of the GFP protein band from neighbour bands of the S30. The SDS-PAGE gels were scanned and the GFP bands quantified and the total amount of GFP was determined by comparison with the reference GFP protein. The active GFP present in each sample was calculated by measuring the fluorescence 430–580 nm of the GFP proteins in the native PAGE. The reference GFP were arbitrarily assigned as 100% and the relative activity of the newly translated GFP protein was calculated.

In this thesis the activity of the GFP from the coupled in vitro system performed in order to determine the EF4 effect on GFP synthesis. The total RTS solution volume was increased to 15 µl by adding additional 5 µl of 1x BB or 1x BB plus EF4, EF4

was used in 3 times over the ribosome. The procedure was started by incubation of the sample in the RTS at 30 °C before and after 30 min samples were taken out then the antibiotic thiostrepton was added in the sample in order to inhibit translation in the system. Every 30 min up to 180 min, samples were taken out and flash frozen after thawing mixed with either native or SDS sample buffer and subjected to both Native and denature15% PAA gels.

Solution Reconstitution procedure

1. *E. coli* Lysate	Reconstitute the lyophilizate with 0.36 ml of Reconstitution Buffer, mix carefully by rolling or gentle shaking. DO NOT VORTEX!
2. Reaction Mix	Reconstitute with 0.30 ml of Reconstitution Buffer, mix by rolling or shaking.
3. Amino Acids	Reconstitute the lyophilizate with 0.36 ml of Reconstitution Buffer, mix by rolling or shaking.
4. Methionine	Reconstitute the lyophilizate with 0.33 ml of Reconstitution Buffer, mix by rolling or shaking.
5.Reconstitution Buffer	1.6 ml; Ready-to-use solution; stable at 2–8°C, can also be stored at − 15°C to − 25°C.
6. Control vector GFP	Briefly centrifuge down the content of the bottle and reconstitute the lyophilizate with 50 µl of sterile DNase- and RNase- free water The solution is stable at −15°C to −25°C.

Table 2.6 Preparation of working solutions (RTS 100 HY *E. coli* Kit)

Contents	**Preparation of working solution for one 50 µl reaction**
	Reaction Solution Into one of the supplied reaction tubes pipette the following components: 1. 12 µl *E. coli* Lysate 2. 10 µl Reaction Mix 3. 12 µl Amino Acids 4. 1 µl Methionine 5. 5 µl Reconstitution Buffer 6. 0.5 µg of circular DNA template or 0.1–0.5 µg of linear template in 10 µl of water or TE-buffer. Mix carefully by rolling or gentle shaking. DO NOT VORTEX!

3. Results

3.1 In vivo experiments

3.1.1 Phenotype determination of EF4 using BW25113 and JW2553 (ΔEF4) strains from Keio Collection

Previously Dibb and Wolf have concluded from knock-out experiments that *lepA* coding for EF4 is a non-essential gene and has no phenotype (Dibb and Wolfe 1986). In this chapter we analyse, whether EF4 is important under stress conditions. Acidic pH is one of the conditions we took into account, since the Kuster group in Amsterdam (Bijlsma, Lie et al. 2000) identified genes essential for *Helicobacter pylori* growth at acidic pH, *lepA* was one of 10 genes that were identified.

3.1.1.1 The first approach for EF4 phenotype determination

At first we tested the wild type (WT) strain BW25113 and the mutant (MT) strain JW2553 that were obtained from Keio collection. The mutant design is based on single gene deletion, where the *lepA* ORF is replaced with a kanamycin cassette, only the start codon and 29 nucleotides of the *lepA* gene remained (**Figure 2.1 Materials and Methods, page 46**) (Baba, Ara et al. 2006).

The JW2553 strain, where *lepA* gene is replaced with a kanamycin cassette, was verified with colony PCR and compared with the WT strain. The sizes of the amplified fragments were as expected ~ 2200 bp, which is larger than the WT fragment by 400 bp, and this is large enough to see the difference on gel electrophoresis (**Figure 3.1 B)**. Additional colony PCR was performed in order to confirm the lack of *lepA* gene with a so-called III primer; this is specific for *lepA* gene at position 1400 bp. Amplification with this primer and forward primer gives a fragment, in contrast to the mutant JW2553 (MT), which lacks the gene (**Figure 3.1 A**).

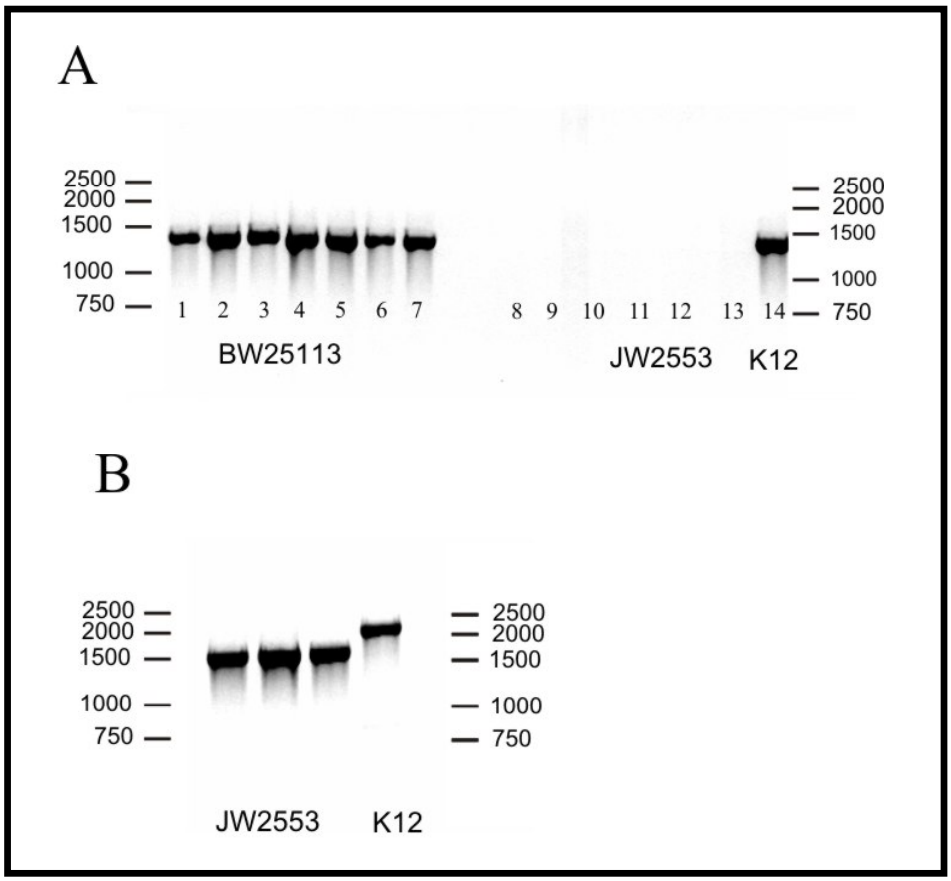

Figure 3.1 Colony PCR. A) With* lepA *N-terminal and inside III (1400) primer an amplified product of ~ 1400 bp for WT (BW25113) is obtained, whereas no PCR product is detected for the MT. B) PCR amplification with forward-flank and reverse-flank primers; K12 strain is used as a positive control, which gives a product above 2000 bp in agreement with the expected PCR product 2231 bp. For JW2553 (MT) the size is about ~1800 bp and the expected amplified product is 1782 bp.

3.1.1.1.1 Growth curves of WT and MT in LB medium

Growth of WT and MT were first separately monitored in LB medium in the presence and absence of high ionic strength (100 mM $MgCl_2$, 200 mM KCl). **Figure 3.2** illustrates that there are no obvious differences in growth between the two strains at either normal condition or at high ionic strength,

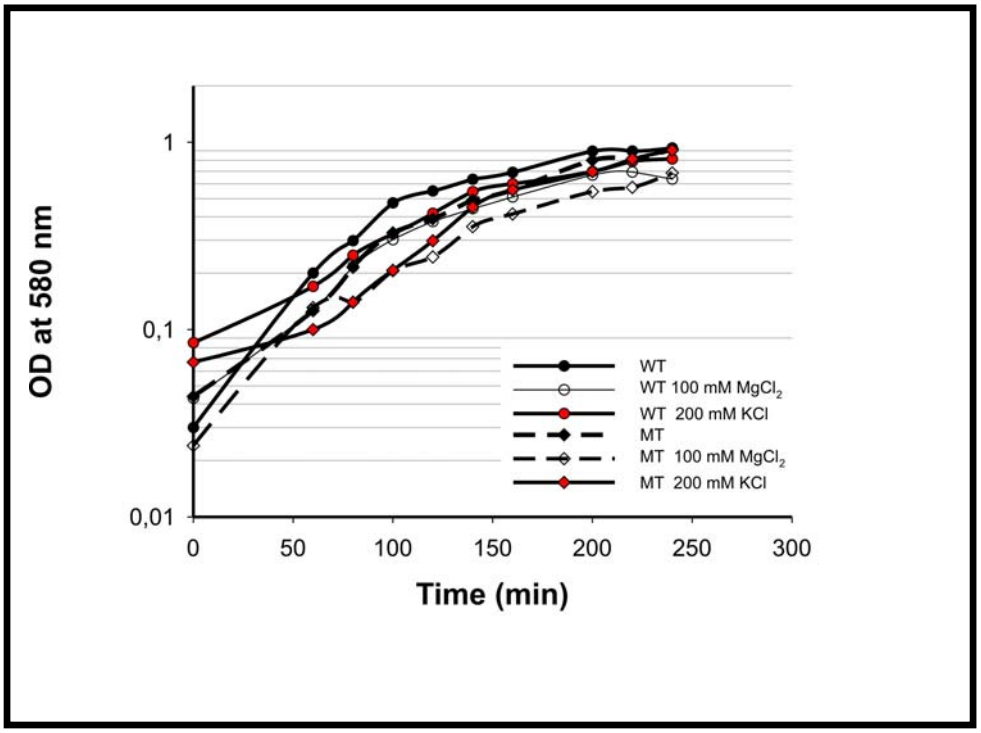

Figure 3.2. Growth curves of WT and MT in LB medium and - where indicated - 100 mM $MgCl_2$ or 200 mM KCl.

3.1.1.1.2 Growth curves of WT and MT in M9 medium

Minimal medium (M9) is mimicking better natural condition, where growth rate is limited by carbon and energy supply. In the M9 medium we also included different pHs. Cells were grown in M9 medium in a pH range between 5-8 with varying ionic conditions (100 mM $MgCl_2$, 200 mM KCl, 100 mM NaCl). At pH 7 in presence or absence of ions, MT cells were growing in parallel with WT cells. After 10 folds dilution the MT cells have a prolonged lag phase in comparison to the WT, which has no lag phase **(Figure 3.3 A)**.

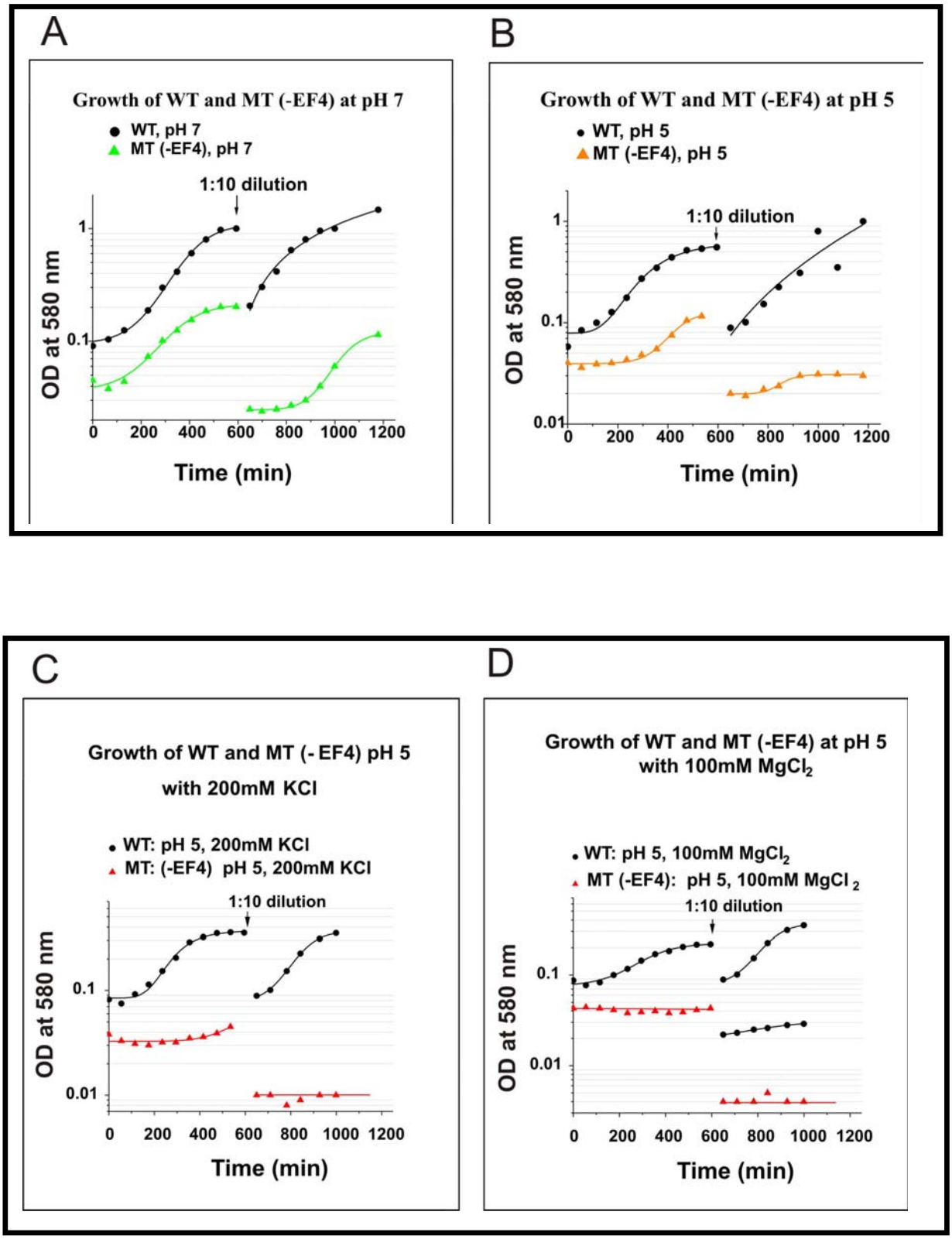

Figure 3.3. Representative growth curves of WT BW25113 and MT JW2553 at A) pH 7. B) pH 5. C) pH 5 with 200 mM KCl. D) pH 5 with 100 mM $MgCl_2$.

Interestingly, MT cells grown at low pH between 5- 6 had different growth pattern. The growth rate was inhibited slightly, but when salts like Mg^{2+} and K^{+} were added,

the growth rate was highly inhibited and after a 10-fold dilution the cells did not recover at all **(Figure 3.3 B, C and D).** According to the results with the mutant from the Keio collection, low pH and high salt concentration induced significant growth defects and after 10-fold dilution cell-death followed.

In this way a systematic analysis was performed, a summary of the parameters is shown with the parameters sun (**Figure 3.4**) of both the WT and MT at a pH range between 5-8 under various ionic conditions.

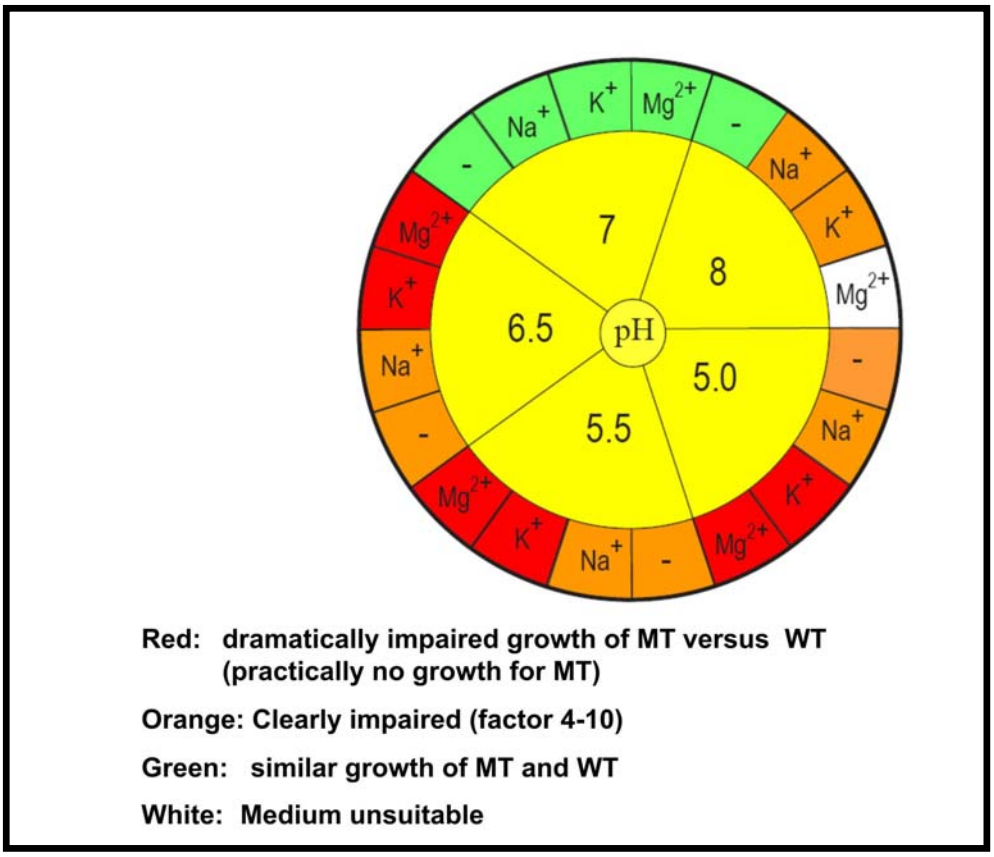

Figure 3.4 The parameter sun is a summary of growth curves of both the WT and MT at a pH range between 5-8 with varying ionic conditions. The colour code classifies qualitatively the growth differences between MT and WT.

For control reasons we ordered a second mutant lacking the *lepA* gene from the Keio collection in Japan, the mutant was derived from the same mother strain. To our disappointment we were not able to reproduce the above described results, the repeated growth curve patterns were very different from the previous ones **(Figure 3.5)**, where the MT was not growing to densities above OD_{580} 0.3-0.5 in M9 under all

tested stress conditions. With the new MT strain a reduced growth was only observed in M9 medium for both MT and WT. When growth rates of MT and WT were checked in LB medium the growth rates were comparable.

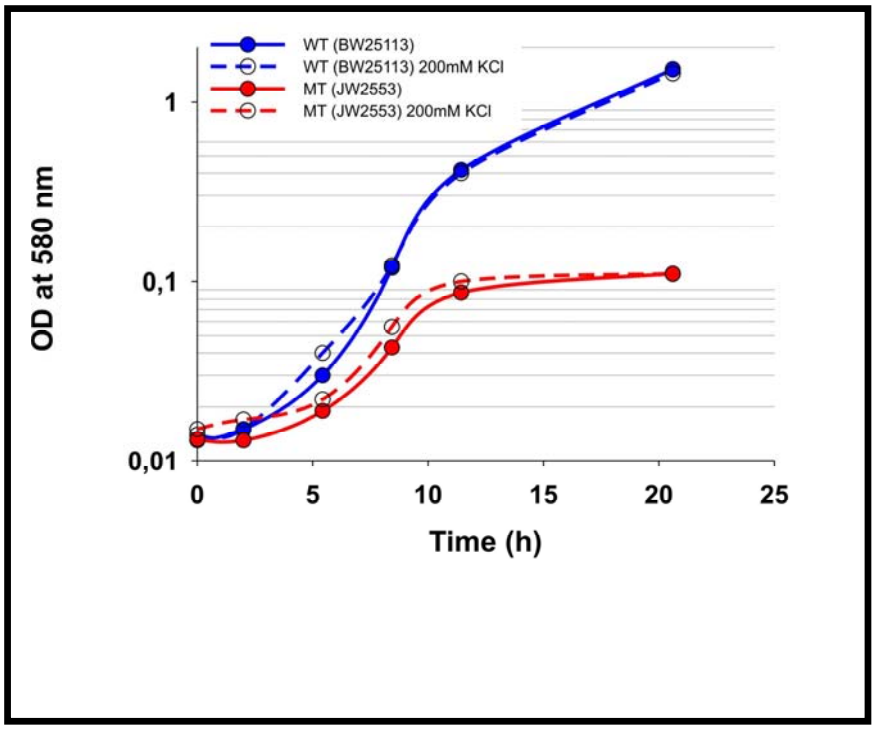

Figure 3.5 Growth curves of WT and MT: Cells were streaked out from the mother glycerol stock, then single colony was inoculated in to 5 ml fresh LB medium and grown over night. Main culture was started in M9 medium with either pH 7 in the presence or absence of 200 mM KCl and growth curves were monitored at OD_{580}.

A further striking observation was made, when cells were streaked out on LB/ Kan plates: The colonies were more or less heterogeneous. Therefore growth curves were made from both large and small colonies with almost the same results.

We suspected that the WT and MT were not isogenic outside the *lepA* gene. As a crude check we decided to compare the cell morphology by electron microscopy. WT and MT cells were grown in M9 medium at pH 7 and pH 6. Samples were prepared as described in Materials and Methods, after negative staining cells were pictured and WT and MT strains were compared. Surprisingly, we observed dissimilarity between WT and MT cells: MT but not WT cells showed long flagella **(Figure 3.6).** Formation of flagella requires more than 50 genes (Terashima, Kojima et al. 2008). It is therefore clear that WT and MT were not isogenic outside the *lepA* gene.

In other words, the images of BW25113 and JW2553 clearly illustrate that the mutant strain was not designed from the wild type BW25113 as Keio collection claimed.

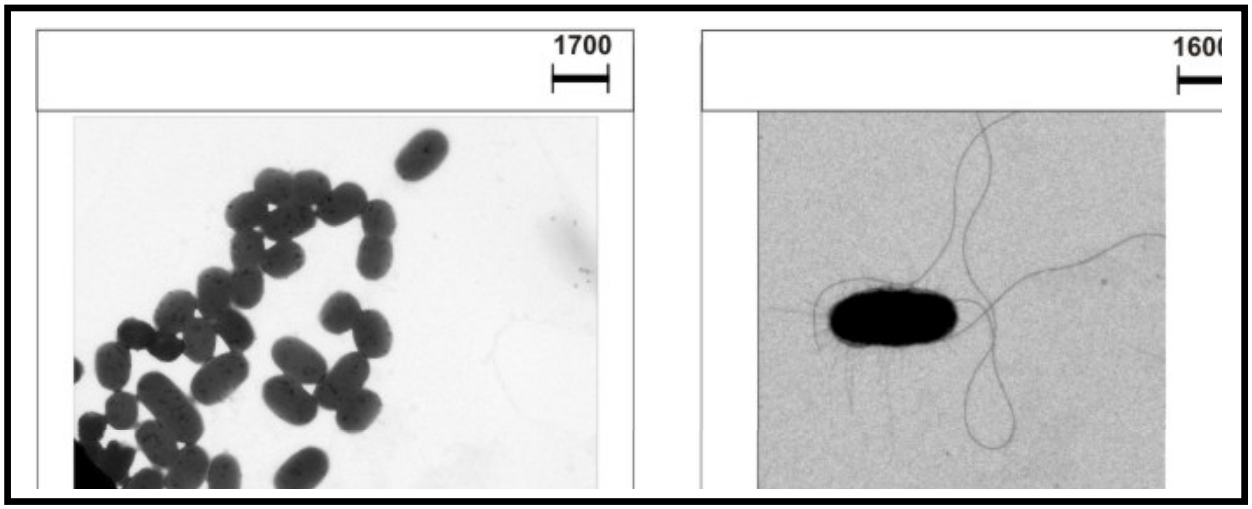

Figure 3.6 EM pictures of BW25113 (WT) left and JW2553 (ΔEF4) right.

3.1.1.2 Second approach for EF4 phenotype determination

After the first disappointing trial, a new mutant was designed using the kanamycin cassette that replaced the *lepA* gene. The *lepA* fragment together with the kanamycin cassette was taken and reintroduced into the BW25113 genome with the method of P1Kc transduction kindly performed by our colleague Dr. Madoka Kitakawa, Kobe, and described in Materials and Methods. The new construct was confirmed (i) with PCR using primers designed for neighbouring genes and also one primer pair hybridizing to a sequence inside the *lepA* gene; and (ii) the *lepA* gene deletion could be confirmed by sequencing. The new mutant was termed MDEF4 (EF4 deletion mutant). The confirmation of the gene deletion is shown in **Figure 3.7,** where the colony PCR with outside primers from neighboring genes (forward-flank and reverse-flank primer) on the left side yields a PCR product of >2,000 bp for the WT and of ~1,500 for MDEF4 confirming the expected nucleotide length of MDEF4 and WT with 1,400 bp and 2,231 bp respectively. On the right side, inside gene III (1400) primer is used. The results clearly prove the absence of the *lepA* gene in the mutant.

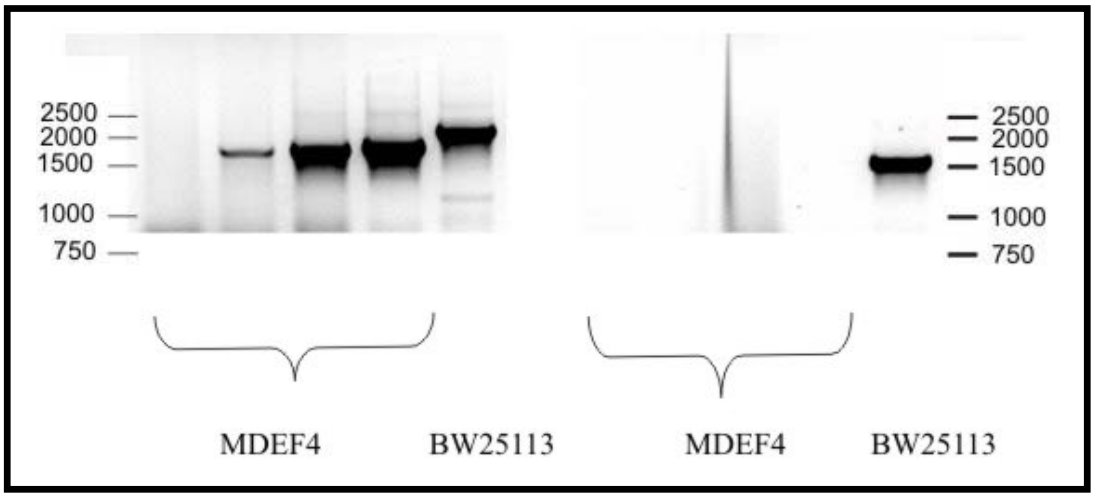

Figure 3.7 Colony PCR. On the left side, outside PCR (from neighboring genes using forward-flank and reverse-flank primers). On the right side, PCR using inside primers called lepA N-terminal and inside III (1400) primers.

Eventually the gene was sequenced using the neighbouring primers, the results showed that in the MDEF4 strain the *lepA* gene was absent. Finally, the morphology of the strains was checked again by EM, **Figure 3.8** shows that the same morphology of MT and WT cells is evident. Cell sizes were compared and the average length and width of both WT and MDEF4 were measured at different pHs as depicted in **Table 3.1**. Both the WT and MDEF4 at pH 7 had a length of 1.5 and 1.6 µm respectively, and a width of ~1.0 µm. At pH 6 the lengths and widths were the same, 1.6 µm.

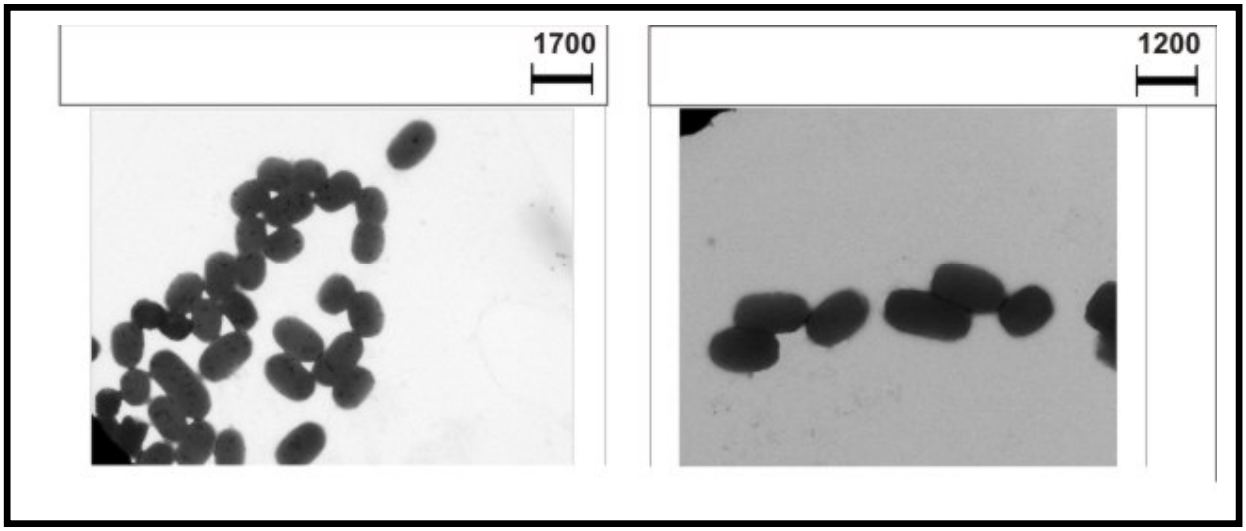

Figure 3.8 Comparison of BW25113 and MDEF4 morphology with EM. Left panel illustrates BW25113 and on right panel P1 transducted BW25113 (MDEF4) is seen.

Table 3.1 Comparison of BW25113 and MDEF4 cell sizes at pH 7 and pH 6 with electron microscopy.

Strains at different	*E. coli* length (µm) Average value for ~ 15 cells	*E. coli* width (µm) Average value for ~ 15 cells
pH 7, WT	1.5	1.03
pH 7, MDEF4	1.67	1.02
pH 6, WT	1.63	1.12
pH 6, MDEF4	1.6	1.18
Standard deviation < 10%		

3.1.1.2.1 EF4 gene is required for cell growth maintenance at low pH and high ionic strength or low temperature

The lack of EF4 has no clear phenotype at pH 7, when WT and MT grown in rich LB medium or M9 medium **(Figure 3.9)**. However, subtle growth differences cannot be detected with this method. A more sensitive assay is the growth competition assay allowing a comparison over many generations. Various growth conditions were applied **(Table 2.4)**.

The assay goes as follows: Equal volumes from both strains at the same cell density were mixed and the population distribution between WT cells and mutant were monitored by plating the mixed culture on LB and LB/ kanamycin plates during various times, first every 4 hours during 24 hours with appropriate dilution, then the cell culture was diluted 1:100 every 24 hours for growth for additional 3 days

approximately 30 generations. **Figure 3.10** is an example of the mixed cultures plated on LB and LB/ Kan plates.

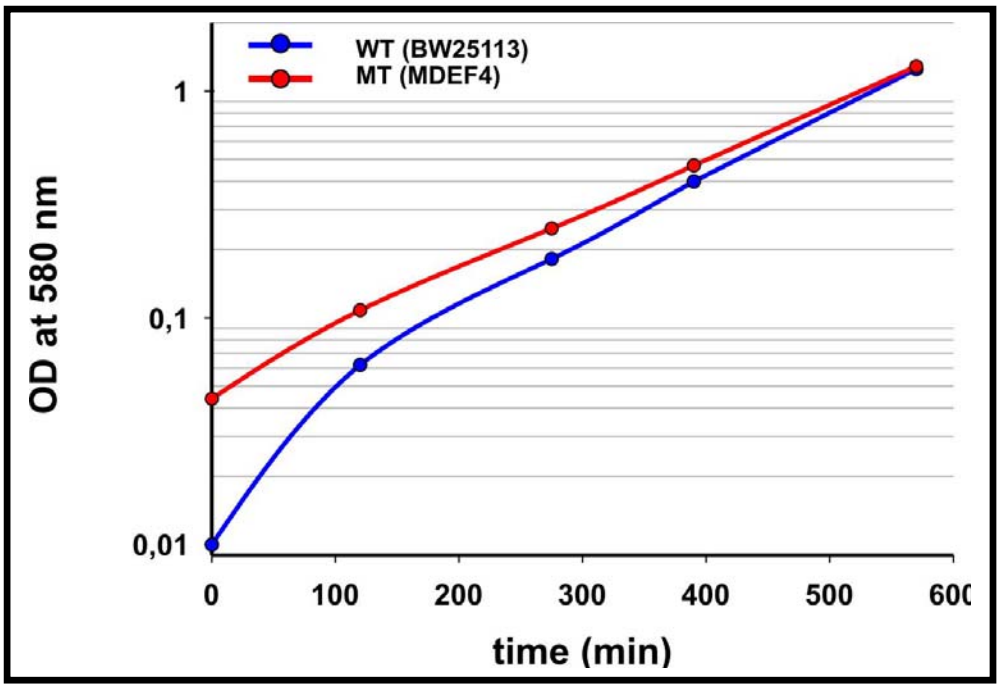

Figure 3.9. Growth curves in M9 medium at pH 7 of WT and MDEF4.

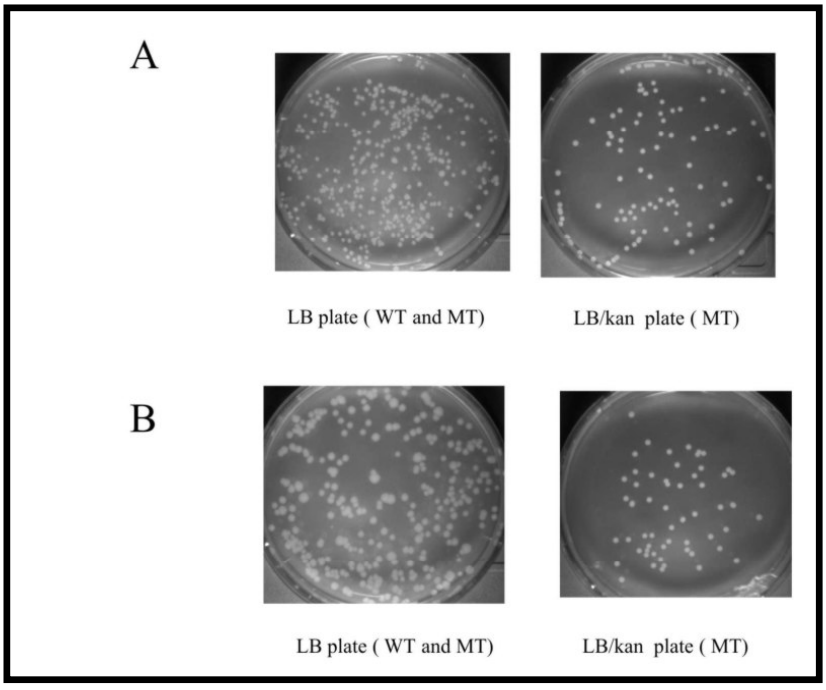

Figure 3.10 Growth competition. Cells were plated on both LB and LB 50 µg/ ml kanamycin. A) Growth competition at pH 6, 200 mM KCl after 25 generations. B) Growth competition at pH 6, 100 mM $MgCl_2$ after 30 generations.

At pH 7 minimal media growth of the mutant cells was slightly impaired, decreasing from 58 to 48% after ~15 generations **(Figure 3.11, dark blue curve)**. Addition of

100 mM $MgCl_2$ to the growth medium led to a more significant decrease down to 18% after 25 generations **(Figure 3.11, light blue curve with open circle).** A similar decrease after only 10 to 15 generations was observed at pH 6 with or without added 100 mM $MgCl_2$ (**Figure 3.11, dark red and light red with closed and open squares, respectively)**. At low temperature (16°C) cell growth performance was monitored, after 10 generations an outspoken reduction of MT cells was observed **(Figure 3.11, pink with diamonds).**

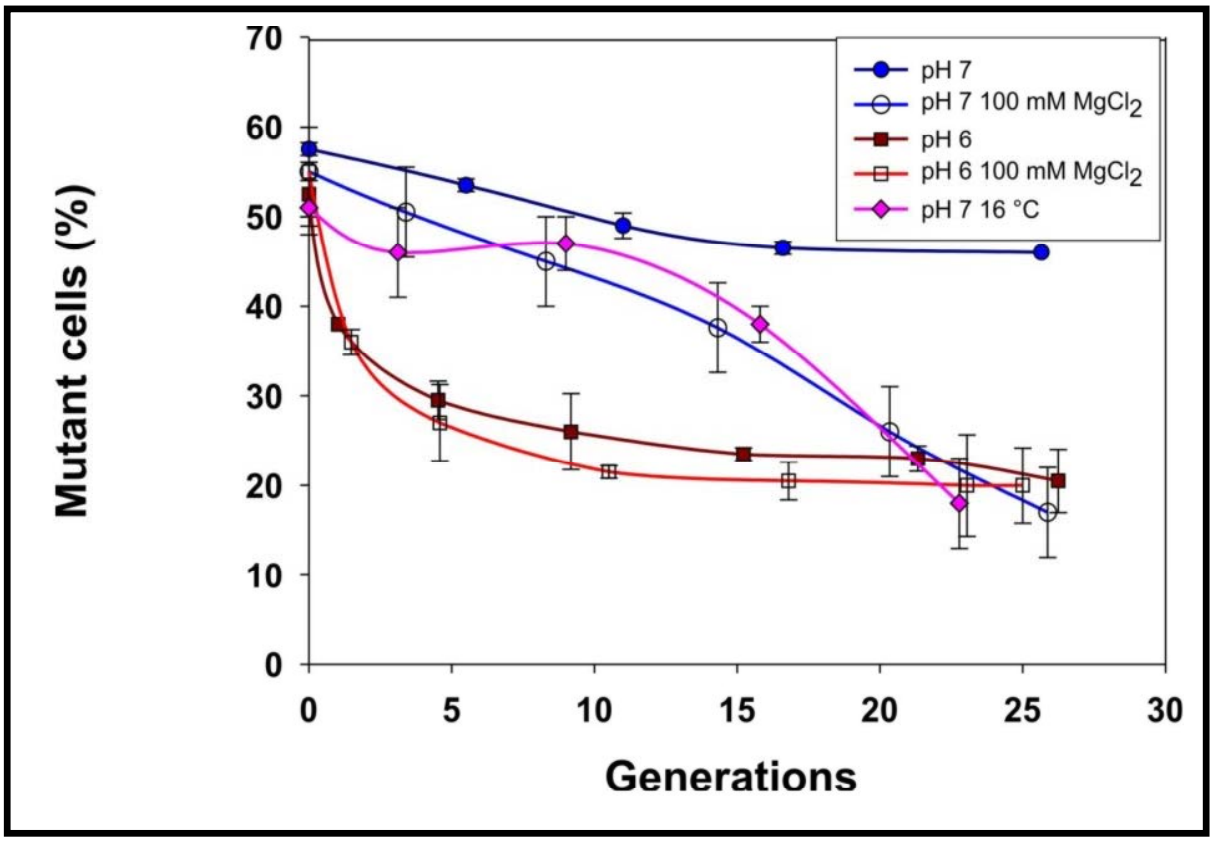

Figure 3.11 Growth competition at pH 7 and pH 6 in the presence and absence of 100 mM $MgCl_2$ and pH 7 at 16 °C.

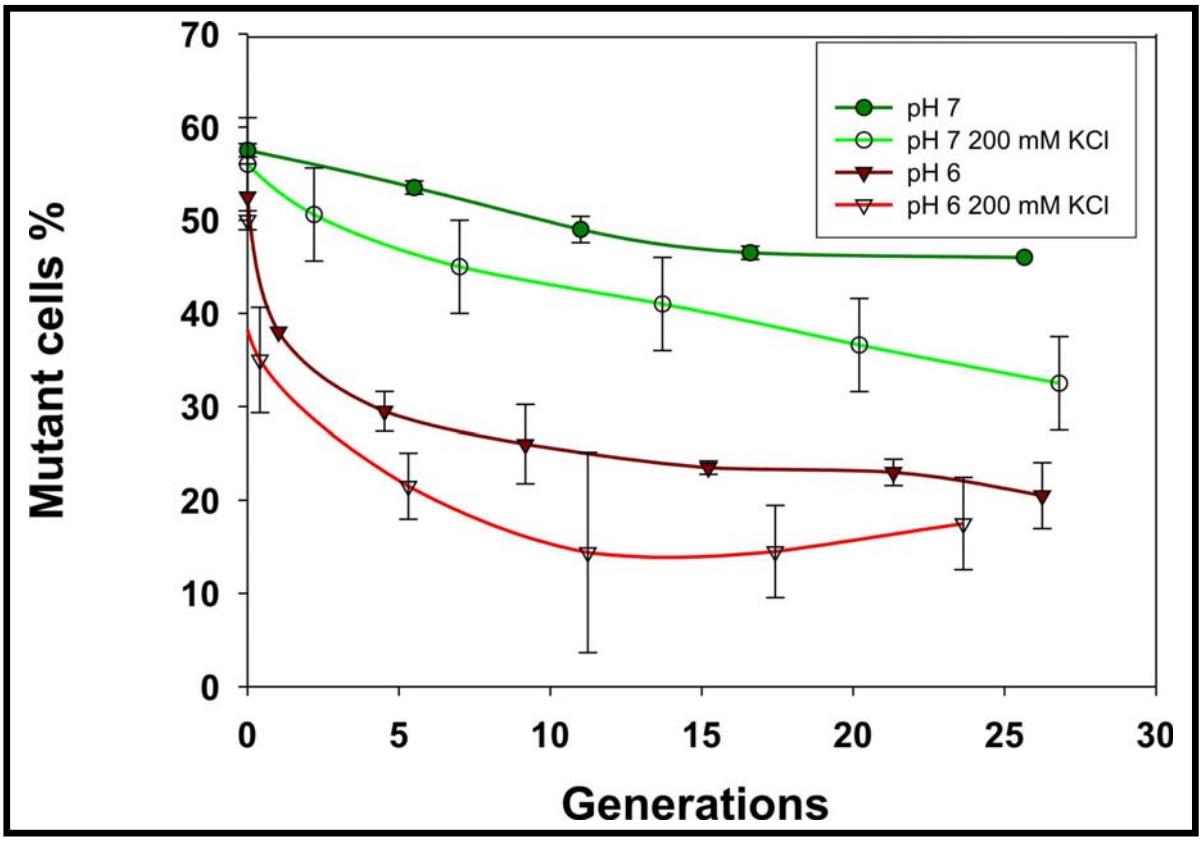

Figure 3.12. Growth competition at pH 7 and pH 6 in the presence and absence of 200 mM KCl.

Growth competitions were also performed at pH 7 and pH 6 in the presence and absence of 200 mM KCl, similar cell growth decrease to 20% was observed in the presence of 200 mM KCl **(Figure 3.12, light green and light red)**.

These results demonstrate clearly that EF4 plays an important role for bacterial growth under osmotic stress and at low temperature. A stable growth of mutant cells at about 20% is probably due to the second phase of osmoregulation in bacteria.

3.1.1.2.2 Polysome profiling of MDEF4 strain comparison to WT strain

In the next step we checked whether MDEF4 polysome pattern was changing in the absence of *lepA* gene. Cells were grown in LB medium at 37°C, and then harvested at ~ 0.6 working fast and in the cold as described in Materials and Methods. The polysome profile that was obtained from MDEF4 was the same as the WT polysome profile, this means that the ribosome assembly is not affected by the absence of EF4 **(Figure 3.13).**

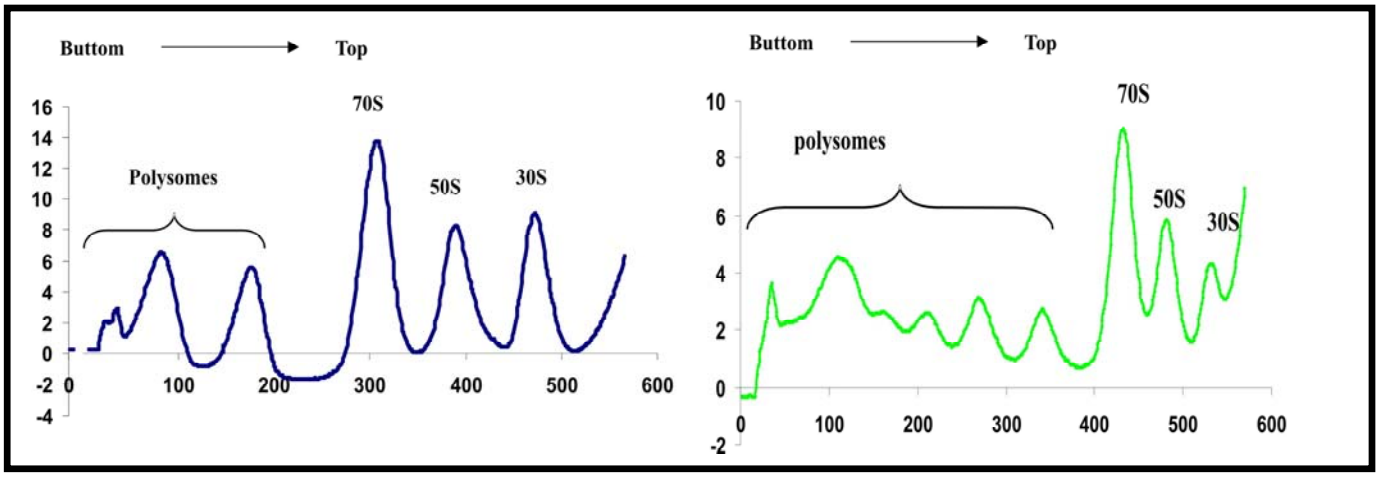

Figure 3.13 Polysome profile of WT (left) and MDEF4 (right).

3.1.1.3 the distribution of EF4 between cytoplasm and membrane changes at different conditions

March and Inouye already have demonstrated that overexpressed EF4 is found in the membrane (March and Inouye 1985). *In vitro* experiments have shown that EF4 is improving the protein yield and specific activity at a molar ration of 0.3:1 (EF4: 70S), while increased EF4 concentration results in inhibition of protein synthesis as a consequences of futile translocation and back translocation (Qin, Polacek et al. 2006). A release of EF4 from membrane to cytoplasm could be possible, and if so might represent an important step of regulation. To further examine this possibility we determined the molar ratio of EF4 between cytoplasm and membrane fractions at various conditions with Western blott analysis using EF4 polyclonal antibody.

At first the separation of membrane and cytosol fraction were optimized and samples of cytosol and membrane fractions were run on SDS-PAGE gel and Coomassie stained. A successful separation of membrane and cytosol fractions can be recognized, since in the membrane and the cytosol protein patterns are different and diagnostic bands for either fractions exist **(Figure 3.14)**.

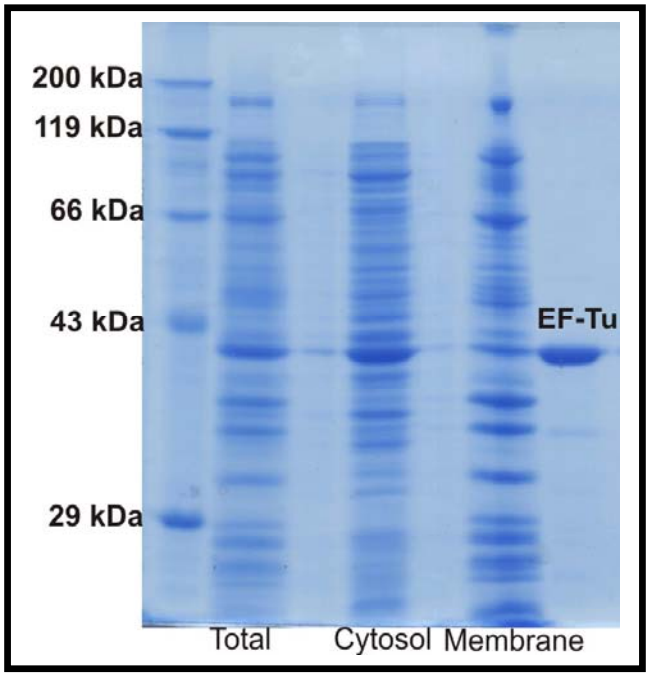

Figure 3.14 SDS-PAGE of protein distribution between membrane and cytosol. As control EF-Tu is used.

Under optimal conditions (pH 7, 37°C, LB medium) the cytosol:membrane distribution of EF4 was 25:75 or lower **(Figure 3.15 A)**. The situation is reversed for cells grown at pH 6 and 100 mM $MgCl_2$: cytosol:membrane distributions 85:15 were observed **(Figure 3.15 D).** Conditions such as pH 7 plus 100 mM $MgCl_2$ at 37°C **(Figure 3.15 B)**, pH 6 at 37°C **(Figure 3.15 C)** and pH 7 at 16°C **(Figure 3.16 B)** changes the distribution to ~ 50:50 between the cytosol and membrane. In milder stress conditions such as 25°C the distribution is about 40:60, obviously less amount of EF4 is needed in the cytosol **(Figure 3.16 A)**. These results suggest that EF4 is stored under optimal conditions in the membrane, and that EF4 is delivered to the cytoplasm under stress conditions, when this factor is required.

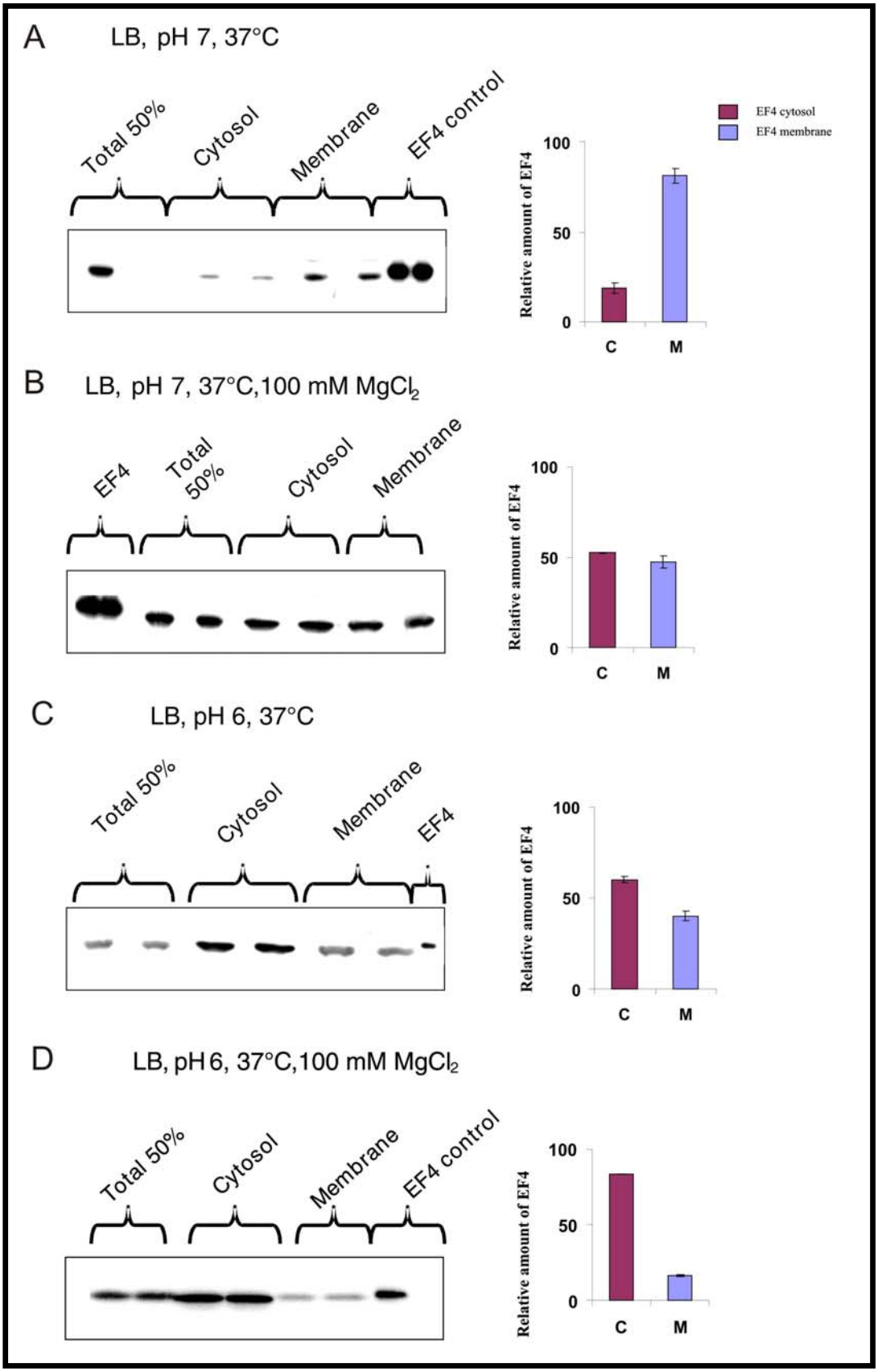

Figure 3.15. EF4 distribution between cytosol and membranes at A) pH 7, 37°C; B) pH 7, 37 °C, 100 mM $MgCl_2$; C) pH 6, 37 °C; and D) pH 6, 37 °C, 100 mM $MgCl_2$. On the left panel immunoblotting pictures using polyclonal anti-EF4 antibody. Right panel, relative amounts of EF4 in the cytosol and membrane in percent.

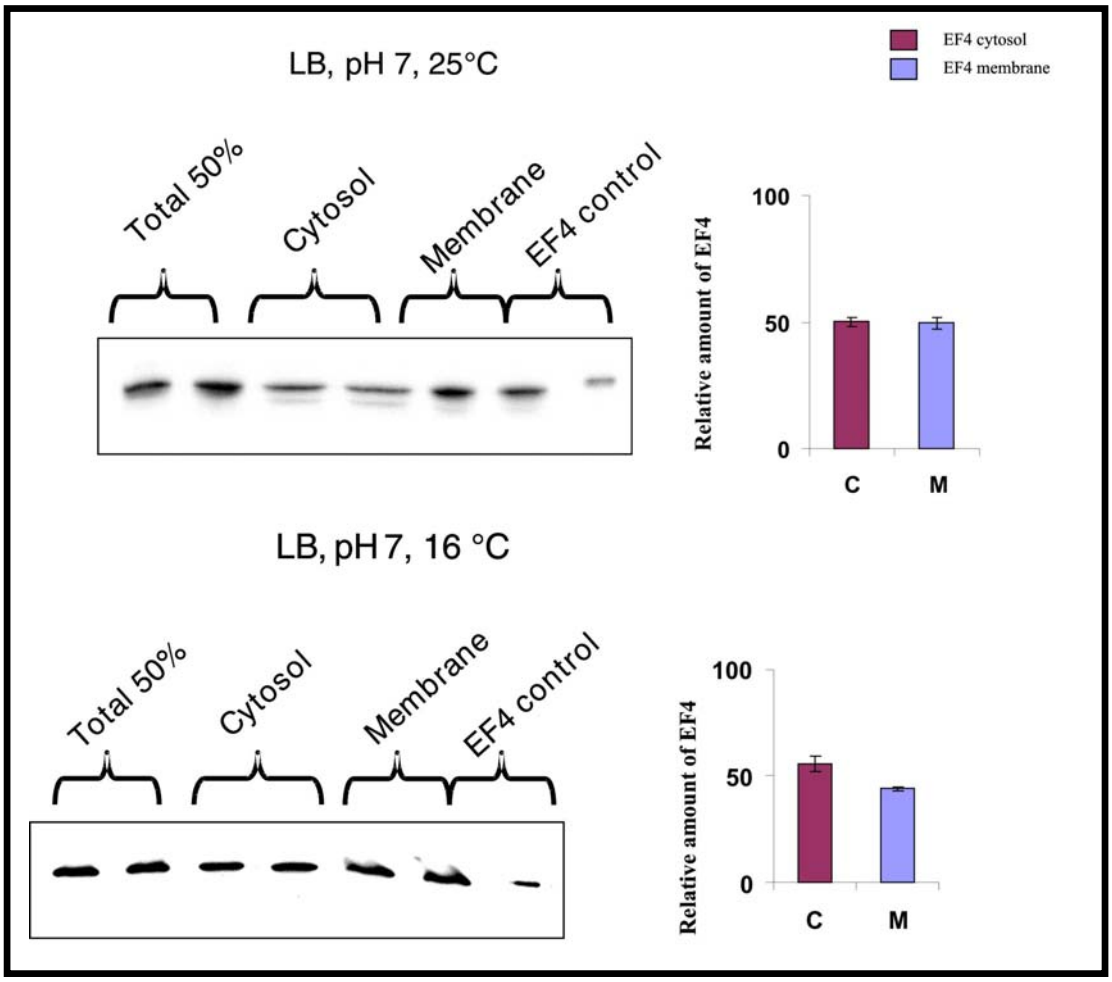

Figure 3.16. EF4 distribution between cytosol and membranes at A) pH 7, 25°C, B) pH 7, 16°C.

3.1.2 An estimate of EF4 concentrations *in vivo*

The square root of ribosome content is a linear function of the growth rate in *E. coli*. Ribosome synthesis rates in *E. coli* are mechanistically coupled to the energetic status (nucleoside triphosphate concentrations). The molar ratios of both the ribosomal elongation factors EF-Ts and EF-G to the ribosomes are ca. 1:1 and is also proportionally regulated to the growth rate as the ribosomes. The molar ratio of EF-Tu is about 10 per ribosome (Furano 1975). Here we determine the molar ratio of EF4 to the ribosomes in total cell extract under optimal conditions (LB medium, 37°C). Cells were harvested at semi log phase, where protein synthesis is optimal. The results show that EF4 ratio to ribosomes is about 0.1, which means 1 EF4 per 10 ribosomes.

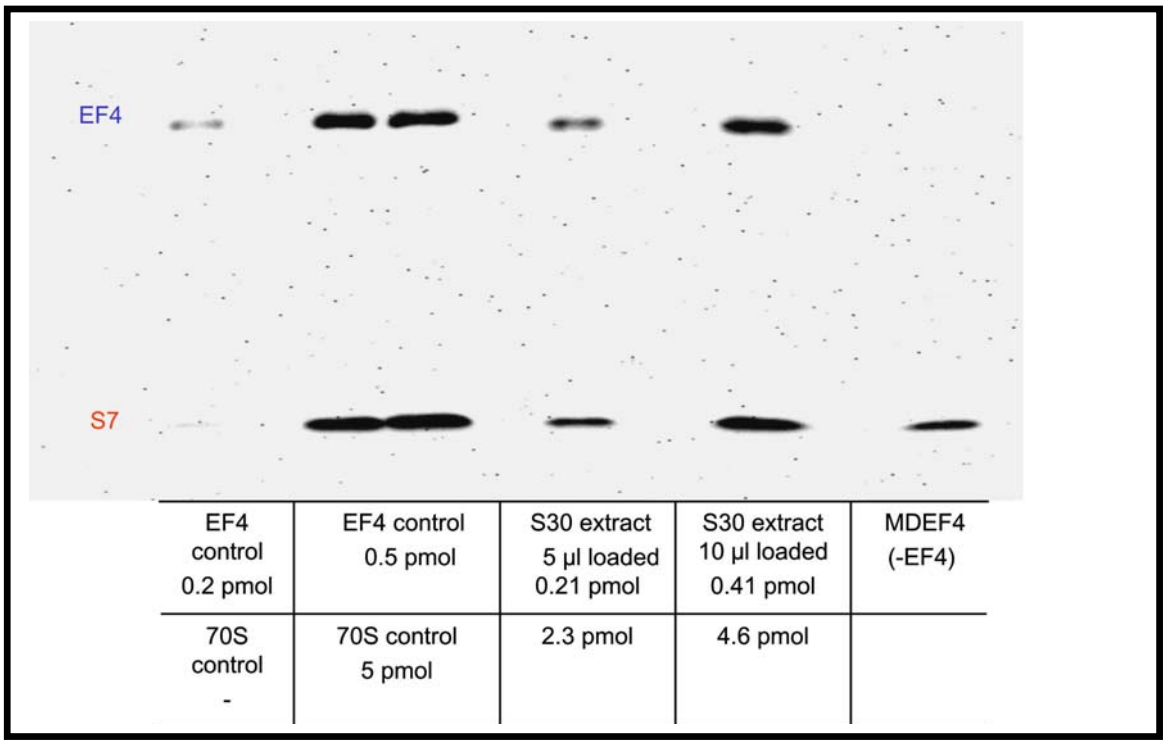

Figure 3.17. EF4 concentration estimation* in vivo*. S30 lysate from exponentially growing cells were loaded onto an SDS gel (5 and 10 µl). The cells were harvested at an OD_{600} of ~0.6/ml (10 ml total volume). Western blotting of each fraction identified EF4 and the ribosomal protein S7 as an 30S indicator. Control amounts of EF4 and 70S ribosomes added to the gel allowed via pixel measurement the determination of the corresponding molar ratios.

3.1.3 Molar ratio of EF4 to ribosomes in the cytosol

The goal of this experiment was to see whether the amount of EF4 changes proportionally with that of the ribosomes. S30 extract was prepared under optimal and stress conditions previously mentioned. The amount was estimated with polyclonal antibodies anti-S7 and anti-EF4, the ratio was estimated by pixel calculations as in the previous section. During growth in rich medium at 37°C there is only 1 EF4 per 20 ribosomes present in the cytosol, whereas under stress conditions (salt or low temperature) the molar ratio EF4:70S increases three times, from 0.05 to about 0.15 **(Table 3.2)**, still a low value as compared to EF-G of EF-Ts.

Table 3.2 EF4:S7 ratio in S30 extract

LB medium, pH 7, 37°C

Control				S30 extract				Ratio EF4:S7
EF4		S7		EF4		S7		
pixel	pmol	pixel	pmol	Pixel	pmol	Pixel	pmol	0.05
24544	0.5±0.002	24617	5±0.2	3883	0.08±0.02	5037	1.25±0.3	

LB medium, pH 6 100 mM $MgCl_2$

Control				S30 extract				Ratio EF4:S7
EF4		S7		EF4		S7		0.16
pixel	pmol	pixel	pmol	Pixel	pmol	Pixel	pmol	
160830	0.5±0.026	192583	5±0.008	115261	0.36±0.017	87736	2.28±0.08	

LB medium, pH 7, 16°C

Control				S30 extract				Ratio EF4:S7
EF4		S7		EF4		S7		
pixel	pmol	pixel	pmol	Pixel	pmol	Pixel	pmol	0.14
53599	0.5±0.01	40145	5±0.7	109057	0.36±0.04	167867	2.57±0.5	

3.1.4 Distribution of EF4 relative to EF-P between the cytosol and the membrane

Elongation factor P (EF-P) is a protein with unknown function. It has a three-domain structure, which mimics tRNA (Hanawa-Suetsugu, Sekine et al. 2004) indicating that it interacts with the ribosome. Indeed, the crystal structure of an EF-P•70S complex shows that EF-P binds to a 70S initiation complex next to the P-site fMet-tRNA at the side of the E site (Blaha, Stanley et al. 2009). The EF-P homologue in eukarya and archaea is initiation factor 5A (eIF-5A), which has domains corresponding to domains I and II of EF-P. EF-P is not essential for cell growth in LB medium, however first indications with growth competition experiments in our group revealed that EF-P has

an important role during growth in minimal medium, since the strain lacking EF-P is fast over-grown by WT cells after a few generation the mutant cells are down to 5%; (Kijek, 2009).The EF-P distribution between the cytosol and the membrane is extremely biased **(Figure 3.18)**, in that EF-P is almost exclusively observed in the cytosolic fraction: ~ 90% of the protein is present in the cytosol and less than 10% in the membrane, just the opposite of EF4, which is in rich LB medium (pH 7) mainly in the membrane (~85-90%).

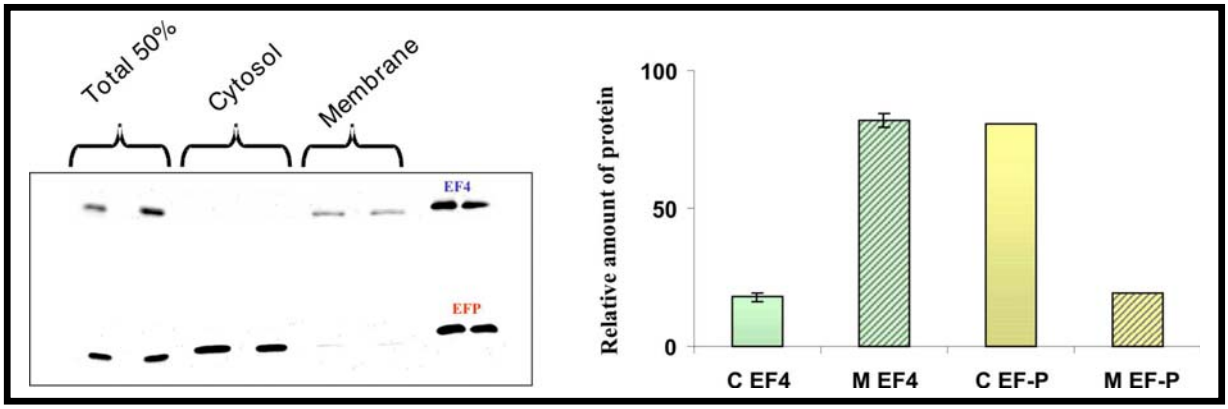

Figure 3.18 EF4 and EF-P distribution between cytosol and membrane at pH 7, 37°C. Left panel, immunoblotting using polyclonal anti-EF4 and anti- EF-P antibodies as described in Materials and Methods. Right panels, estimates of the relative amounts (%) of EF4 and EF-P in membrane and cytosol fractions based on the intensities of the corresponding immunoblotting bands. C, cytosol; M, membrane.

The EF-P distribution was also checked under different conditions and in **Figure 3.19** a representative is shown at 16°C where the EF-P amount is not changing, while the EF4 amount is changing dramatically from 10-15% to 55% in the cytosol. Overall we can say that EF-P is predominantly a cytosolic protein in contrast to EF4. At the same time these results demonstrate an effective separation of membrane and cytosolic fraction.

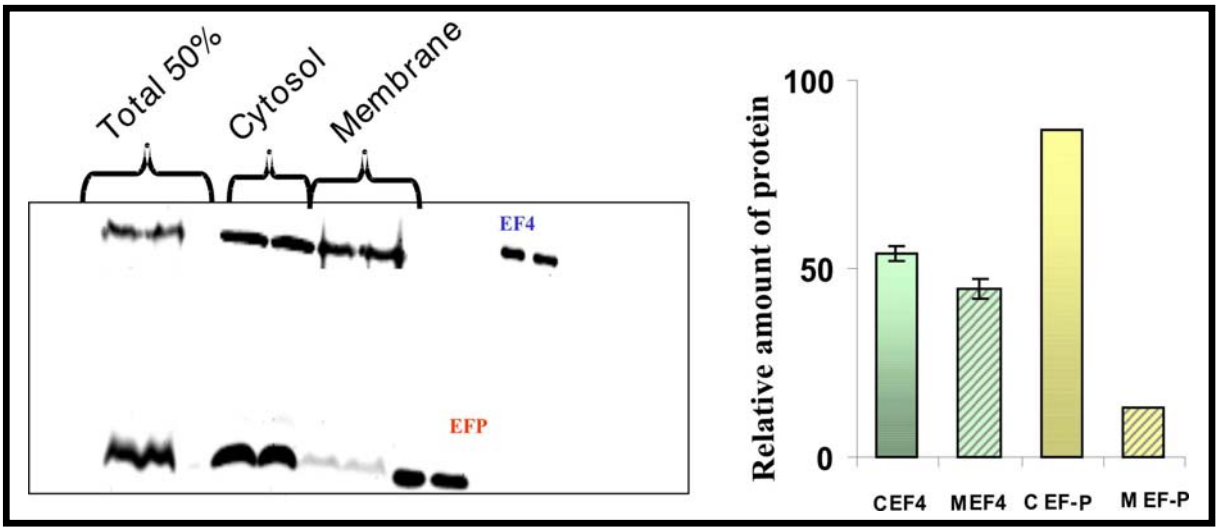

Figure 3.19 EF4 and EF-P distribution between cytosol and membranes at pH 7, 16°C. Left panel, immunoblotting using polyclonal anti-EF4 and anti- EFP antibodies. Right panel, estimates of the relative amounts (%) of EF4 and EF-P in membrane and cytosol fractions based on the intensities of the corresponding immunoblotting bands. C, cytosol; M, membrane.

3.2. Toxicity effect of EF4

3.2.1 Toxicity check with low copy plasmid pZS*24-MCS-1

pZS*24-MCS-1 is a low copy plasmid which has a plac/ara promoter, the expression of the protein can be controlled with this promoter up to 1,800 folds (Lutz and Bujard 1997). This plasmid is therefore well suited for toxicity determination of an expressed gene, since the total amount of protein expression can be controlled with either IPTG or arabinose induction. Results of the toxicity of EF4 and human Mito EF4 (Hsm-EF4) are shown in **Figures 3.20 and 3.21**.

The growth of the *E. coli* cells containing pZS*24-MCS-1-lepA plasmid were slightly decreased but rather not inhibited by induction with 5 mM IPTG plus 0.05% arabinose. With EF4 polyclonal antibody the amount of overexpressed protein was compared roughly with the EF4 protein control **(Figure 3.22).**

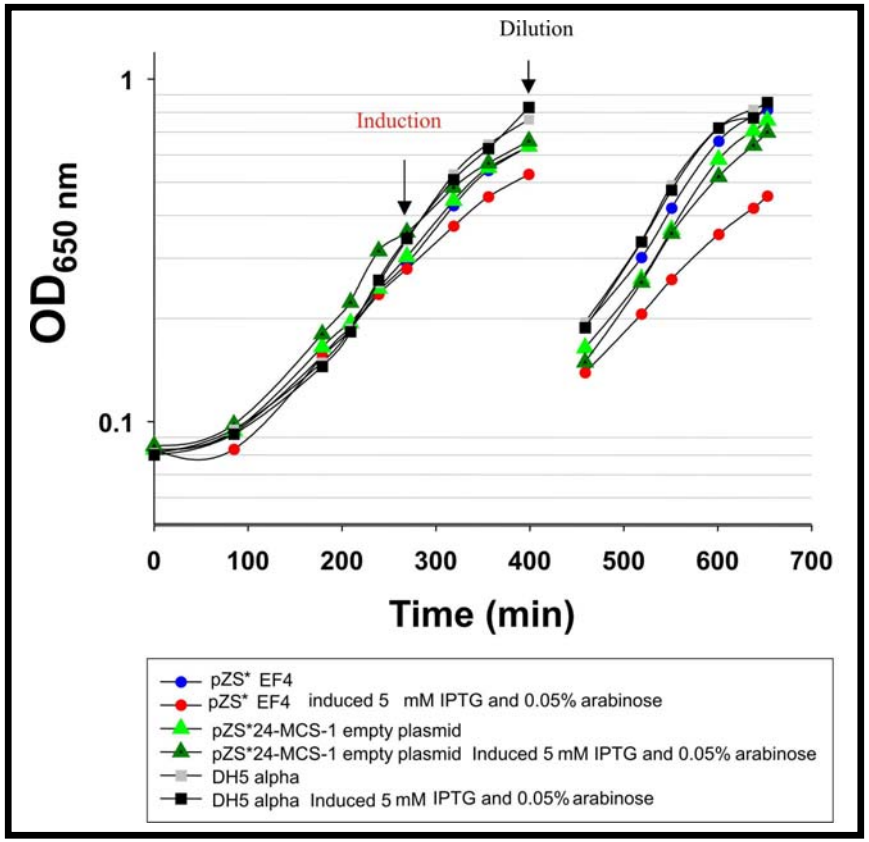

Figure 3.20 Toxicity of E. coli EF4. Cells were grown in LB medium, at an OD_{600} of 0.2 cells were induced with 5 mM IPTG and 0.05% arabinose, later on diluted 1:10 in fresh LB medium containing 5 mM IPTG and 0.05% arabinose.

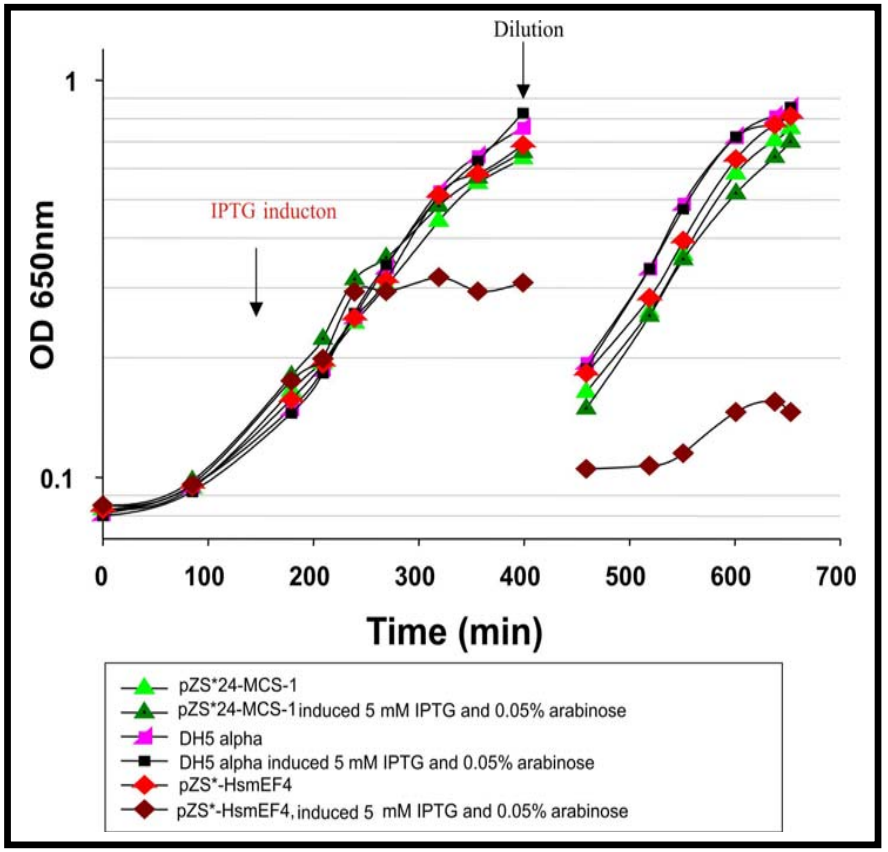

Figure 3.21 Toxicity determination of Hsm-EF4. Cells grown in LB medium and induced with 5 mM IPTG and 0.05% arabinose at OD_{600} of 0.2, later on diluted 1:10 in fresh LB medium containing 5 mM IPTG and 0.05% arabinose.

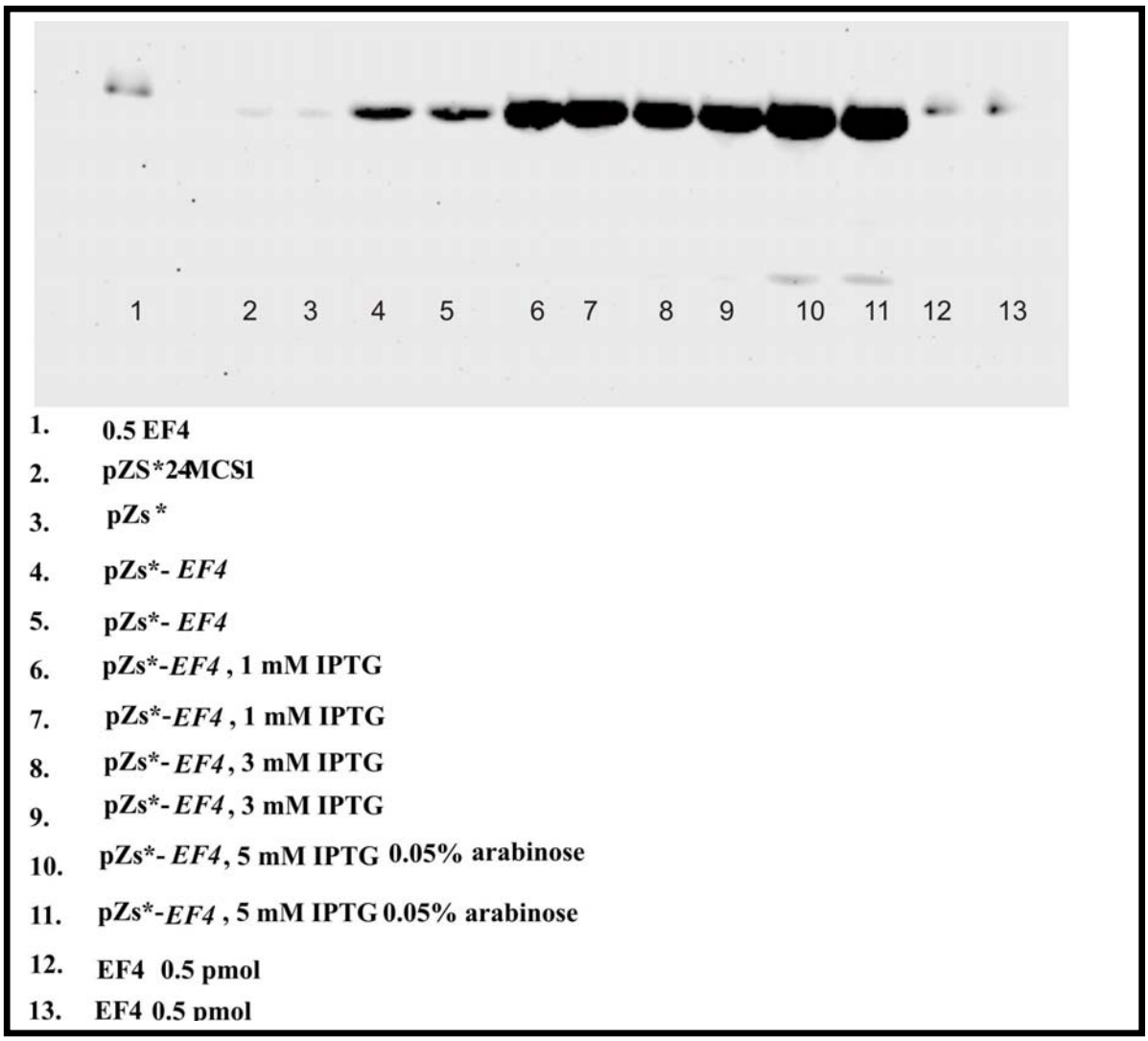

Figure 3.22 The Western blotting analysis of EF4 expressed in pZS* 24-MCS-1 vector with increasing concentrations of IPTG and addition of arabinose.

The amount of expressed protein was not detectable for human mito-EF4 (Hsm-EF4). The growth of DH5α cells bearing pZS*Hsm-EF4 was inhibited and the cells were not recovering after 1:10 dilution in LB medium containing 5 mM IPTG and 0.05% arabinose indicating the extreme toxicity of the human mitochondrial orthologue of EF4.

3.3 EF4 protein purification

Special care was taken on getting the pure protein without partial degradation that might affect the activity of the protein. In our previous EF4 purifications one of the

main issues was, when purified EF4 was stored at salt concentrations below 500 mM K^+, the protein precipitates. For these reasons some steps has been taken into consideration as will be described below.

The EF4 protein carrying a His-tag was purified from an over-expression strain with nickel column and further with cation-exchange (MonoS). EF4 is mainly eluted at 200 mM imidazole **(Figure 3.23 A, elution 3)**. Unfortunately the eluted EF4 was not pure enough to be used in our functional assays. Smaller protein fragments are seen on the SDS-PAGE gel that might be degradation products or impurities **(Figure 3.23 B, marked with red arrow).** The purification of EF4 was continued in order to remove the additional bands that might interfer with the full-length protein. The eluted fractions were subjected to FPLC (fast protein liquid chromatography) using a cationic exchange column. The results show that the protein has an additional specific band, which is shorter than EF4 and might be a degradation product of EF4 **(Figure 3.23 B Lane; F3 and F6 (unbound fractions) comparison to lane H11-H16 (elution fractions)).** The peak marked with asterisk is where the pure EF4 is eluted and fractions combined. High salt is affecting the activity of the 70S ribosome. Since the EF4 protein was eluted at high salt, we had to desalt it for storage purposes. The high salt buffer was then replaced by EF4 storage buffer ($H_{20i}K_{500}SH_4glycerol_{10\%}$) (**Figure 3.23 C).**

Protein marker from
Fermentas #SM0431

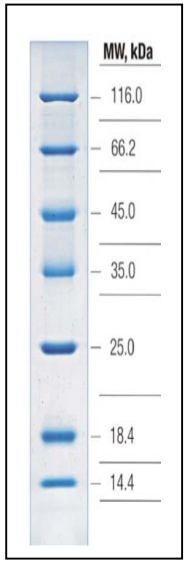

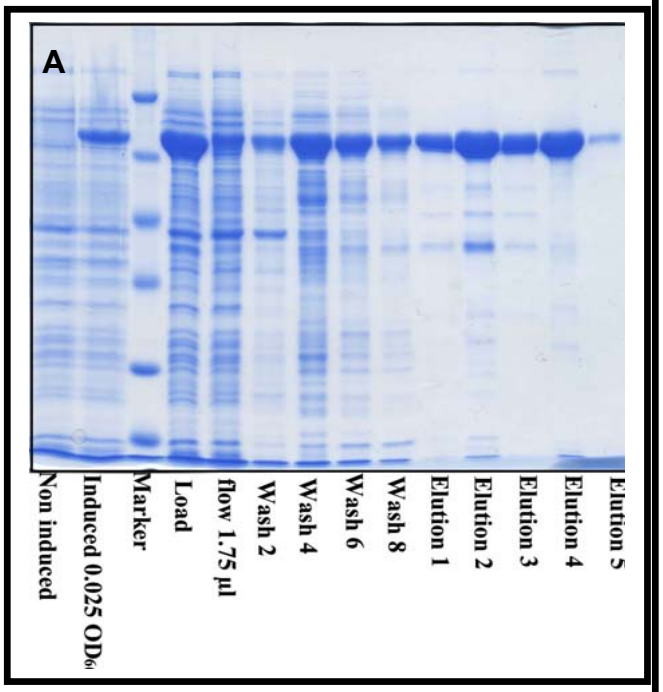

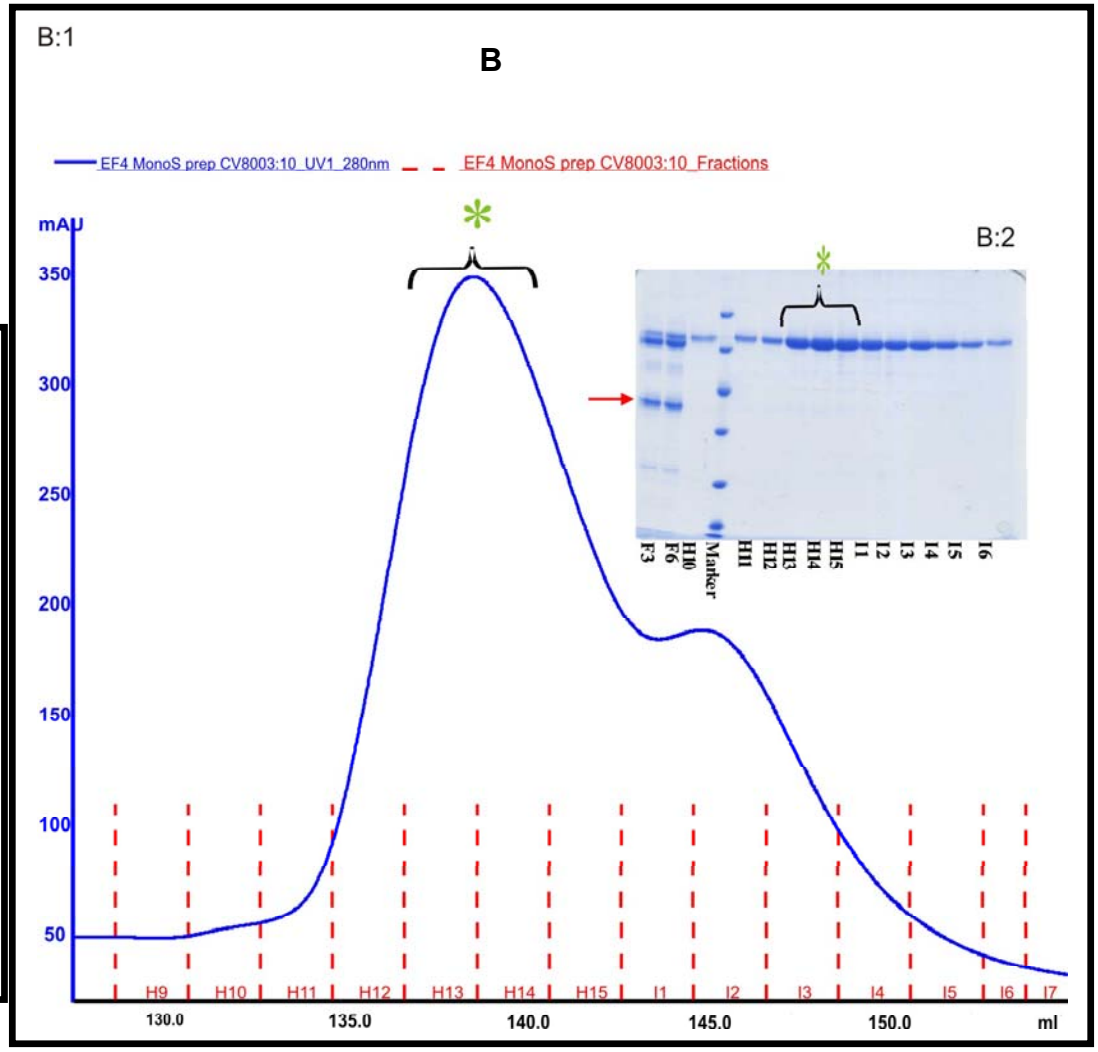

C

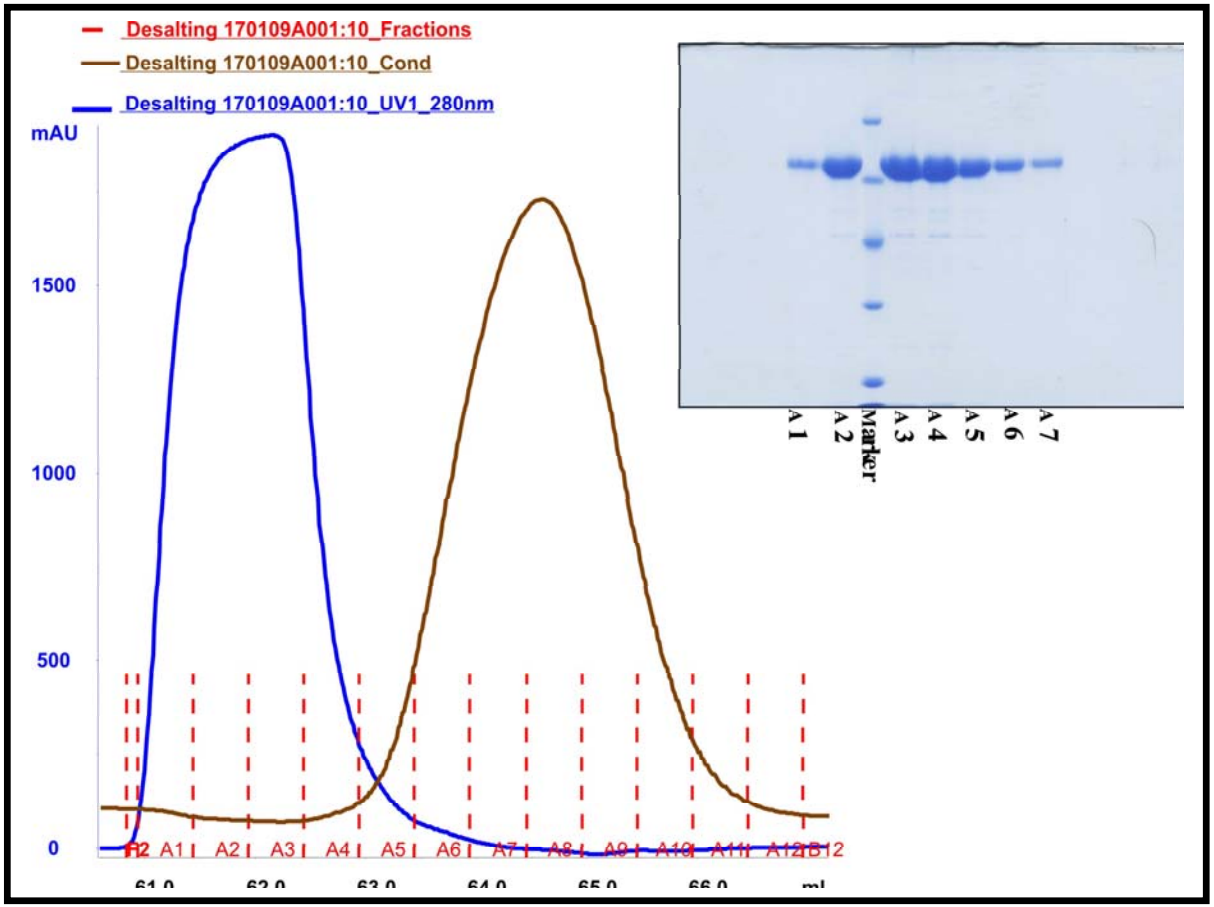

Figure 3.23 EF4 protein purification steps. A) Protein expression and NiNTA protein elution: elution fraction 1, 2 (100 mM imidazole); elution fraction 3, 4 (200 mM imidazole), elution fraction 5, 6 (300 mM imidazole). B: 1) FPLC protein cationic exchange chromatogram with 0.2 - 1 M K^+ gradient; each letter corresponds to an elution fraction the asterisk indicates peak fractions that were combined. .B: 2) SDS-PAGE gel of all fractions asterisk is indicating the same fraction that were further used. The SDS-PAGE gel shows the corresponding elution fractions. C) FPLC desalting chromatogram; fractions A2-A5, A3-A4, A6 were pooled. Insert: SDS-PAGE gel of desalted fractions.

3.4 Importance of EF4

3.4.1 Poly(U) dependent poly(Phe) synthesis and mis- incorporation of leucine (Leu) at 4.5 and 14 mM Mg^{2+}

Our highly optimised assay poly(U) dependent poly(Phe) synthesis with 4.5 mM Mg^{2+} and polyamines (Szaflarski, Vesper et al. 2008) proves a stable post translocational state (POST state) with a stable E site occupation by deacylated tRNA (Rheinberger and Nierhaus 1987) and a Phe incorporation of 100-500 Phe per ribosome. The mis-incorporation of near-cognate tRNA, in this case Leu, is as low as 1 Leu per ~3,000 Phe. Since Leu is the "classical" mis-incorporated amino acid in the presence of an UUU codon at the A site, because it only differs at the wobble position UUA/UUG, it is used in our mis- incorporation assays. The 40 pmol addition of $tRNA^{Phe}$ has been a topic of discussion. The $tRNA^{bulk}$ extracted from *E. coli* contains the tRNAs in physiological concentration ratios and in principal it should be sufficient to perform protein synthesis, however in our poly(U) dependent poly(Phe) synthesis $tRNA^{Phe}$ is added due to the exclusive presence of UUU codons. In this section, we examined

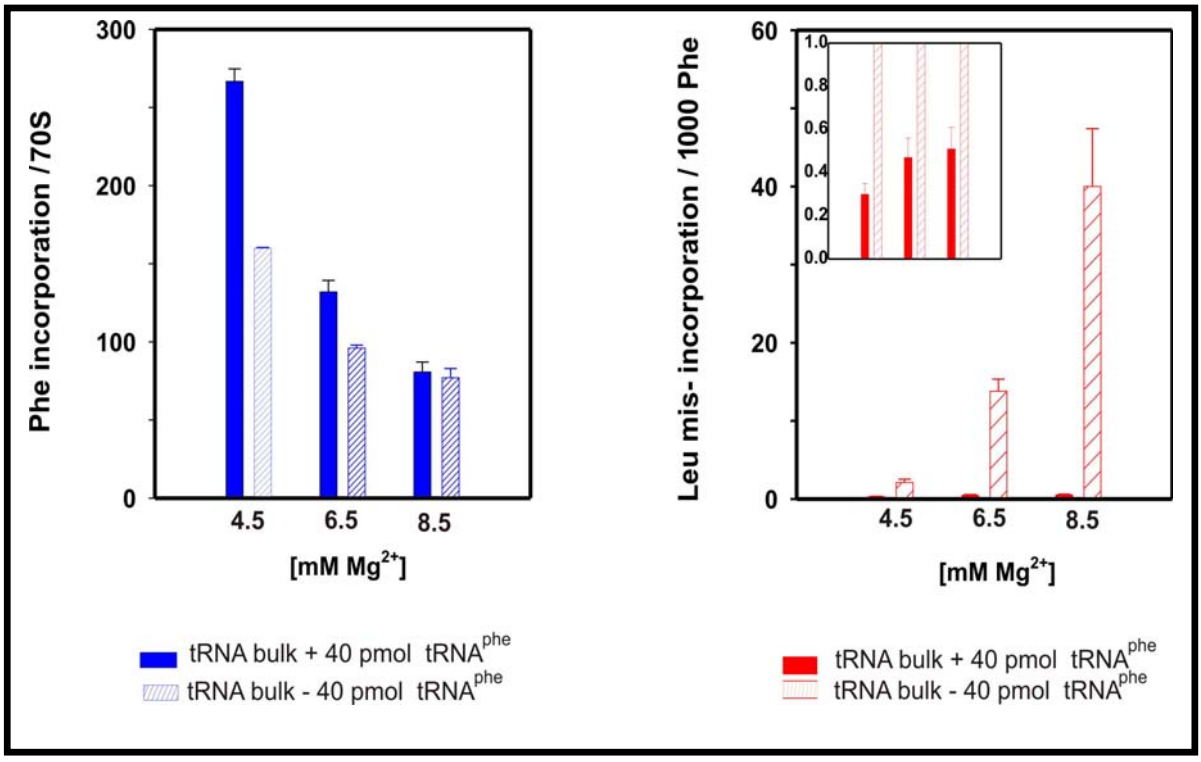

Figure 3.24 Poly(U) dependent poly(Phe) synthesis performed under optimised conditions (4.5 mM Mg^{2+}) and under higher Mg^{2+} concentrations at 6 and 8 mM with and without addition of 40 pmol $tRNA^{Phe}$, $tRNA^{bulk}$ (200 pmol) is present in all conditions.

the Phe synthesis and near-cognate incorporation efficiency in the presence and absence of 40 pmol $tRNA^{Phe}$. **Figure 3.24** clearly shows that the addition of $tRNA^{Phe}$ is only beneficial in the optimized 4.5 system, whereas under unfavourable Mg^{2+} concentrations $tRNA^{Phe}$ within the $tRNA^{bulk}$ is not limiting due to the slow Phe incorporation **(Figure 3.24, left hand side)**. Increasing Mg^{2+} concentrations increases also the mis-incorporation of Leu, an effect much more outspoken in the absence of the additional 40 pmol $tRNA^{Phe}$ **(Figure 3.24, right hand side)**. This is due to the fact that the molar ratio of cognate $tRNA^{Phe}$ *versus* near-cognate $tRNA^{Leu}$ dictates the mis-incorporation level. It follows that our optimised 4.5 poly(U) dependent poly(Phe) system requires the addition of 40 pmol $tRNA^{Phe}$.

Ribosome activity is optimal at 4.5 mM Mg^{2+} as mentioned above, whereas at high Mg^{2+} protein synthesis slows down dramatically, and the error rate is increased up to 20-fold. Our *in vivo* experiments suggest that EF4 may be of importance at high ionic strength.

Poly(U) dependent poly(Phe) experiment was performed in the absence and presence of EF4 at different Mg^{2+} concentrations (4.5, 6.0, 8.0, 10.0, and 14.0 mM). Phe incorporation per 70S ribosome and mis-incorporation of Leu was monitored. **Figures 3.24-25** show that the protein synthesis decreased with increasing Mg^{2+} concentration. This is also shown in (Szaflarski, Vesper et al. 2008). When EF4 is present, the Phe incorporation is not effected under optimal conditions (4.5 mM Mg^{2+}), whereas EF4 is accelerating Phe incorporation at unfavourable Mg^{2+} concentrations but does not affect the mis-incorporation level, i.e. the fidelity or protein synthesis **Figure 3.25**. The experiment was repeated kinetically under 4.5 and 14 mM Mg^{2+} in order to determine the initial rate of Phe incorporation differences in the presence and absence of EF4. As expected at 4.5 mM Mg^{2+} EF4 is not needed while in the presence of EF4 the Phe synthesis is accelerating and increasing in parallel with time, while the system without EF4 is hampered and protein synthesis is almost impossible. The mis-incorporation was also monitored and EF4 appeared to have no effect on accuracy **Figure 3.26**.

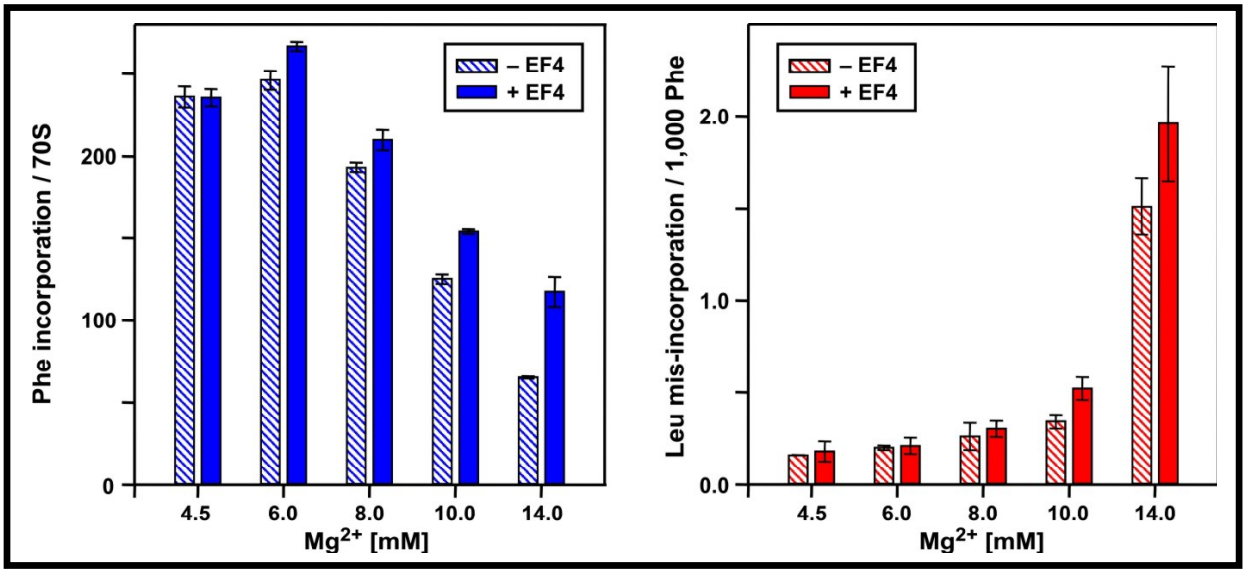

Figure 3.25. Phe incorporation per 70S in the absence and presence of EF4 (left panel). Leu mis-incorporation per 1000 Phe is shown in the right panel. EF4 does not affect the fidelity of protein synthesis.

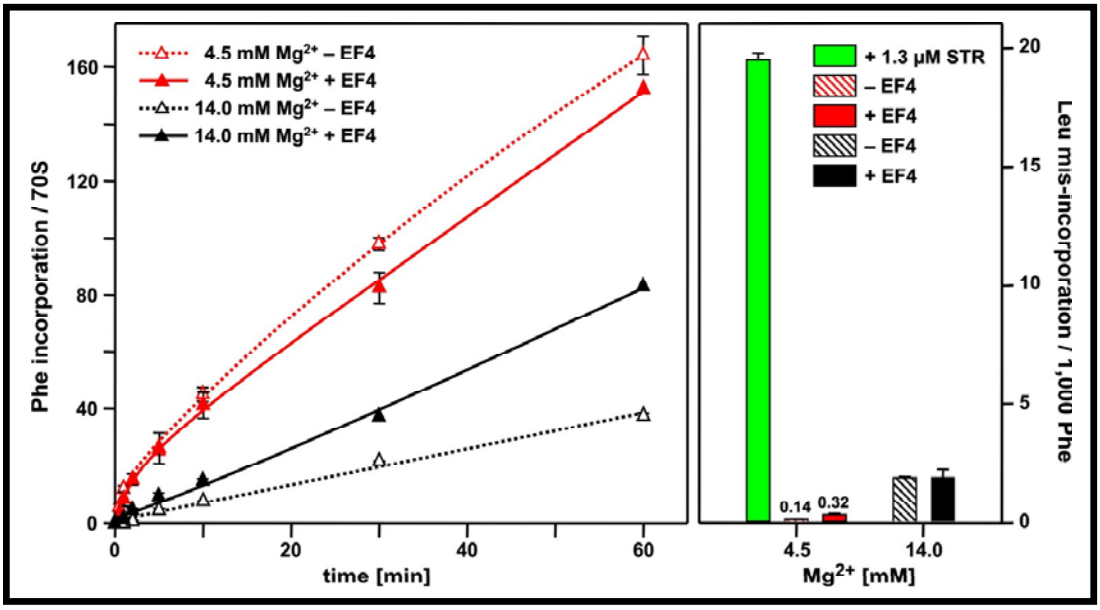

Figure 3.26. Left side is the kinetic of Phe synthesis without (dashed line) and with EF4 (solid lane). Black curves, 14 mM Mg^{2+}; red curves, 4.5 system. Right side is showing mis-incorporation of Leu at 4,5 and 14 mM Mg^{2+} in the presence and absence of EF4, Streptomycin is used as a positive mis-incorporation control.

The acceleration effects of protein synthesis observed in the described experiments might be minimal effects, since the S100 enzymes used might contain EF4 thus reducing the effect when EF4 is added. Therefore we performed similar experiments but now with precharged Phe-$tRNA^{Phe}$ und purified elongation factors thus avoiding the presence of S100 enzymes. A control assay constructing a PRE state and translocating it to a POST state is shown at 4.5 and 14 mM, under both conditions highly specific complexes can be made, the yield of complexes is even better at 14

mM (**Figure 3.27 A)**. Now indeed a more dramatic effect of EF4 is seen with an accelerating effect of the initial rate of up to 10 times in the presence of 14 mM Mg^{2+}, whereas again no effect can be observed under optimal condition. Further more we wanted to find out whether we could stall the ribosomes to up to100% by increasing ionic strength and also to find out how EF4 will react to such a hyper-ionic change. The experiment was repeated with increasing amount of Mg^{2+}, and the poly(Phe) synthesis was checked both in the presence and absence of EF4 2x times over the ribosomes. The surprising results were that EF4 can indeed accelerate the poly(Phe) synthesis even at 30 mM Mg^{2+}, where practically all ribosomes were stalled in the absence of EF4 **(Figure 3.27C)**.

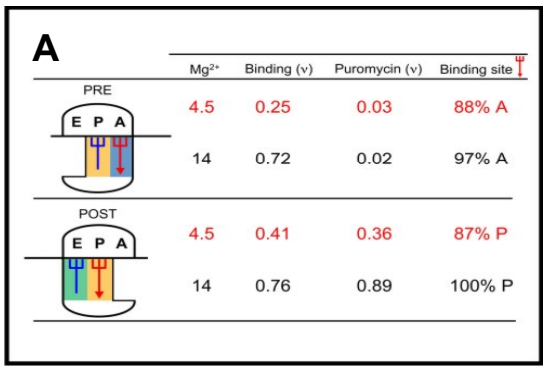

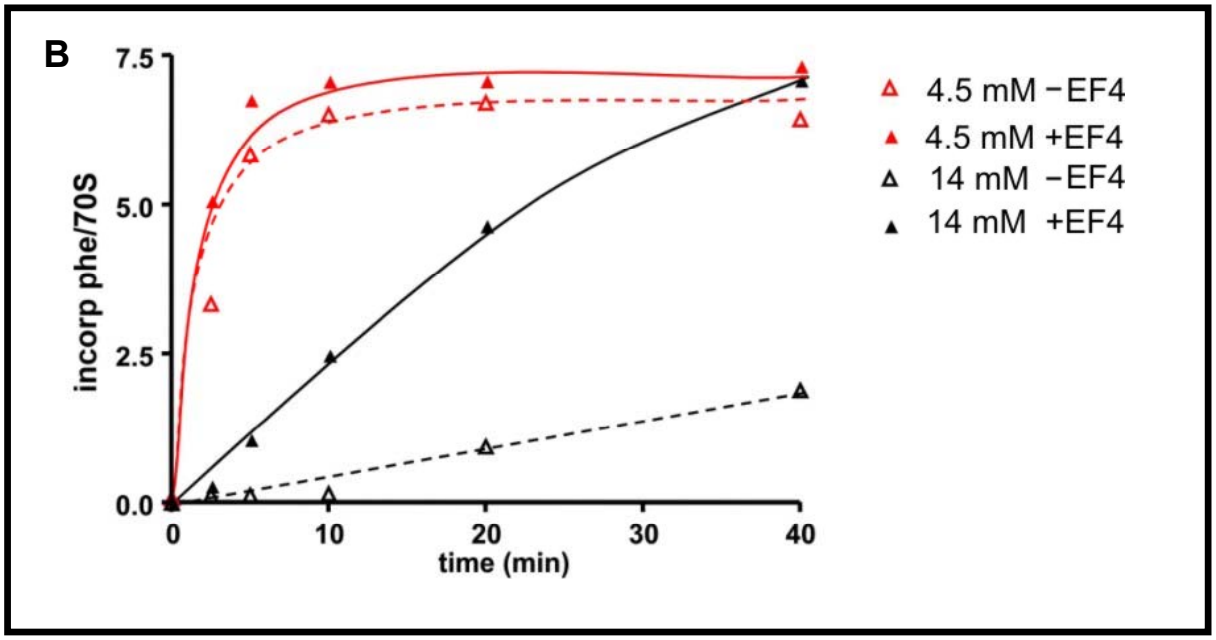

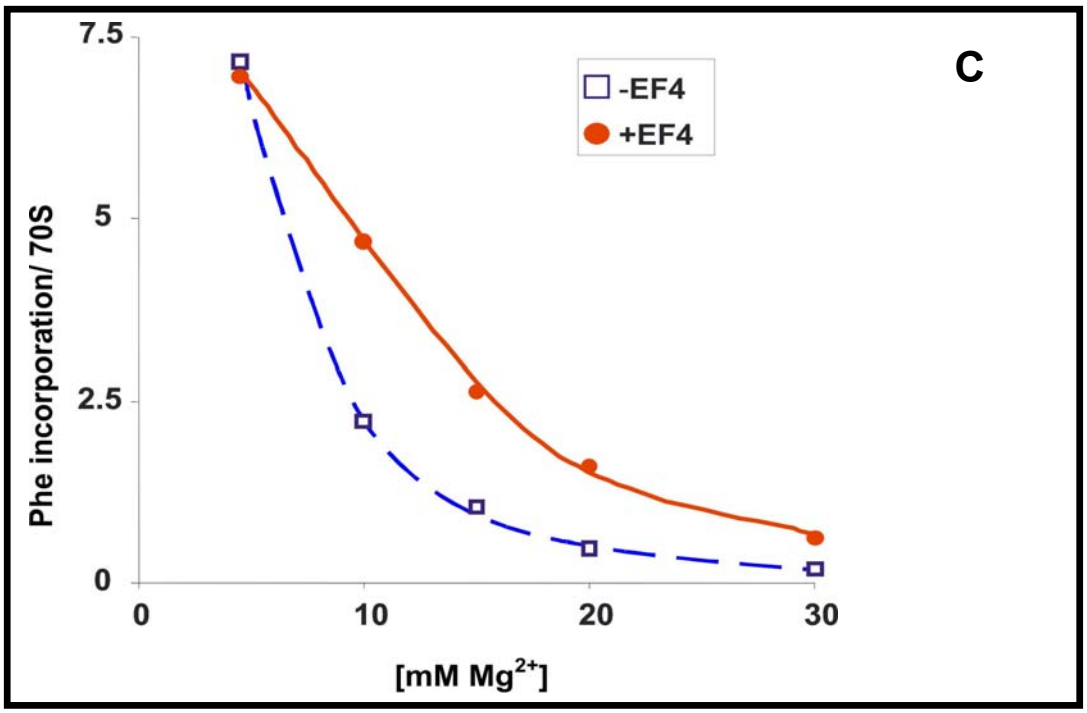

Figure 3.27 The effect of EF4 on poly(Phe) synthesis. A, tRNA binding assay, A and P site at 4.5 and 14 mM Mg^{2+}. B, Phe incorporation per 70S during 40 min at 4.5 and 14 mM Mg^{2+} in a purified system using precharged Phe-$tRNA^{Phe}$ and elongation factors, but no S100 enzymes. EF4 2-times over the ribosomes. C, Poly(U) dependent poly(Phe) synthesis without S100, and with increasing amount of mg^{2+} (4.5, 10, 15, 20, 30 mM.

3.5 EF4 GTPase activity in the presence of antibiotics

About 70% of all antibiotics target the ribosome and the purpose here is to study the uncoupled GTPase activity of EF4 with empty 70S ribosome in the presence of various antibiotics **(Table 3.3)** EF-G is in all the GTPase activity assays used as a positive control, since the antibiotic effects on the GTPase activity of EF-G are well studied already. Kanamycin as described in the table above is not affecting the GTPase activity, and thus is used as a negative control. As seen in **Figure 3.28** there is no inhibition of the GTPase activity of both EF4 and EF-G.

Table 3.3 Description of antibiotics that have been used in the following experiment

Antibiotics	Functions and effects on ribosome and factors
Kanamycin	An aminoglycoside that stimulates missense errors (Jelenc and Kurland 1984)
Thiostrepton	A modified peptide antibiotic that has several effects on translation. A prominent one is inhibition of uncoupled GTPase, it also prevents spontaneous EF-G dependent translocation, and furthermore the antibiotic inhibits transitions between PRE and POST state in both directions (Hausner, Geigenmüller et al. 1988).
Micrococcin	Has a binding site nearby to that of thiostrepton, while it has an contrasting effect on the GTPase activity of EF-G (Spahn and Prescott 1996)
Viomycin	Blocks EF-G dependent translocation but not GTP hydrolysis (Rodnina, Savelsbergh et al. 1999).
Neomycin	Aminoglycoside, causes mRNA miscoding, inhibits mRNA-tRNA translocation.
Fusidic acid	Steroidal antibiotic, allows translocation and GTP hydrolysis but prevents the release of P_i and stabilizes the EF-G (GTP) conformation on the ribosome. (Laurberg, Kristensen et al. 2000).

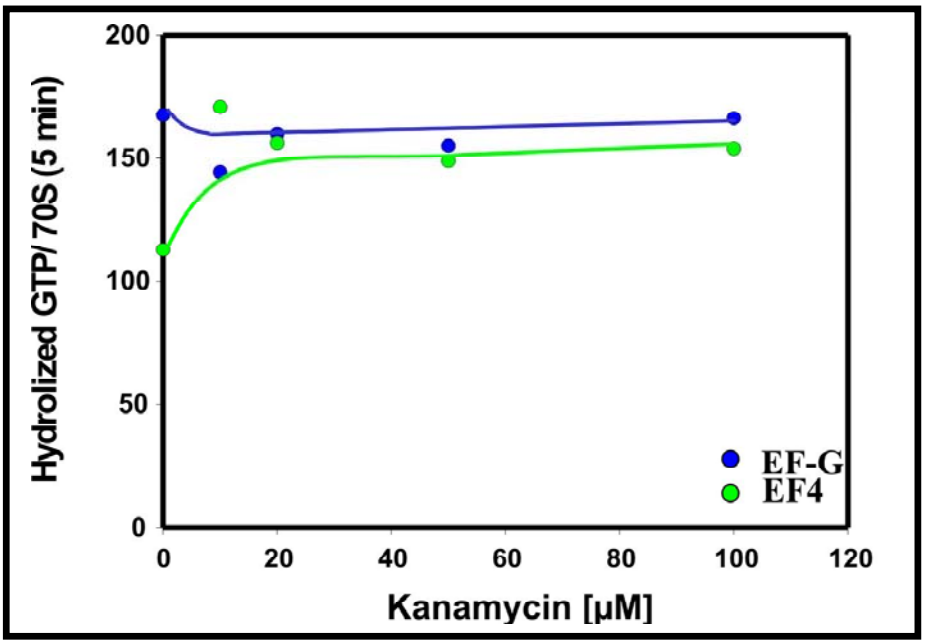

Figure 3.28 GTPase activity assay; 10 pmol factor, 5 pmol 70S, 50 μM [^{32}P] GTP, kanamycin 10, 20, 50 and 100 μM, incubation at 37°C for 5 minutes. EF4 and EF-G, green and blue, respectively.

Thiostrepton binds in the cleft between the ribosomal protein L11 and helices 43 and 44 of the 23S rRNA, which directly overlaps with the position of domain V of EF-G, and disturbs its function (Harms, Wilson et al. 2008), whereas the uncoupled GTPases activity of IF2 is stimulated (Cameron, Thompson et al. 2002). **Figure 3.29** shows that the GTPase activity of EF4 is inhibited with as low as 1 μM thiostrepton, which is a strong indication that thiostrepton has the same inhibition power on EF4 as well as on EF-G.

In a recent paper it has been shown that micrococcin does not bind to the same position as thiostrepton but nearby (Harms, Wilson et al. 2008). Unlike thiostrepton, micrococcin stimulates the GTPase activity of EF-G, and we tested micrococcin effects on EF4, which surprisingly showed that it inhibits EF4 uncoupled GTPase activity, whereas our results for EF-G are in agreement with previous data of (Cameron, Thompson et al. 2002) **(Figure 3.30)**.

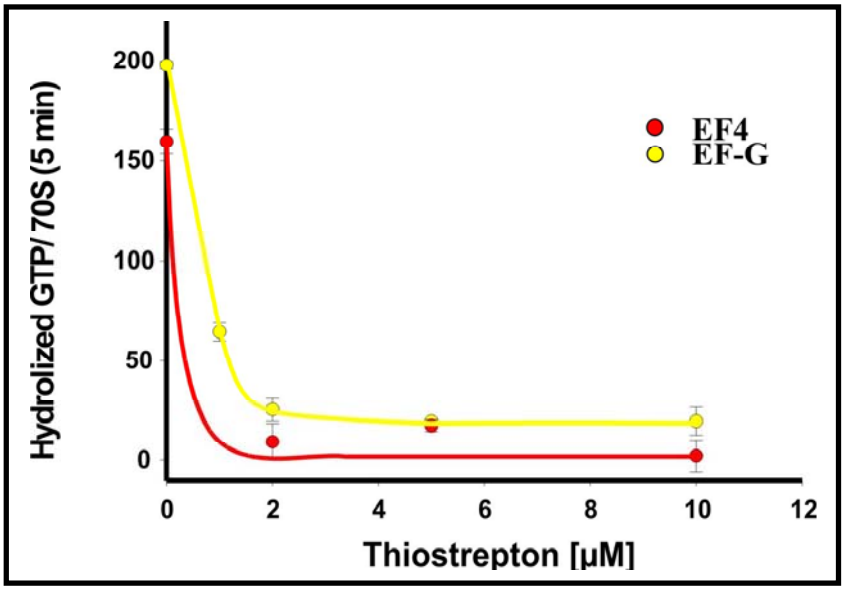

Figure 3.29 GTPase activity of EF4 and EF-G in the presence of thiostrepton. The conditions are as described in Figure 3.28 and the antibiotic thiostrepton dissolved in 50% DMSO with final concentration of 1% in the assay. Thiostrepton concentrations were 0.5, 1, 2, 5 µM.

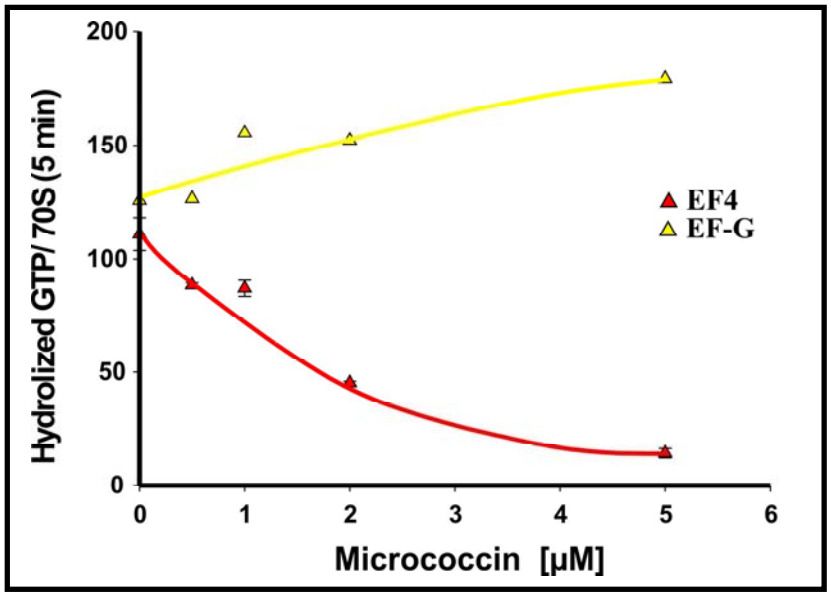

Figure 3.30 Inhibition and stimulation of uncoupled GTPase activity of EF4 and EF-G, respectively. For conditions see legend of Figure 3.29, micrococcin was dissolved in 50% methanol and the final concentration of methanol in the reaction was 1%.

Neomycin and viomycin were also tested, it is already known that GTP hydrolysis of EF-G is not affected by viomycin (Rodnina, Savelsbergh et al. 1997). Viomycin blocks EF-G dependent translocation but not GTP hydrolysis consistent with the results shown in **Figure 3.31,** viomycin seems even to stimulate the GTPase activity of EF4. For Neomycin the assay shows that the GTP hydrolysis of both EF-G and EF4 is also not affected or blocked (data not shown).

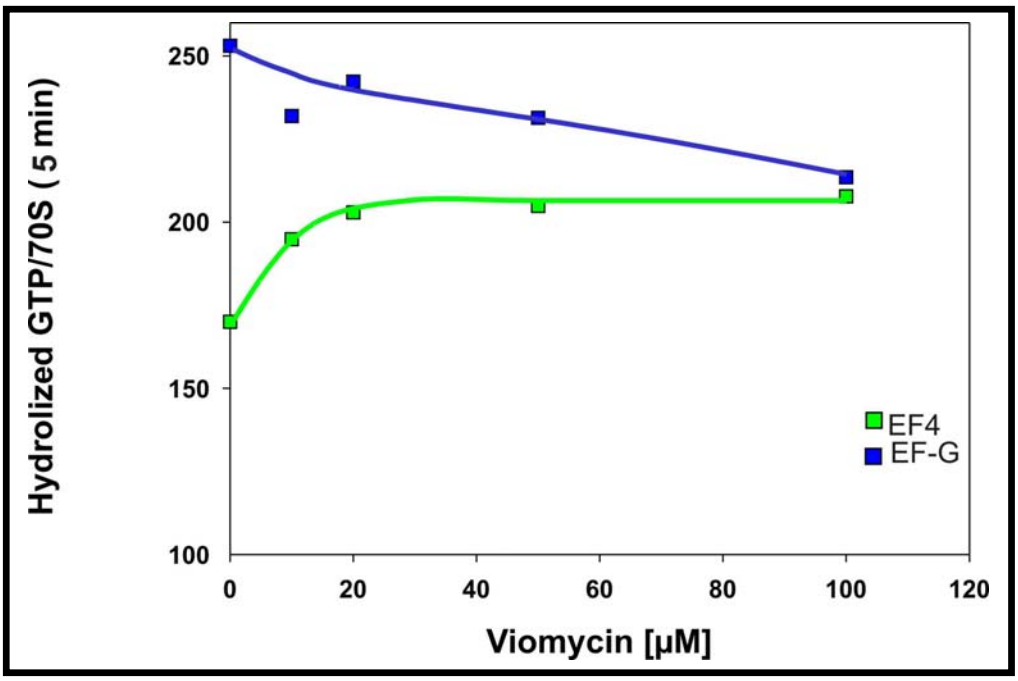

Figure 3.31 The viomycin effect on EF-G (blue) and EF4 (green). GTPase activity assay is performed as described in Figure 3.29. Viomycin concentrations were 10, 20, 50, 100 µM.

Fusidic acid is inhibiting protein synthesis by directly acting on EF-G (Laurberg, Kristensen et al. 2000). In the presence of fusidic acid EF-G remains bound to the ribosome after GTP hydrolysis, and this in turn prevents and blocks the protein synthesis. Due to structural similarities between EF-G and EF4 it was of particular interest to test fusidic acid effects on EF4. The results show clear inhibition of EF-G dependent GTP hydrolysis and less pronounced also for EF4 **(Figure 3.32).** This might due to some differences in the fusidic-acid binding pocket of EF-G and EF4, respectively (for more details see discussion).

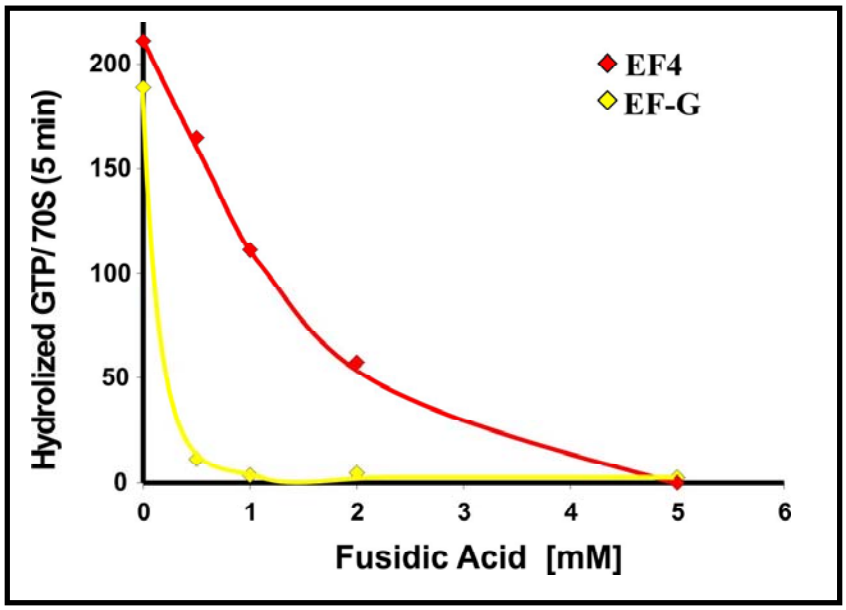

Figure 3.32 Inhibition of EF-G and EF4 GTPase activity with increasing amounts of fusidic acid (0.5, 1, 2, 5 mM).

3.6 Discrimination between EF-G, EF4 and EF-Tu on the ribosome for the same binding site

3.6.1 EF4 and EF-G

Some domains of EF-G, EF-Tu and EF4 are structural homologous and share nearly identical binding sites on the ribosome; these are the GTPase associated center (GAC) and the sarcin-ricin loop (SRL). The SRL is relatively immobile, while GAC, which consists of helices 43 and 44 and L11 and L10•(L7/L12)4 is flexible and make extensive movements. The GAC mobility is well studied; it can adopt mainly two different conformations "open" and "closed". The open conformation of GAC is characteristic for the POST state with EF-Tu•GTP, and closed conformation is favouring with EF-G•GTP. It is already known that EF-G and EF-Tu dependent GTPases show positive cooperativity effects on empty ribosomes (Mesters, Potapov et al. 1994).

In this section EF4 cooperativity with either EF-G or EF-Tu is checked on empty 70S. In this assay 3 pmol 70S, 3 pmol EF-G and increasing amounts of EF4 (0,1, 2, 4, 6 times over the 70S) were used and the GTP hydrolysis was monitored by [γ-^{32}P]GTP. The results shown in **Figure 3.33** demonstrate that EF-G alone and EF-G plus increasing amounts of EF4 have the same activity clearly indicating that EF-G and

EF4 compete with each other for the binding site, since as shown in **Figure 3.34** each of them has about the same GTPase activity.

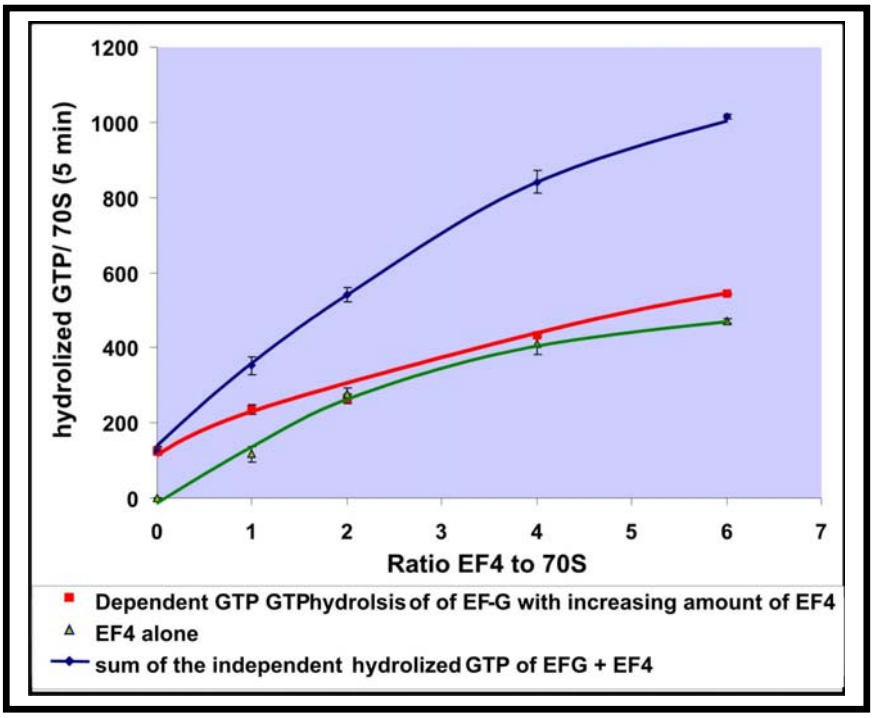

Figure 3.33 Hydrolized GTP per 70S monitored with increasing amounts of EF4. 70S (3 pmol), EF-G (3 pmol), EF4 (0, 3, 6, 12, 18 pmol), 50 µM GTP, total volume 50 µl.

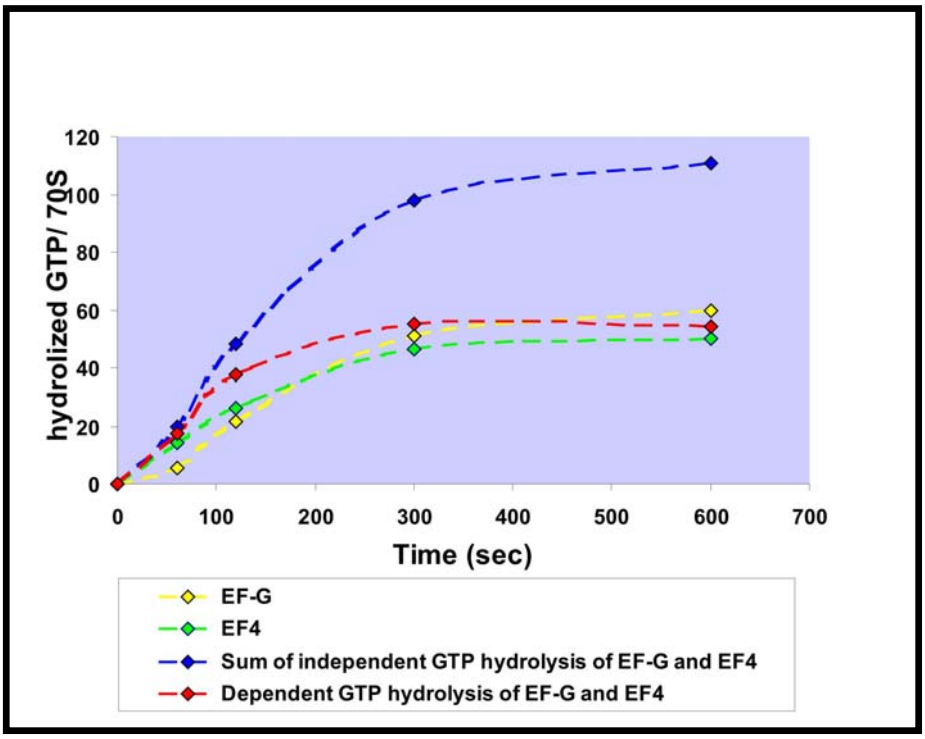

Figure3.34 Kinetics of hydrolized GTP per 70S. 70S (3 pmol), EF-G (3 pmol), EF4 (3 pmol), 50 µM GTP, total volume 50 µl.

3.6.2 EF4 and EF-Tu

Next we checked a possible cooperativity between EF4 and EF-Tu. The known EF-Tu and EF-G cooperativity is used as a positive control in this section. Uncoupled GTP hydrolysis of EF-Tu is extremely low in comparison to EF-G and EF4. Nevertheless the cooperativity still can be monitored in the case of EF-G **(Figure 3.35 A)**. The GTP hydrolysis of EF-G appears to be higher than the theoretical sum of the individual GTPase activities of EF-Tu and EF-G together confirming the previous results of (Mesters, Potapov et al. 1994). EF4 with increasing amounts of EF-Tu shows, surprisingly, also a cooperativity to a similar extent as in the case EF-G and EF-Tu **(Figure 3.35 B).**

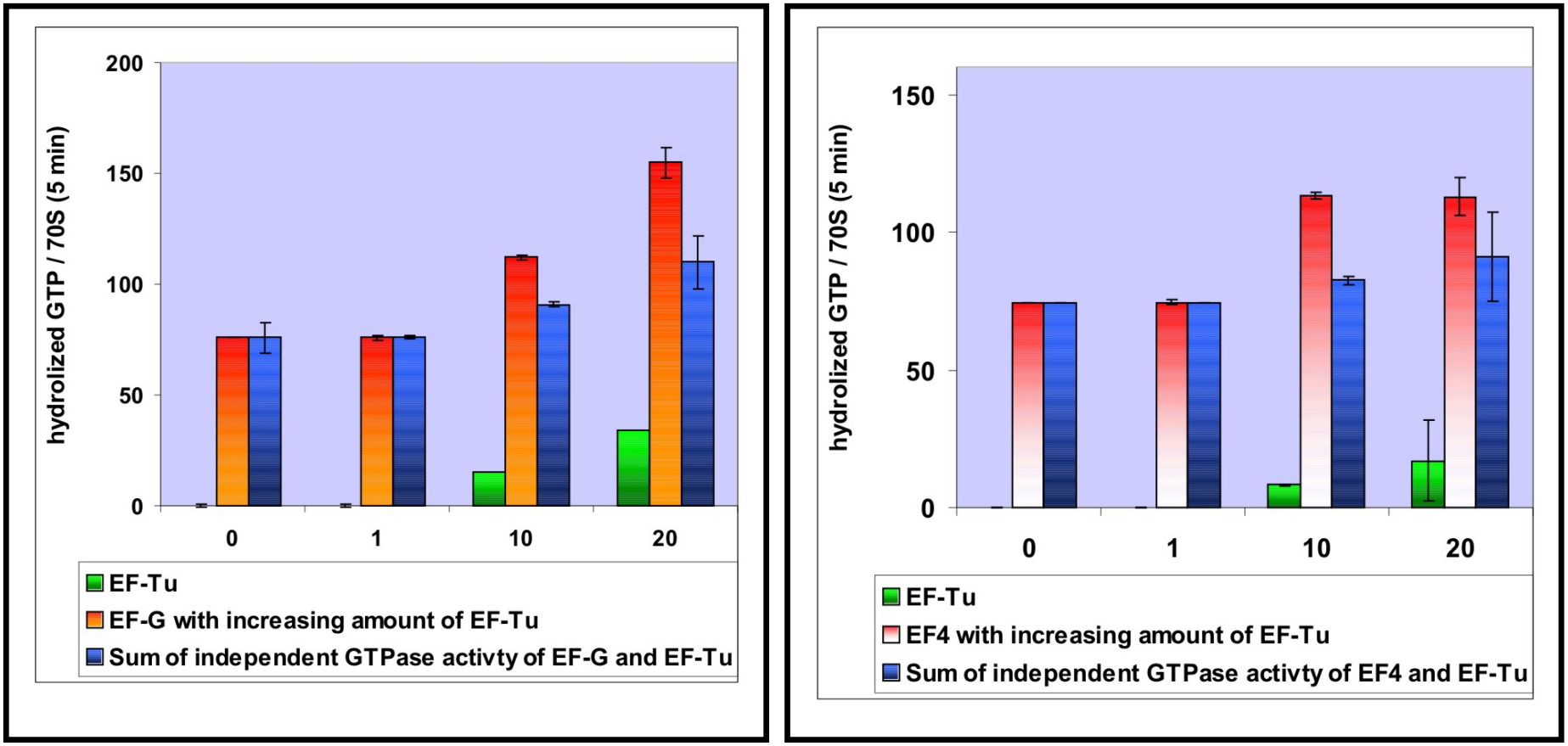

Figure 3.35 A) Cooperativity between EF-G and EF-Tu. 70S (3 pmol), EF-G (3 pmol), EF-Tu (3, 35 and 60 pmol), GTP (50 µM). Total volume/ reaction 50 µl.B) Cooperativity between EF4 and EF-Tu. 70S (3 pmol), EF4 (3 pmol), EF-Tu (0, 3, 30 and 60 pmol), GTP (50 µM). Total volume/ reaction 50 µl.

3.6.3 GFP activity test using RTS system

The total protein and active fraction of GFP was estimated in the presence and absence of EF4. The GFP synthesis in the RTS system was blocked by addition of 50 µM thiostrepton, and the total and active amounts were determined subsequently. The results are demonstrating that EF4 is increasing the active fraction of GFP post-translationally. It follows that EF4 has in addition to its ribosomal co-translational effects a chaperone like function.

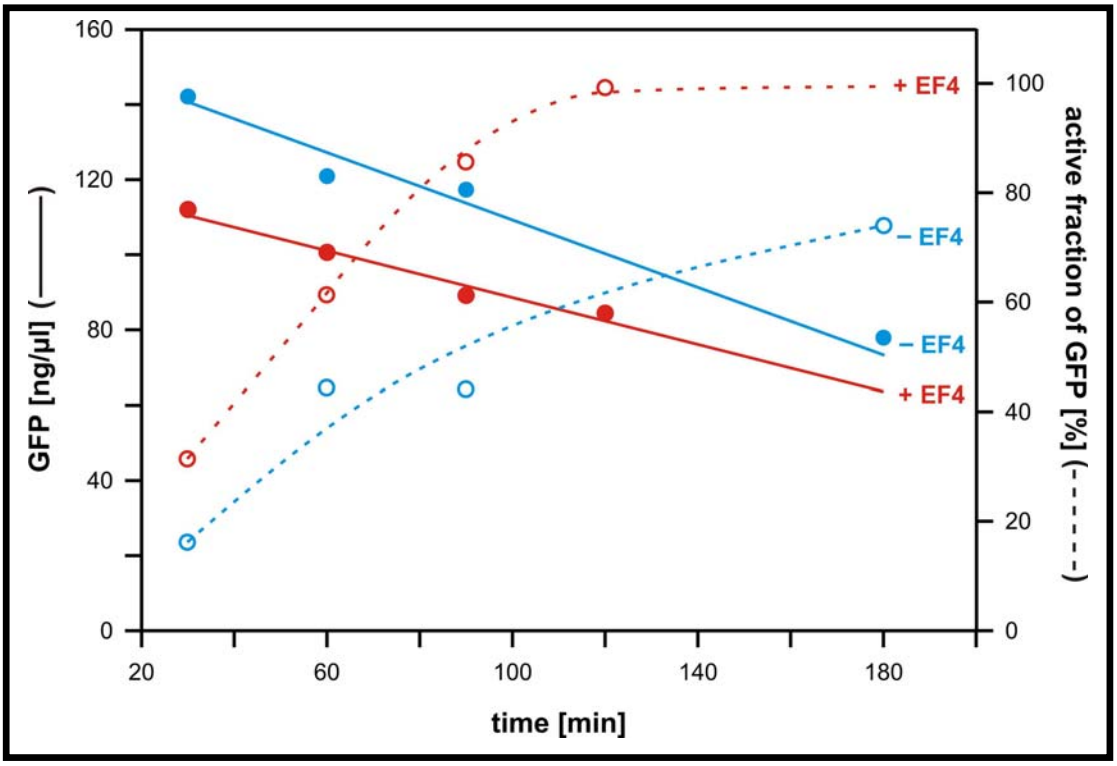

Figure 3.36 kinetic measurements of the reporter protein GFP synthesis after addition of thiostrepton with the RTS system presence and absence of EF4.

4 Discussion

4.1 EF4 is an old factor with a newly discovered function

The bacterial elongation factor EF4 is one of the most conserved proteins, more conserved than IF3 and EF-Ts with strong structural resemblance to EF-G. EF4 contains all EF-G domains except the 130 amino acid domain IV. This EF-G domain interacts with the decoding centre of the A-site part on the small ribosomal subunit; therefore it is considered to function as a “doorstop” by occupying the decoding region of the A site after the tRNAs have been translocated from A and P sites to P and E sites.

The first evidence that EF4 has a back translocation ability of tRNAs on ribosomes came from two distinct functional assays performed in our lab: puromycin reaction and dipeptide formation. Both Pi and POST states with AcPhe-tRNA as a donor at the P site are good substrates for both puromycin and aminoacyl-tRNA as an acceptor at the A site. EF4 blocked both puromycin reaction and peptide formation, when the ribosome is in its POST state, while leaving the Pi state unaffected. Furthermore, the toeprinting assay was clearly demonstrating that EF4 in the presence of GTP or GDPNP back-translocates the tRNA2•mRNA complex by a codon length from the POST state to the PRE state. Eventually, EF4 at low concentration enhanced the green fluorescent protein (GFP) synthesis in a coupled transcription-translation system and also increased the active fraction. This beneficial function was shown to be coupled to high Mg^{2+} concentrations, which distort the ribosomal structure and impair ribosomal reactions such as translocations. Such ill-translocated ribosomes might display their A-site codon in a suboptimal fashion and thus were thought to be one source of the well documented fact that high Mg^{2+} concentrations slow down protein synthesis and impair the accuracy of aminoacyl-tRNA selection at the A site.

Therefore, the function of EF4 was described in the following way: it recognizes improperly translocated ribosomes, back translocates them, and thus giving EF-G a second chance to catalyze a proper translocation reaction (Qin, Polacek et al. 2006). In this way it was thought to prevent misincorporations: An error-prone ill-translocated ribosome is back-translocated and thus resolves the dangerous situation and – overall – improves the accuracy of aminoacyl-tRNA selection.

This scientifically sound interpretation, however, bears a problem. It is known that a protein is surprisingly tolerant against misincorporations, only 1 in ~ 400 mis-incorporations is harmful for the protein's activity (Kurland, Jørgensen et al. 1990). The basic reason is that (i) practically exclusively near- cognate aminoacyl-tRNAs are selected instead of the cognate one and (ii) the current genetic code lexicon is organized in a way that the two to five near-cognate tRNAs bears an amino acid that is chemically similar to cognate tRNA. For example, if the amino acid of a cognate aminoacyl-tRNA is hydrophobic, the near-cognate aminoacyl-tRNAs are also hydrophobic. This is true even in error-inducing situations such as high Mg^{2+} concentrations or in the presence of aminoglycosides that can increase the misincorporations 30 to 100-fold (Szaflarski, Vesper et al. 2008). In contrast, the dangerous non-cognate aminoacyl-tRNAs representing the majority often are of different chemical nature as compared to that of the cognate one, and the selection of these ones is effectively prevented by intricate mechanisms of the ribosome (for review see (Nierhaus 2006)).

This fact prompted us to investigate again the physiological importance of EF4, the results are presented in this thesis.

4.2 EF4 is needed under high ionic strength in vivo

In vivo assays performed by Dibb and Wolf in 1986 (Dibb and Wolfe 1986) demonstrated that an EF4 gene knockout has no phenotype, the main reason that for about two decades no one was interested studying this protein. Only the flood of deciphered genomes revealed two important facts concerning EF4: (i) it is one of the best conserved proteins known, and (ii) it is extremely widely distributed, present in all bacteria, in mitochondria and chloroplasts. These facts prompted our group to study the importance of this protein and continued prompting us to find out the physiological importance of EF4 under non-permissive conditions. Using a sensitive method called growth competition, which is mainly used when a clear phenotype is not seen (Gutgsell, Deutscher et al. 2005), we tested the mutant to compete with the wildtype in an extended range of growth conditions.

Stress conditions such as high salts or low pH (e.g. pH 6) or low temperatures increase the intracellular K+ concentrations dramatically form 50 to 100 mM under relaxed conditions up to 1,000 mM (Wood, Bremer et al. 2001)! Under these

conditions the growth rate of cells lacking EF4 (MDEF4) is initially slow compared to that of wildtype cells, reason enough to become extinct in nature, but after 10 – 20 generations the growth rate of both cell types equalize, and remains so for many additional generations **(**see **Figures 3.11 and 3.12,** page 83-84**)**. This observation is consistent with the known two-phase response of bacterial osmoregulation. During the first phase the intracellular K^+ concentration, normally maintained at 60-100 mM, increases rapidly, reaching values as high as 1 M in *E. coli* (Richey, Cayley et al. 1987). In the second phase the disaccharide trehalose is synthesized resulting in a reduction of K^+ concentration down to its normal range (for review see Csonka and Hanson 1991).

Wild-type cells respond to the first surge phase in K^+ concentration by rapidly increasing the cytoplasmic level of EF4. This is not an option for the EF4-lacking cells, and this lack obviously causes a disadvantage for growth indicated by the decreased growth rate vis-à-vis that of wildtype. Interestingly, hyperosmotic conditions generally leave the interior of Archaea and Eukarya cells largely unchanged (Kunte 2006), including K^+ concentrations, which correlates with the lack of EF4 in these organisms.

EF4 is a large protein (599 amino acid residues in *E. coli*), raising the question of whether the wildtype cell has sufficient time to synthesize such a relatively large protein in sufficient amounts when the intracellular K^+ concentration rises. Alternatively, it could be that EF4 is stored in the membrane, from which it is released during the first phase of stress response. The latter certainly appears to be at least a major part of the story, given the large shift in the cytosol:membrane distribution of EF4, from 25:75 to 85:15 or to 55:45 induced by high Mg^{2+} (pH 6) or low temperature, respectively see **Figures 3.15 and 3.16,** pages 87-88.

4.3 Antibiotic affect on EF4

4.3.1 Thiostrepton and micrococcin affect differently the EF4 dependent GTPase

The ribosome is the major target of antibiotics, and it is known that they exclusively bind to the ribosomal RNAs. One of the antibiotic-binding sites on the ribosome is the GTPase associated centre (GAC), which is responsible for binding and stimulation of GTPase activity of translational factors such as EF-Tu, EF-G and EF4 and consists

of the helices H43 and 44 together with the proteins L11 and L10, the latter one is part of the pentameric complex $(L7/L12)_2$•L10. The structural similarities between EF-G and EF4 encouraged us to test, whether EF4 is also affected to the same extent by antibiotics that bind to the GTPase associated centre.

Thiostrepton and micrococcin bind to the GAC and affect the translation factor function, e.g. those of EF-G and IF2. Structural analyses of the binding sites of thiostrepton and micrococcin reveals that the two antibiotics have different binding position in the GAC, this is also in agreement with the protection assay showing one major difference in that the nucleotide A1067 in the 23S rRNA localized in the GAC is protected by thiostrepton (rather than by micrococcin), and that this drug causes inhibition of uncoupled GTPase activity of EF-G but exhibits enhanced reactivity upon micrococcin binding **(Figure 4.1)**. Thiostrepton is inhibiting the uncoupled GTPase activity of EF4 with an IC_{50} of 0.25 µM **(Figure 3.29,** page 106**)** revealing a comparable binding position of EF4 and EF-G in the GAC. On the other hand micrococcin inhibits the uncoupled GTPase activity of EF4 (IC_{50} 1.5 µM), which is in contrast to that of EF-G. In conclusion each antibiotic exerts diverse effect on the translation factors.

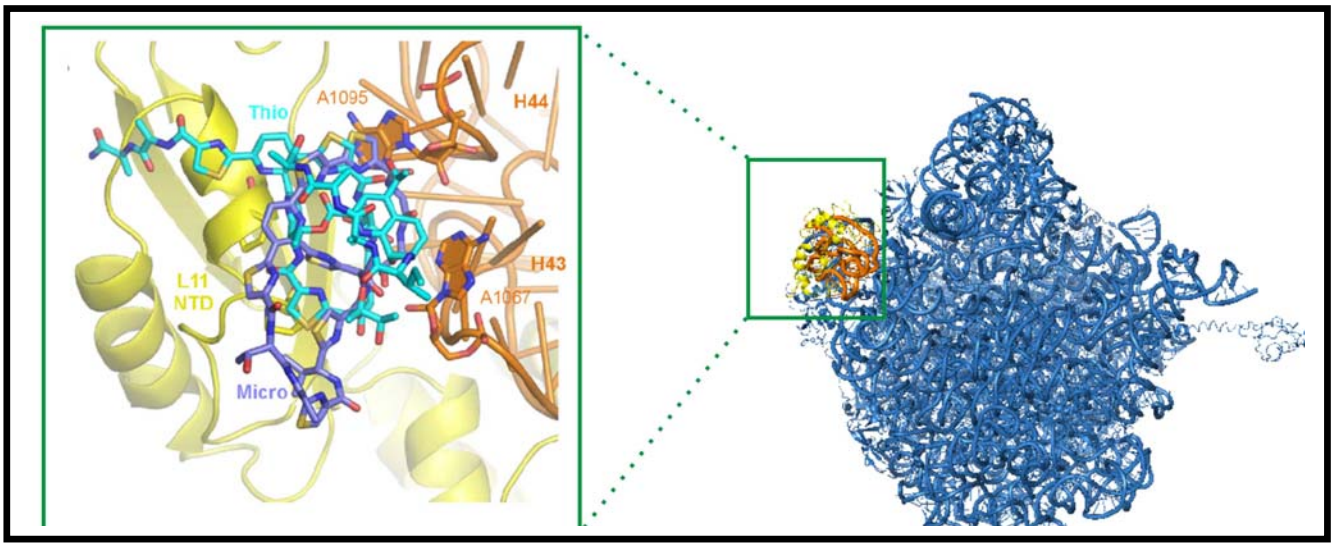

Figure 4.1 50S ribosome with H43 and H44 in orange and L11 in yellow. The zoomed part is showing the micrococcin (Micro) and thiostrepton (Thio) binding (Harms, Wilson et al. 2008). 50S structure was modified from PDB file (3I1N).

4.3.2 Fusidic acid binds to EF4

It is already known that fusidic acid binds to EF-G and blocks EF-G in the GDP conformer on the ribosome (Laurberg, Kristensen et al. 2000). Here we show that

fusidic acid blocks the uncoupled GTPase activity of EF-G, and interestingly it does the same with EF4, however, at higher concentrations. The 50% inhibition of the uncoupled EF-G inhibition was found at 0.25 mM and that of EF4 at 1.3 mM. We extrapolate our finding and assume that EF4 is also blocked on the ribosome in its GDP conformer in the same way as EF-G. **Figure 4.2** shows an alignment of both factors (EF4 in dark blue, EF-G in white-grey) in the region of the fusidic-acid binding pocket. The residues in pink in the zoomed insert indicate residues, that when mutated mediate resistance of EF-G against the drug.

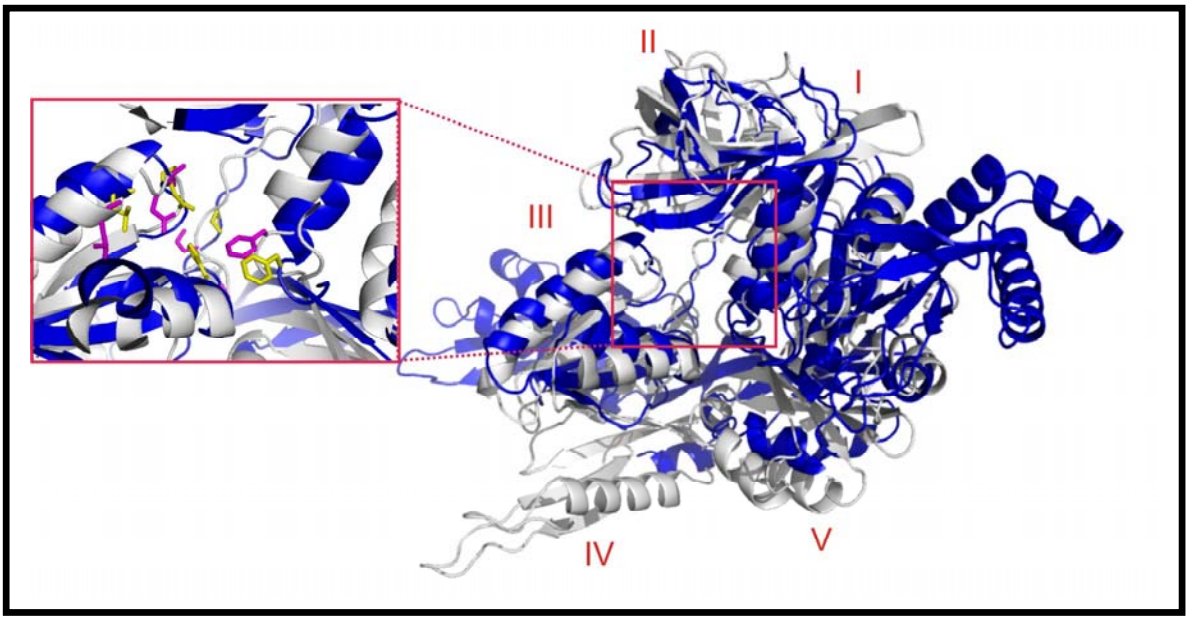

Figure 4.2 Structural alignment of EF4 (blue) and EF-G (white-grey), insert is enlarged figure of the fusidic acid pocket, which is based on mutational analysis (Laurberg, Kristensen et al. 2000). Amino acid residues from EF4 are in yellow and those of EF-G in purple. PDB files (EF4 (3DEG), EF-G (2J7K))

The fusidic acid biding pocket on EF-G is localized in the centre of the protein, which seems to be also true for EF4. The amino acid alignment of residues in the pocket **(**see **Table 4.1)** shows that there is one different amino acid: EF-G H-458 changed to EF4 Gly-344, which might cause an instable binding of fusidic acid in EF4 and thus explain why the concentrations of fusidic acid for blocking EF4 is higher than that for EF-G.

Table 4.1 the Amino acid alignment in the fusidic acid pocket of both EF-G and EF4

EF-4	EF-G
Phe-84	Phe-90
Pro-293	Pro-405
Leu-317	Leu-431
Asp-322	Asp-435
Ala-344	**Pro-436**
Gly-344	**H-458**

4.4 Cooperativity between EF4 and EFG versus EF4 and EF-Tu

All three translational GTPases mentioned in the heading are sharing near-identical binding sites on the GAC. The GAC is adopting two distinct conformations designated “open” and “close” referring to POST and PRE ribosomal states, respectively. EF-G is binding to PRE state ribosomes, while EF-Tu favors POST-state ribosomes. This also indicated by empty ribosomes, which might still have a “memory” for the PRE and POST states, since a cooperativity was observed concerning of uncoupled GPTase activity, when both EG-G and EF-Tu were present: The activity was higher than the sum of both individual activities (Mesters, Potapov et al. 1994), an observation that we reproduced in **Figure 3.35 A,** page 111. Both factors bind to the same ribosomal binding site enabled by the molecular mimicry between them (Nyborg, Nissen et al. 1996). Therefore it was of interest to study whether a similar cooperativity exists between EF4 and either EF-G or EF-Tu. Since EF-G is translocase and EF4 a back-translocase we anticipated that these two factors might show a cooperativity of their GTPases. Surprisingly, we found that EF4 is antagonizing EF-G **(Figures 3.33 and 3.34,** pages 109**)** and is competing for the same binding site, most likely a closed conformation of GAC. In contrast, cooperativity between EF-Tu and EF4 was observed at a level comparable to that of EF-G and EF-Tu **(Figure 3.35 B,** page 111**)**. Obviously, the empty ribosome cannot distinguish between the EF-G and EF4 due to structural similarities, however in the presence of tRNAs, the story might be different.

4.5 The importance of EF4: Reconciling the in vivo and in vitro effects

Under moderate conditions such as ~pH 7, EF4 is presence only in traces in the cytoplasm, but we observed large amounts in the membrane. Obviously EF4 is not needed under this condition explaining the lack of a phenotype, when EF4 is knocked out. In contrast we observe impaired growth at high ionic conditions: the strain lacking EF4 is easily overgrown by wild-type cells in growth competition experiments. In this unfavorable growth conditions a dramatic shift of EF4 from the membrane to the cytoplasm is observed. Obviously, the membrane is a storage organ for EF4.

The surprising *in vivo* experiments prompted us to pursue an *in vitro* EF4 analysis. Starting with our optimized poly(U) dependent poly(Phe) synthesis assay, which can yield 200 to 500 incorporated Phe on average per ribosome present in the assay (not considering the active fraction of ribosomes!), two surprising observations were made:

1: Under optimal condition (4.5 mM Mg^{2+} and polyamines) the error measured as incorporation of the near-cognate Leu is very low, about 1 Leu per 3,000 incorporated Phe, an accuracy also seen *in vivo*. Increasing the Mg^{2+} concentration up to 14 mM Mg^{2+} increases the error by several ten-folds, but **adding EF4 does not increase the error** (**Figure 3.26,** page 101). This is at variance with the assumption of Qin et al (Qin, Polacek et al. 2006). It follows that the observed increase of the active fraction upon EF4 addition has nothing to do with an improved accuracy but has to be explained in a different way.

2: In the same Figure the kinetics of poly(Phe) demonstrate another important feature, when EF4 was added: The **rate of poly(Phe) is significantly increased at higher Mg^{2+} concentrations upon EF4 addition**. Without EF4 the known effect of increasing the Mg^{2+} concentrations is seen: The higher the Mg^{2+} the slower the poly(Phe) synthesis obviously due to an increase of the fraction of stalled ribosomes (Szaflarski, Vesper et al. 2008). In these assays S100 enzymes were used, which probably contain EF4, therefore the changes seen upon addition of EF4 are minimal effects. In order to obtain a more precise picture of the EF4 effects, we applied a purified system for poly(Phe) synthesis using pre-charged Phe-tRNA and purified elongation factors EF-Tu, EF-Ts and EF-G. Now the EF4 effects are dramatic at higher Mg^{2+} concentrations, again under optimal 4.5 mM Mg^{2+} EF4 plays not role. At

a concentration of 30 mM Mg^{2+} all ribosomes are stalled and accordingly brings the poly(Phe) synthesis to a standstill. The strongest EF4 effect of poly(Phe) synthesis was seen around 14 mM Mg^{2+} with an acceleration factor of 2- to 5-fold **(Figure 3.27 B and C**, pages 102 and 103**)**.

We underline that the EF4 acceleration effect of protein synthesis is a total surprise, since the function of a back-translocation should *prima vista* result in a retardation rather than acceleration of protein synthesis. And in line with this idea, the EF4 effect of increasing the accuracy was thought to be related to an assumed retardation of protein synthesis according to the general wisdom "*the slower, the better*", or adapted to our case "the slower, the more accurate". The overall acceleration effect of EF4 and its back-translocation function suggests that EF4 recognized stalled ribosomes, mobilizes them and thus provokes acceleration. On polysomes mobilization of a single ribosome has even a negative amplification as consequence, namely all the following ribosomes on the same mRNA are also blocked by just a single stalled ribosomes **(Figure 4.3)**. We conclude that back-translocation and acceleration of protein synthesis are just two sides of the same coin, and that mobilization of stalled ribosomes is the central function of EF4.

But how we explain the increase in the active fraction observed by Qin et al (Qin, Polacek et al. 2006) A recent paper by Ignatova's group might give the answer (Zhang, Hubalewska et al. 2009). They observed that rare codons are preferentially used after domains, so that ribosomes pause after synthesizing a domain and thus support the folding of this domain. If artificially the pausing sites are moved into the middle of a domain, the active fraction of the corresponding proteins is reduced. One important consequence concerning EF4 is that under non-stressed conditions EF4 should not interfere with pausing ribosomes that are beneficial for co-translational folding. This explains why it might even advantageous not to have EF4 in the cytoplasm under these conditions explaining the trace amounts of EF4 observed.

If at higher ionic strength unscheduled pausing shows up that do not follow or observe domain borders within a protein, folding might be significantly impaired. It is this point that requires now the presence of EF4 in the cytoplasm: It recognizes and mobilizes unscheduled stalling ribosomes thus having two beneficial effects for the cell, namely the overall acceleration of protein synthesis and the increase of the active fraction. It might be important to have EF4 ready at the storage place

“membrane”, so that now time is wasted for synthesizing significant amounts of EF4 with its length of 599 amino acids.

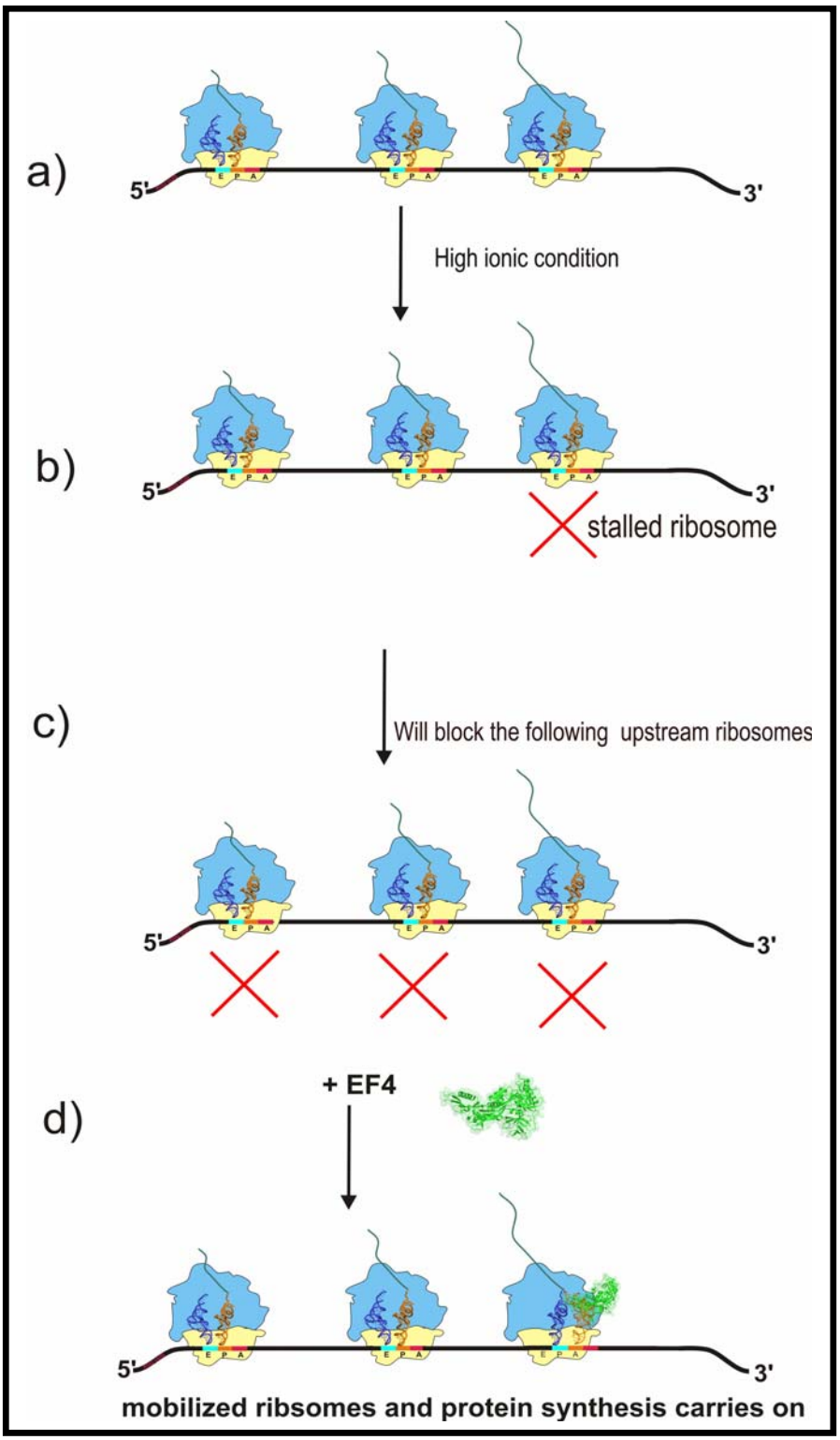

Figure 4.3 Model demonstrating EF4 importance at high ionic strength. A) Normal protein synthesis; B) high ionic strength leads to a single stalled ribosome on a polysome; C) upstream ribosomes are therefore blocked stopping protein synthesis on this mRNA. D) EF4 addition rescues the stalled ribosome by provoking a back-translocation towards PRE state that can be correctly translocated by EF-G allowing translation of the following ribosomes as well.

5 Appendix

5.1 Appendix I

5.1.1 Purification of Homosapiens mitochondria EF4 (HsmEF4)

HsmEF4 is highly conserved in mitochondria and exhibits strong amino acid similarities to bacterial EF4. The function of HsmEF4 is still not known. Our purpose in this section is to purify the active protein, which can be used for further analysis.

5.1.2 HsmEF4 protein purification protocol

The HsmEF4 gene was cloned into pET-28a carrying a N terminal His-tag. and transformed into *E. coli* BL21 (DE3) strain then plated on LB + Kan (50 µg/ ml). One single colony was inoculated into 200 ml LB + KAN (50 µg/ ml) incubated at 37 °C with 170 rpm overnight. The Main culture was prepared by inoculating 16 l of LB medium + Kan (50 µg/ ml) with 1:100 dilution of the preculture then the culture was incubated until it reached OD_{600} 0.4 and induced with 1 mM IPTG, followed by additional incubation for 2 hours. The cells are then harvested by centrifugation at 6,000 rpm for 10 min at 4 °C and resuspended in buffer A. The cells were then disrupted with 3 passages through the microfluidizer to lysate the cells. Subsequently the cell lysate was centrifuged at 35,000 rpm for 1 hour at 4 °C to separate the supernatant from the cell debris and prepared for NiNTA- agarose. 3.5 ml of the NiNTA was used in polypropylene columns, and the column was equilibrated with buffer A by washing with 2 X column volume (CV). The supernatant was applied on the column and washed with 8x CV buffer A+ 10 mM imidazole. The protein is then eluted with using buffer A with different imidazole concentrations (100 mM, 200 mM, 300 mM). The fractions where the protein is eluted is pooled diluted 2:3 with buffer B1 this gives a final concentration of 200 mM K^+. And then subjected to FPLC where further purified with anionic exchange chromatography (MonoQ).The protein is then eluted via step gradient from 200 mM K^+ to 1000 mM K^+. The collected fractions are dialysed with the storage buffer 3x 45 min in 100x the current volume.

5.1.3 Purification outcome

HsmEF4 is a mitochondrial protein and the expression of this protein in *E. coli* is very low, due to that fact the amount of culture medium was increased to 16 l in order to get sufficient amount of cells.

The eluted samples from NiNTA fractions number E2-4 shows that the overproduced protein is consistent of many bands that might be either degradation products or impurities. Nevertheless the fractions E2-E4 were pooled and with anionic exchange we tried to catch the correct size of the protein, the first trial with cationic exchange didn't work we improved the binding conditions to the monoQ column by decreasing the B1 and B2 buffer pH to 6.9. But unfortunately the first cationic exchange trial was not pure as depicted in **Figure 5.2**. The purified protein had many additional bands. To eliminate the "impurities" the sample for the second time was subjected to MonoQ with smaller step gradient interval in order to be able to separate the two upper bands shown in **Figure 5.1**.

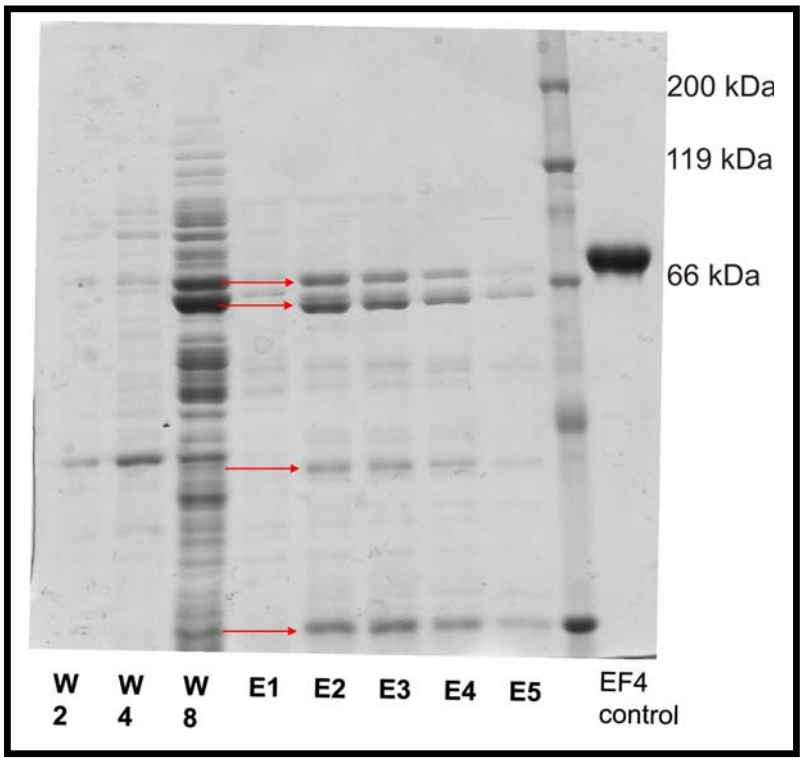

Figure 5.1 The NiNTA elution of HsmEF4, W (wash), E (elution). 25 pmol EF4 as control.

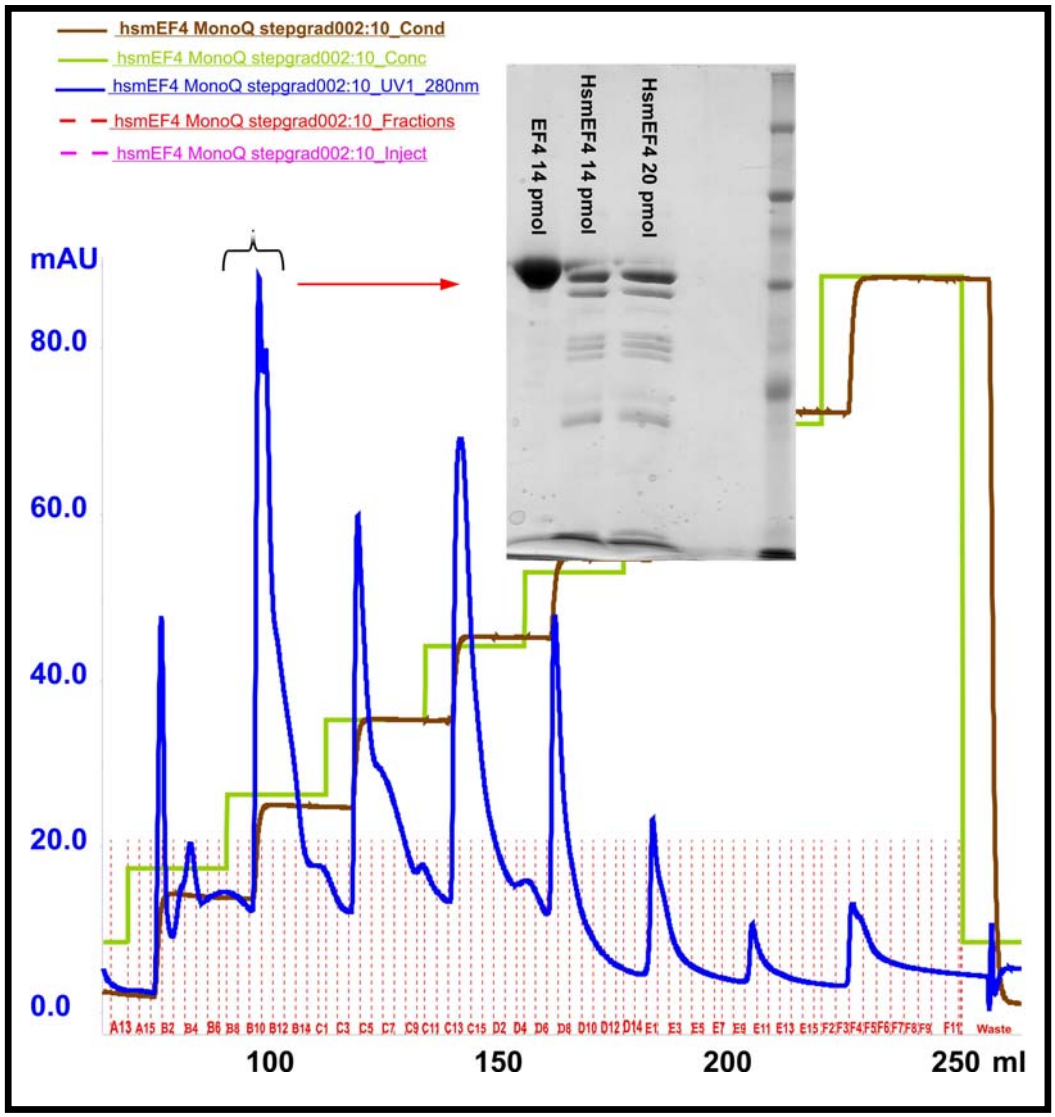

Figure 5.2 A step gradient FPLC with anionic exchange (200-1000 mM K^+). The marked peak fractions were combined and run on an SDS-PAGE gel. Insert shows the purified protein after concentration.

This time, we were able to remove many of the additional bands and also to separate the two major protein fractions present in the second and third peak **(**SDS-PAGE gel insert in **figure 5.3).** The pooled fractions (number 2) contain the purest charge, which will be further analysed in our functional assays for EF4.

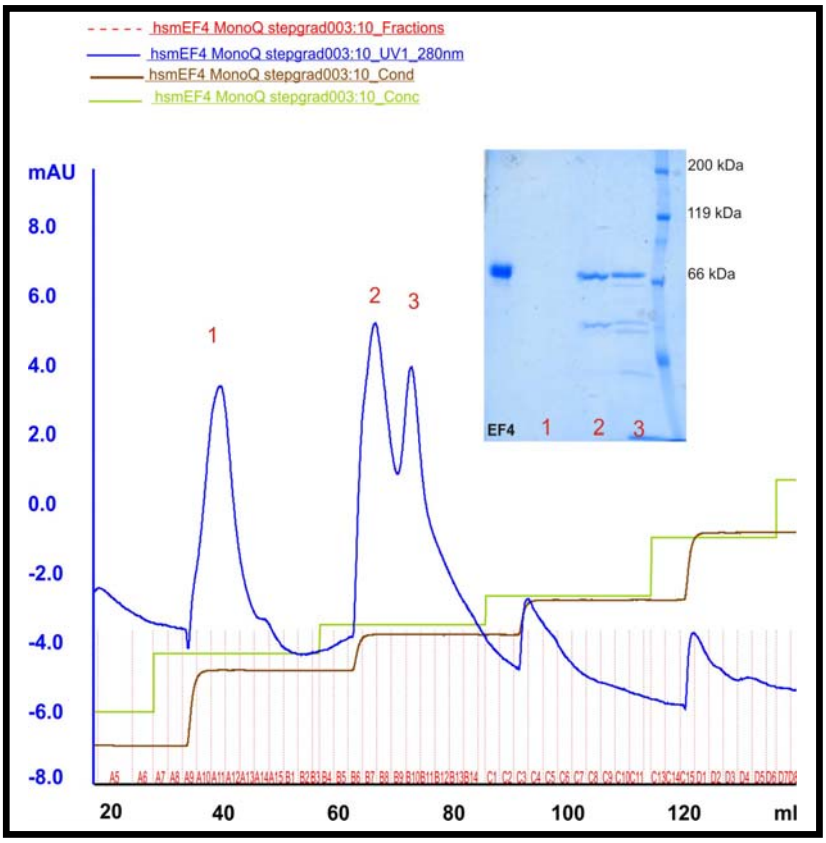

Figure 5.3 Step gradient extending for 200-1000 mM K^+, with small fraction collection 2.5 ml/ fraction (due to many fractions the numbering of the fractions can not be seen). The SDS-PAGE gel insert is showing the following three peaks protein content.

Table 1 Buffers for purification of HsmEF4

Buffer A (Ni-NTA) pH 8.0	Na_2HPO_4 NaH_2PO4 NaCl	46.6 mM 3.4 mM 300 mM
Buffer B_1 (MonoQ) pH 6.9	Hepes- KOH	20 mM
Buffer B_2 (MonoQ) pH 6.9	Hepes-KOH K-Acetate	20 mM 1 M
Buffer C (storage buffer)	Hepes-KOH pH 7.6 K- Acetate BME Glycerol	20 mM 500 mM 4 mM 10%

EF4 AB buffer (Adjustment buffer)	Hepes-KOH pH 7.6 Mg-Acetate ß-Mercaptoethanol Spermidine Spermine	20 mM 6 mM 30 mM 2.7 mM 0.07 mM

Appendix II

Primers that are used in this thesis.

Primers 5 ➡ ’3’ used for PCR confirmation of Knockout strain JW2553

Forward flank ^{2705983}	GAAACATCTTCggAAgACgCgAgCC (25 mer)
Reveres-Flank ^{2703752}	CCAgTACCggAAAAACAgAAgCACC (25 mer)
EF4 internal primer	GAAgTTgTAATCCAgAgACgC
EF4 N-terminal	gAATATACgTAACTTTTCgATCAT
EF4 C-terminal	gTCTTTgCCgACgTgCAg

Primers 5’➡ 3’ used for EF4 cloning into pET-28a

Ecolepfor	gAgAAgTTCATATgAAgAATATACgTAAC
Ecoleprev	TAgggATCATTATTTgTTgTCTTTgCCg

Primers 5’ ➡ 3’ used for EF4 cloning into pZS*24-MCS-1-28a

Fw lepA	ggggTACCATgAAgAATATACGTAACTTTTCg
Rv lepA	gggggggATCgATTTATTTgTTgTCTTTgCCgACgTg

Primers 5’ ➡ 3’ used for HsmEF4 cloning into pZS*24-MCS-1-28a

Fw mito	gCggTACCATggCgCCGACCCTTggg
Rv mito	gggggCATCgATTCAgCTTTTTTTCCCTTCTg

Bibliography

Agrawal, R. K., C. M. T. Spahn, et al. (2000). "Visualization of tRNA movements on the *Escherichia coli* 70S ribosome during the elongation cycle." J. Cell. Biol. **150**: 447-459.

Allen, D. W. and P. C. Zamecnik (1962). "The effect of puromycin on rabbit reticulocyte ribosomes." Biochim. Biophys. Acta **55**: 865-874.

Baba, T., T. Ara, et al. (2006). "Construction of Escherichia coli K-12 in-frame, single-gene knockout mutants: the Keio collection." Mol. Syst. Biol. **2**: 2006 0008.

Ban, N., P. Nissen, et al. (2000). "The complete atomic structure of the large ribosomal subunit at 2.4 Å resolution." Science **289**: 905-920.

Barondes, S. H. and M. W. Nirenberg (1962). "Fate of a Synthetic Polynucleotide Directing Cell-Free Protein Synthesis II. Association with Ribosomes." Science **138**(3542): 813-817.

Bauerschmitt, H., S. Funes, et al. (2008). "The membrane-bound GTPase Guf1 promotes mitochondrial protein synthesis under suboptimal conditions." J. Biol. Chem. **283**(25): 17139-17146.

Bergemann, K. and K. H. Nierhaus (1983). "Spontaneous, elongation factor G independent translocation of *Escherichia coli* ribosomes." J. Biol. Chem. **258**(24): 15105-15113.

Bijlsma, J. J., A. L. M. Lie, et al. (2000). "Identification of loci essential for the growth of *Helicobacter pylori* under acidic conditions." J. Infect. Dis. **182**(5): 1566-1569.

Blaha, G., R. E. Stanley, et al. (2009). "Formation of the first peptide bond: the structure of EF-P bound to the 70S ribosome." Science **325**(5943): 966-970.

Blattner FR, P. G. r., Bloch CA, Perna NT, Burland V, Riley M, Collado-Vides J, Glasner JD, Rode CK, Mayhew GF, Gregor J, Davis NW, Kirkpatrick HA, Goeden MA, Rose DJ, Mau B, Shao Y. (1997). "The complete genome sequence of Escherichia coli K-12." Science **277**(5331): 1453-62.

Bretscher, M. S. (1968). "Translocation in protein synthesis: a hybrid structure model." Nature **218**(142): 675-7.

Brodersen, D. E., W. M. Clemons, Jr., et al. (2002). "Crystal structure of the 30 S ribosomal subunit from Thermus thermophilus: structure of the proteins and their interactions with 16 S RNA." J. Mol. Biol. **316**(3): 725-68.

Cameron, D. M., J. Thompson, et al. (2002). "Initiation factor IF2, thiostrepton and micrococcin prevent the binding of elongation factor G to the Escherichia coli ribosome." J. Mol. Biol. **319**(1): 27-35.

Carter, A. P., W. M. Clemons, Jr., et al. (2001). "Crystal structure of an initiation factor bound to the 30S ribosomal subunit." Science **291**(5503): 498-501.

Caskey, T., E. Scolnick, et al. (1969). Peptide chain termination, codon, protein factor, and ribosomal requirements. Cold Spring Harbor Symp. Quant. Biol. **34:** 479-491.

Cate, J. H., M. M. Yusupov, et al. (1999). "X-ray crystal structures of 70S ribosome functional complexes." Science **285**: 2095-2104.

Celano, B., R. T. Pawlik, et al. (1988). "Interaction of Escherichia coli, translation-initiation factor IF-1 with ribosomes." Eur. J. Biochem. **178**(2): 351-5.

Connell, S. R., C. Takemoto, et al. (2007). "Structural basis for interaction of the ribosome with the switch regions of GTP-bound elongation factors." Mol. Cell **25**(5): 751-764.

Connell, S. R., M. Topf, et al. (2008). "A new tRNA intermediate revealed on the ribosome during EF4-mediated back-translocation." Nat Struct Mol Biol **15**(9): 910-5.

Cornish, P. V., D. N. Ermolenko, et al. (2008). "Spontaneous intersubunit rotation in single ribosomes." Mol. Cell **30**(5): 578-588.

Crick, F. H. C. (1966). "Codon-anticodon pairing: The wobble hypothesis." J. Mol. Biol. **19**: 548-555.

Csonka, L. N. and A. D. Hanson (1991). "Prokaryotic osmoregulation: genetics and physiology." Annu Rev Microbiol **45**: 569-606.

Cukras, A. R., D. R. Southworth, et al. (2003). "Ribosomal proteins S12 and S13 function as control elements for translocation of the mRNA:tRNA complex." Mol. Cell **12**(2): 321-328.

Deutscher, M. P., C. W. Marlor, et al. (1984). "Ribonuclease T: New exoribonuclease possibly involved in end-turnover of tRNA." Proc. Natl. Acad. Sci. USA **81**: 4290 - 4293.

Di Giacco, V., V. Marquez, et al. (2008). "Shine-Dalgarno interaction prevents incorporation of noncognate amino acids at the codon following the AUG." Proc. Natl. Acad. Sci. U S A **105**(31): 10715-10720.

Dibb, N. J. and P. B. Wolfe (1986). "lep operon proximal gene is not required for growth or secretion by *Escherichia coli*." J. Bacteriol. **166**(1): 83-87.

Evans, R. N., G. Blaha, et al. (2008). "The structure of LepA, the ribosomal back translocase." Proc. Natl. Acad. Sci. U S A **105**(12): 4673-4678.

Frank, J. and R. K. Agrawal (2000). "A ratchet-like inter-subunit reorganization of the ribosome during translocation." Nature **406**: 318-322.

Frank, J., H. Gao, et al. (2007). "The process of mRNA-tRNA translocation." Proc. Natl. Acad. Sci. U S A **104**(50): 19671-19678.

Furano, A. V. (1975). "Content of elongation factor Tu in *Escherichia coli*." Proc. Natl. Acad. Sci. U S A **72**(12): 4780-4784.

Gao, H., J. Sengupta, et al. (2003). "Study of the structural dynamics of the *E. coli* 70S ribosome using real-space refinement." Cell **113**: **789–801**.

Gavrilova, L. P. and A. S. Spirin (1971). "Stimulation of 'non-enzymic' translocation in ribosome by p -chloromercuribenzoate." FEBS Lett. **17**(2): 324-326.

Gnirke, A., U. Geigenmüller, et al. (1989). "The allosteric three-site model for the ribosomal elongation cycle." J. Biol. Chem. **264**: 7291-7301.

Green, R. and H. F. Noller (1997). "Ribosomes and translation." Annu. Rev. Biochem. **66**: 679-716.

Grunberg-Manago, M., P. Dessen, et al. (1975). "Light-scattering studies showing the effect of initiation factors on the reversible dissociation of *Escherichia coli* ribosomes." J. Mol. Biol. **94**(3): 461-478.

Gutgsell, N. S., M. P. Deutscher, et al. (2005). "The pseudouridine synthase RluD is required for normal ribosome assembly and function in *Escherichia coli*." RNA **11**: 1141–1152.

Halic, M., T. Becker, et al. (2004). "Structure of the signal recognition particle interacting with the elongation-arrested ribosome." Nature **427**(6977): 808-814.

Hanawa-Suetsugu, K., S. Sekine, et al. (2004). "Crystal structure of elongation factor P from *Thermus thermophilus* HB8." Proc. Natl. Acad. Sci. U S A **101**(26): 9595-9600.

Harms, J., F. Schluenzen, et al. (2001). "High resolution structure of the large ribosomal subunit from a mesophilic eubacterium." Cell **107**(5): 679-688.

Harms, J. M., D. N. Wilson, et al. (2008). "Translational Regulation via L11: Molecular Switches on the Ribosome Turned On and Off by Thiostrepton and Micrococcin." Mol. Cell **30**(1): 26-38.

Hausner, T. P., U. Geigenmüller, et al. (1988). "The allosteric three site model for the ribosomal elongation cycle. New insights into the inhibition mechanisms of aminoglycosides, thiostrepton, and viomycin." J. Biol. Chem. **263**(26): 13103-13111.

Hirokawa, G., N. Iwakura, et al. (2008). "The role of GTP in transient splitting of 70S ribosomes by RRF (ribosome recycling factor) and EF-G (elongation factor G)." Nucleic Acids Res. **36**(21): 6676-6687.

Jelenc, P. C. and C. G. Kurland (1984). "Multiple effects of kanamycin on translational accuracy." Mol. Gen. Genet **194**(1-2): 195-199.

Komoda, T., N. S. Sato, et al. (2006). "The A-site finger in 23 S rRNA acts as a functional attenuator for translocation." J. Biol. Chem. **281**(43): 32303-32309.

Kunte, H. (2006). "Osmoregulation in bacteria: Compatible solute accumulation." Osmosensing Environ. Chem. **3**: 94-99.

Kurland, C. G., F. Jørgensen, et al. (1990). Through the accuracy window. The Ribosome- Structure, Function, and Evolution. A. Dahlberg, W. E. Hill, R. A. Garrettet al. Washington, D. C., Amer. Soc. Microbiol.**:** 513-526.

Laurberg, M., O. Kristensen, et al. (2000). "Structure of a mutant EF-G reveals domain III and possibly the fusidic acid binding site." J. Mol. Biol. **303**(4): 593-603.

Lipmann, F. (1963). "Messenger ribonucleic acid." Prog. Natl. Acid. Res. **1**: 135-161.

Lutz, R. and H. Bujard (1997). "Independent and tight regulation of transcriptional units in Escherichia coli via the LacR/O, the TetR/O and AraC/I1-I2 regulatory elements." Nucleic Acids Res. **25**(6): 1203-1210.

Manen, D., G. Xia, et al. (1994). "A locus involved in the regulation of replication in plasmid pSC101." Mol. Microbiol. **11**(5): 875-884.

March, P. E. and M. Inouye (1985). "Characterization of the lep operon of *Escherichia coli*. Identification of the promoter and the gene upstream of the signal peptidase I gene." J. Biol. Chem. **260**(12): 7206-7213.

March, P. E. and M. Inouye (1985). "GTP-binding membrane protein of *Escherichia coli* with sequence homology to initiation factor 2 and elongation factors Tu and G." Proc. Natl. Acad. Sci. U S A **82**(22): 7500-7504.

Margus, T., M. Remm, et al. (2007). "Phylogenetic distribution of translational GTPases in bacteria." BMC Genomics **8**: 15.

Marquez, V., D. N. Wilson, et al. (2004). "Maintaining the ribosomal reading frame: The influence of the E site during translational regulation of release factor 2." Cell **118**(1): 45-55.

Martemyanov, K. A. and A. T. Gudkov (1999). "Domain IV of elongation factor G from Thermus thermophilus is strictly required for translocation." FEBS Lett. **452**(3): 155-159.

Mesters, J. R., A. P. Potapov, et al. (1994). "Synergism between the GTPase activities of EF-Tu.GTP and EF-G.GTP on empty ribosomes. Elongation factors as stimulators of the ribosomal oscillation between two conformations." J. Mol. Biol. **242**(5): 644-654.

Moazed, D. and H. F. Noller (1989). "Intermediate states in the movement of transfer RNA in the ribosome." Nature **342**: 142-148.

Munro, J. B., R. B. Altman, et al. (2007). "Identification of two distinct hybrid state intermediates on the ribosome." Mol. Cell **25**(4): 505-517.

Nakabachi, A., A. Yamashita, et al. (2006). "The 160-kilobase genome of the bacterial endosymbiont Carsonella." Science **314**(5797): 267.

Nierhaus, K. H. (2006). "Decoding errors and the involvement of the E-site." Biochimie **88**: 1013-1019.

Nissen, P., J. Hansen, et al. (2000). "The structural basis of ribosome activity in peptide bond synthesis." Science **289**(5481): 920-930.

Nissen, P., J. A. Ippolito, et al. (2001). "RNA tertiary interactions in the large ribosomal subunit: the A-minor motif." Proc. Natl. Acad. Sci. USA **98**(9): 4899-903.

Nyborg, J., P. Nissen, et al. (1996). "Structure of the ternary complex of EF-Tu: Macromolecular mimicry in translation." Trends Biochem Sci **21**(3): 81-82.

Ogle, J., A. Carter, et al. (2003). "Insights into the decoding mechanism from recent ribosome structures." TIBS **28**(5): 259-266.

Ogle, J. M., D. E. Brodersen, et al. (2001). "Recognition of cognate transfer RNA by the 30S ribosomal subunit." Science **292**(5518): 897-902.

Pan, D., S. V. Kirillov, et al. (2007). "Kinetically competent intermediates in the translocation step of protein synthesis." Mol. Cell **25**(4): 519-529.

Qin, Y., N. Polacek, et al. (2006). "The highly conserved LepA is a ribosomal elongation factor that back-translocates the ribosome." Cell **127**(4): 721-733.

Rheinberger, H.-J., H. Sternbach, et al. (1981). "Three tRNA binding sites on *Escherichia coli* ribosomes." Proc. Natl. Acad. Sci. USA **78**(9): 5310-5314.

Rheinberger, H. J. and K. H. Nierhaus (1987). "The ribosomal E site at low magnesium: coordinate inactivation of ribosomal functions at magnesium concentrations below 10 mM and its prevention by polyamines." J. Biomol. Struct. Dyn. **5**(2): 435-46.

Richey, B., D. S. Cayley, et al. (1987). "Variability of intracellular environment of *Escherichia coli*." J. Biol. Chem. **262**: 7157-7164.

Rodnina, M. V., A. Savelsbergh, et al. (1997). "Hydrolysis of GTP by elongation factor G drives tRNA movement on the ribosome." Nature **385**(6611): 37-41.

Rodnina, M. V., A. Savelsbergh, et al. (1999). "Thiostrepton inhibits the turnover but not the GTPase of elongation factor G on the ribosome." Proc. Natl Acad. Sci. USA **96**: 9586-9590.

Schuette, J. C., F. V. t. Murphy, et al. (2009). "GTPase activation of elongation factor EF-Tu by the ribosome during decoding." Embo J **28**(6): 755-65.

Schuwirth, B. S., M. A. Borovinskaya, et al. (2005). "Structures of the bacterial ribosome at 3.5 A resolution." Science **310**(5749): 827-834.

Shine, J. and L. Dalgarno (1974). "The 3'-terminal sequence of *E. coli* 16S rRNA: Complementarity to nonsense triplets and ribosome binding sites." Proc. Natl Acad. Sci. USA **71**(4): 1342-1346.

Shoji, S., S. E. Walker, et al. (2009). "Ribosomal Translocation: One Step Closer to the Molecular Mechanism." ACS Chem. Biol.

Spahn, C. M., M. G. Gomez-Lorenzo, et al. (2004). "Domain movements of elongation factor eEF2 and the eukaryotic 80S ribosome facilitate tRNA translocation." EMBO J. **23**(5): 1008-1019.

Spahn, C. M. T. and C. D. Prescott (1996). "Throwing a spanner in the works: antibiotics and the translational apparatus." J. Mol. Med. **74**: 423-439.

Steven, A. C., B. L. Trus, et al. (1988). "Molecular substructure of a viral receptor-recognition protein. The gp17 tail-fiber of bacteriophage T7." J. Mol. Biol. **200**(2): 351-365.

Szaflarski, W., O. Vesper, et al. (2008). "New features of the ribosome and ribosomal inhibitors: Non-enzymatic recycling, misreading and back-translocation." J. Mol. Biol. **380**: 193-205.

Taylor, D. J., J. Nilsson, et al. (2007). "Structures of modified eEF2 80S ribosome complexes reveal the role of GTP hydrolysis in translocation." EMBO J. **26**(9): 2421-2431.

Terashima, H., S. Kojima, et al. (2008). "Flagellar motility in bacteria structure and function of flagellar motor." Int. Rev. Cell Mol. Biol. **270**: 39-85.

Traub, P. and M. Nomura (1969). "Structure and function of the *Escherichia coli* ribosome. Mechanism of assembly of 30S ribosomes studied *in vitro*." J. Mol. Biol. **40**: 391-413.

Traut, R. R. and R. E. Monro (1964). "The puromiycin reaction and its relation to protein synthesis." J. Mol. Biol. **10**: 63-72.

Valle, M., A. Zavialov, et al. (2003). "Incorporation of aminoacyl-tRNA into the ribosome as seen by cryo-electron microscopy." Nat. Struct. Biol. **10**(11): 899-906.

Valle, M., A. Zavialov, et al. (2003). "Locking and unlocking of ribosomal motions." Cell **114**(1): 123-134.

Watson, J. D. (1964). "The synthesis of proteins upon ribosomes." Bull. Soc. Chim. Biol. **46**: 1399-1425.

Wilson, D. N., G. Blaha, et al. (2002). "Protein synthesis at atomic resolution: mechanistics of translation in the light of highly resolved structures for the ribosome." Curr. Protein Pept. Sci. **3**(1): 1-53.

Wilson, D. N. and K. H. Nierhaus (2003). "The ribosome through the looking glass." Angew. Chem. Int. Ed. Engl. **42**(30): 3464-3486.

Wood, J. M., E. Bremer, et al. (2001). "Osmosensing and osmoregulatory compatible solute accumulation by bacteria." Comp. Biochem. Physiol. A Mol. Integr. Physiol. **130**(3): 437-460.

Yonath, A., J. Müssig, et al. (1980). "Crystallization of the large ribosomal subunits from *Bacillus stearothermophilus*." Biochem. Int. **1**: 428-435.

Yusupov, M. M., G. Z. Yusupova, et al. (2001). "Crystal structure of the ribosome at 5.5 A resolution." Science **292**(5518): 883-896.

Zaher, H. S. and R. Green (2009). "Quality control by the ribosome following peptide bond formation." Nature **457**(7226): 161-166.

Zhang, G., M. Hubalewska, et al. (2009). "Transient ribosomal attenuation coordinates protein synthesis and co-translational folding." Nat. Struct. Mol. Biol. **16**(3): 274-280.

Zwizinski, C. and W. Wickner (1980). "Purification and characterization of leader (signal) peptidase from *Escherichia coli*." J. Biol. Chem. **255**(16): 7973-7977.

Curriculum Vitae

For reasons of data protection, the curriculum vitae is not included in the online version

Acknowledgement

The object of knowledge is what exists and its function to know about reality (Plato). Knud Nierhaus, started his mission in ribosome field already in 70s, bringing remarkable knowledge and findings. His passion and love for his work was one of my driving forces to continue with my exciting topic. Knud, you have supported and encouraged me from the beginning to the final, I thank you for that.

I am indebted to my postdoc college Markus, whose help and intensive discussions about EF4 has been one of the main impacts on my work.

Hiroshi, my friend you have been of great help in many things, thank you! I also would like to show my gratitude to my present lab colleges Daniela, Romi, Jarek, Kaori and past colleges Oliver, Wittek and Alexandros.

I especially thank Renate and Edda for their help and support in many ways.

A very special thanks goes to my friend and my PyMol guru Der David, your support and caring meant a lot to me.

I also want to thank Rudi Lurz and his group for their help in making the EM pictures. A special thank goes to Sergey Baranov for his support, long discussions and friendship.

The prime thanks goes to my precious son, Jara, whose understanding and loving kept me ongoing in my toughest times. I love you kapalli. A special thank goes to my daikm Shaubo, your love and believe in me meant everything. Araz, you were always there for me I thank you for that and I love you. I also want to thank the rest of my family my father Azad and Raz, Nakaroz, Nabaz, Zhwan, Sarawan, Besaran, Kani Dea, Robin, Karwan, Kani and Agreen.

At last but not least I would like to again thank my friend Jaroslaw Kijek aka Jarek for his friendship and support.